

Structure and function of supercomplexes in photosynthetic and respiratory membranes of eukaryotes

Von der Naturwissenschaftlichen Fakultät
der Gottfried Wilhelm Leibniz Universität Hannover

zur Erlangung des Grades

Doktor der Naturwissenschaften

Dr. rer. nat.

genehmigte Dissertation

von

Dipl.-Biol. Jesco Heinemeyer

geboren am 12. Juni 1976 in Hildesheim

2007

Referent: Prof. Dr. Hans-Peter Braun

Koreferent: Prof. Dr. Udo Schmitz

Tag der Promotion: 11.07.2007

Abstract

During the last few years many reports on the supramolecular organization of the oxidative phosphorylation (OXPHOS) system and photophosphorylation (PHOTPHOS) system have been published. In both fields of research many supercomplexes with specific compositions for a number of organisms were described. Interestingly, in the past OXPHOS research was mainly based on Blue-native polyacrylamide gel electrophoresis (BN-PAGE) while PHOTPHOS research often used electron microscopy (EM) in combination with single particle analysis.

By transferring EM in combination with single particle analysis onto the field of OXPHOS research this thesis provides new results on the supramolecular structure of dimeric ATP synthase of *Polytomella* mitochondria. It could be demonstrated that the two ATP synthase protein complexes are connected by their F_0 parts and that their long axes are in an angular orientation to each other within the supercomplex. The angular association of both complexes is proposed to induce a bending of the inner mitochondrial membrane (IMM) important for cristae formation. Furthermore, application of EM was utilized for the structural investigation of the yeast III+IV supercomplex. The results allowed the construction of a pseudoatomic model and revealed that complex IV monomers are attached to dimeric complex III at opposite sides. Interaction of complex IV with dimeric complex III takes place in a way that does not occupy the complex IV sides proposed to be involved in complex IV dimerisation. Due to the observed close proximity of cytochrome c binding sites within the supercomplex a rapid electron transfer via a ping-pong like mechanism is proposed.

The application of BN-PAGE in the field of PHOTPHOS research allowed verifying the supramolecular structures already described by investigations based on EM for *Arabidopsis*. Supercomplexes composed of different numbers of LHC II attached to dimeric PS II as well as a supercomplex of PS I and LHC I were found. Furthermore, analysis by BN-PAGE provides evidence that supercomplexes of PS I and the Cyt b_6f complex are unlikely to exist. This is interesting because these previously proposed structures were assumed to enhance electron transfer during cyclic electron transport. Finally, using the same experimental approach, this PhD thesis shows that the respiratory chain of potato is organized in a supercomplex comprising complex I, III and IV. Presence of these so-called “respirasomes”, which previously were only known for mammals, was described for the first time in plants.

Keywords: Mitochondria, Chloroplasts, Supercomplexes

Zusammenfassung

Während der letzten Jahre wurde in vielen wissenschaftlichen Arbeiten gezeigt, dass das System der Oxidativen Phosphorylierung (OXPHOS) und der Photophosphorylierung (PHOTPHOS) eine supermolekulare Organisation aufweist. In diversen Organismen konnten für beide Systeme definierte Proteinsuperkomplexe nachgewiesen werden. Dabei ist auffallend, dass in der Forschung am OXPHOS-System häufig die Blau-native Polyacrylamid Gelelektrophorese (BN-PAGE) verwendet wurde, während die Forschung am PHOTPHOS-System oft auf einer Kombination von Elektronenmikroskopie (EM) und einer „single particle analysis“ basierte.

Durch den Einsatz von EM und der „single particle analysis“ auf dem Gebiet der OXPHOS-Forschung konnten im Rahmen der vorliegenden Doktorarbeit neue Ergebnisse über die dimeren ATP-Synthase aus den Mitochondrien von *Polytomella* erzielt werden. Es konnte gezeigt werden, dass die monomeren ATP-Synthase Proteinkomplexe durch ihre F_0 -Teile miteinander verbunden sind und dass ihre Längsachsen in einem bestimmten Winkel zueinander stehen. Es wurde geschlussfolgert, dass diese gewinkelte Anordnung das Biegen der inneren Mitochondrienmembran (IMM) verursacht und somit wichtig für die Struktur der Cristae ist. Des Weiteren wurde die EM für die Untersuchung der Struktur eines Proteinsuperkomplexes aus Hefe verwendet, der sich aus den Atmungskettenkomplexen III und IV zusammensetzt. Basierend auf dieser experimentellen Strategie war es möglich, ein pseudoatomares Modell dieses Superkomplexes zu erstellen und zu zeigen, dass Komplex IV Monomere an gegenüberliegenden Seiten eines zentral angeordneten Komplex III Dimers binden. Es konnte weiterhin gezeigt werden, dass die Bereiche, die innerhalb von Komplex IV für eine mögliche Dimerisierung verantwortlich sind, weiterhin frei für eine solche Interaktion sind. Die entdeckte große räumliche Nähe der Cytochrom c-Bindestellen der Komplexe III und IV innerhalb des Superkomplexes lassen auf einen schnellen Elektronentransfer durch eine „ping-pong“-artige Bewegung des Cytochrom c schließen.

Die Tatsache, dass im Bereich der PHOTPHOS-Forschung die Blau-native Gelelektrophorese bisher kaum eingesetzt wurde, war Anlass für eine genaue Untersuchung der supermolekularen Struktur des PHOTPHOS-Systems in *Arabidopsis* mit dieser Strategie. Die durch EM bisher bekannten Superkomplexe, bestehend aus dimerem PS II und LHC II bzw. aus PS I und LHC I, konnten bestätigt werden. Des Weiteren konnte gezeigt werden, dass die Existenz

bisher vermuteter Strukturen aus PS I und Cyt. b_6f eher unwahrscheinlich ist. Dies ist insofern interessant, als dass von diesen vorhergesagten Strukturen angenommen wurde, dass sie die strukturelle Basis für gesteigerten zyklischen Elektronentransport darstellen. Zu guter letzt war es durch die Anwendung der Blau-nativen Gelelektrophorese möglich, neue Superkomplexe aus der Atmungskette von Kartoffel zu beschreiben. Die Existenz von Superkomplexen bestehend aus den Komplexen I, III und IV, die auch als „Respirasome“ bezeichnet werden, war bisher nur für die Säugetiere bekannt.

Schlagwörter: Mitochondrien, Chloroplasten, Superkomplexe

Contents

| | | |
|------------------|---|------------|
| Chapter 1 | General Introduction | 6 |
| | 1.1 Processes of energy metabolism in eukaryotic cells | |
| | 1.2 The Oxidative Phosphorylation System | |
| | 1.2.1 Subcellular localization | |
| | 1.2.2 Components of the Oxidative Phosphorylation System | |
| | 1.3 The Photophosphorylation System | |
| | 1.3.1 Subcellular localization | |
| | 1.3.2 Components of the Photophosphorylation System | |
| | 1.4 New insights into the supramolecular structure of the Oxidative Phosphorylation System and the Photophosphorylation System | |
| | 1.4.1 The discovery of protein supercomplexes | |
| | 1.4.2 New results obtained by Blue-native PAGE | |
| | 1.4.3 New results obtained by single particle electron microscopy | |
| | 1.5 Literature cited | |
| Chapter 2 | Identification and characterization of respirasomes in potato mitochondria (<i>Plant Physiology</i> 134: 1450-1459) | 27 |
| Chapter 3 | Proteomic approach to characterize the supramolecular organization of photosystems in higher plants (<i>Phytochemistry</i> 65: 1683–1692) | 37 |
| Chapter 4 | Structure of dimeric ATP synthase from mitochondria: An angular association of monomers induces the strong curvature of the inner membrane (<i>FEBS Letters</i> 579: 5769–5772) | 47 |
| Chapter 5 | A structural model of the cytochrome c reductase / oxidase supercomplex from yeast mitochondria (<i>JOURNAL OF BIOLOGICAL CHEMISTRY</i> 282: 12240-12248) | 51 |
| Chapter 6 | Respiratory chain supercomplexes in the plant mitochondrial membrane (<i>TRENDS in Plant Science</i> 11: 232-240) | 60 |
| Chapter 7 | Supramolecular structure of the oxidative phosphorylation system in plants (<i>In "Plant Mitochondria", Annual Plant Reviews series, Blackwell Publishing: 171-184</i>) | 69 |
| Chapter 8 | Supplementary Discussion and Outlook | 83 |
| | 8.1 Discussion | |
| | 8.1.1 Function of OXPHOS supercomplexes | |
| | 8.1.2 Function of PHOTPHOS supercomplexes | |
| | 8.2 Outlook | |
| | 8.2.1 Further investigations of the supramolecular organization of membrane bound protein supercomplexes | |
| | 8.2.2 Further investigations of the supramolecular organization of membrane bound protein supercomplexes on the basis of DIGE | |
| | 8.3 Literature cited | |
| Affix | Abbreviations | 100 |
| | Publications | |
| | Curriculum Vitae | |
| | Danksagung | |
| | Eidesstattliche Erklärung | |

General Introduction

1.1 Processes of energy metabolism in eukaryotic cells

All organisms, in order to maintain themselves, to grow and to reproduce need energy. Most of the energy used in this respect in eukaryotic cells is provided by adenosine triphosphate (ATP). ATP can be split into adenosine diphosphate and phosphate. Thereby, the phosphoanhydride bond between both parts of the molecule is cleaved and energy becomes available. The generation of ATP from ADP and phosphate can take place by the use of diverse energy sources like inorganic and organic compounds as well as light. The most prominent processes generating ATP in eukaryotic cells are substrate-chain-phosphorylation, oxidative phosphorylation (OXPHOS) and photophosphorylation (PHOTPHOS).

Substrate-chain-phosphorylation can take place via glycolysis and the citric acid cycle. In glycolysis, the substrate glucose is converted into two molecules of pyruvate. Pyruvate is decarboxylated and the resulting acetyl is converted into two molecules of CO₂ by the citric acid cycle. In both processes the exergonic conversion of specific intermediates into the following one along the substrate chain allows the phosphorylation of ADP or GDP into ATP or GTP. Since the break down of the carbon compounds like glucose or acetyl is accompanied by a de facto oxidation of their c-atoms hydrogen is released and transferred to NAD⁺. NAD⁺ is the oxidized form of nicotinamide adenine dinucleotide (NADH) an universal carrier for electrons.

Oxidative phosphorylation is accomplished by the respiratory chain and the ATP synthase complex. The respiratory chain couples the exergonic transfer of electrons from NADH on to molecular oxygen to the transport of protons from the mitochondrial matrix to the intermembrane space. Thereby an electrochemical gradient is generated which provokes the back flow of protons. This back flow is used by the ATP synthase complex to phosphorylate ADP to ATP (Mitchell 1961).

In photophosphorylation, which takes place during photosynthesis, phosphorylation of ADP is also based on the back flow of protons following an electrochemical gradient as well as the build up of this gradient is achieved by the transfer of electrons. But there are a few major differences (i) the transferred electrons result from the cleavage of water (ii) the energy neces-

sary for this strongly endergonic reaction is supplied by light and (iii) in the process of photosynthesis the electrons are not transferred to molecular oxygen but to NADP^+ . Therefore, photophosphorylation results in the formation of two reactive compounds, NADPH and ATP. In contrast to oxidative phosphorylation in mitochondria, the generated ATP is not exported from the chloroplasts but used as a co-substrate for endergonic reactions within this organelle.

The molecular basis for oxidative phosphorylation and photophosphorylation are large multi-subunit protein complexes. The supramolecular organization of these systems is subject of the presented dissertation.

1.2 The Oxidative Phosphorylation System

1.2.1 Subcellular localization

While glycolysis takes place within the cytosol the citric acid cycle and the oxidative phosphorylation is located in the mitochondria of a cell. Mitochondria are eukaryotic organelles with a round or oval shape and a size of 1 – 3 μm . However, in some organisms they can form a network of fused organelles (Bereiter-Hahn 1990). Mitochondria contain their own DNA often in form of a circular molecule, have a protein synthesis apparatus but are obligate intracellular structures. Therefore, they are designated semiautonomous. The endosymbiosis theory suggests that mitochondria are descendants of an early type of aerobe prokaryote (Sagan 1967), which was taken up by another cell. Since the closest relatives of today's mitochondria belong to only one phylogenetic group of prokaryotes, the alpha proteobacteria (Gray et al. 2001), it is believed that the incorporation only happened once. If this incorporation must be considered to represent the birth of the eukaryotic cell until today is a matter of debate (de Duve 2007).

As a result of an uptake by endocytosis, till today all mitochondria are enveloped by a second lipid membrane, the outer mitochondrial membrane. The membrane is unfolded and has large protein pores which allow the passage of molecules with a size of up to 10 kDa. Therefore this membrane is highly permeable. The pores connect the eukaryotic cytosol with the intermembrane space. The intermembrane space is followed by the inner mitochondrial membrane, the original barrier that demarcates the mitochondrial lumen or matrix from the outside. To function in this respect the inner membrane has a highly selective permeability, mediated

by several transport systems. In contrast to the outer membrane the inner membrane is heavily folded. These foldings are highly dynamic and are called cristae (for recent review see Manella 2006). They protrude into the matrix and depending on their shape they can be classified into lamellar, tubular or vesicular cristae. Despite the fact that the crista lumen belongs to the intermembrane space it can be regarded as an additional compartment because the connections, the crista junctions, are very constricted. Beside the large invaginated areas of the inner mitochondrial membrane there are parts which directly face the outer membrane. These parts are designated the inner boundary membrane.

The structural complexity of mitochondria reflects their physiological role. The highest diversity of reactions can be found in the mitochondrial matrix, e.g. represented by the mitochondrial protein synthesis, the citric acid cycle and the β -oxidation of fatty acids (not in plants). However, the lion's share of energy production in mitochondria involves the inner mitochondrial membrane and the Oxidative Phosphorylation System.

1.2.2 Components of the Oxidative Phosphorylation System

The Oxidative Phosphorylation System in eukaryotes consists most of the time of 5 distinct protein complexes embedded in the inner membrane and two mobile electron carrier ubiquinone and cytochrome c. The complexes are the NADH-ubiquinone oxidoreductase (complex I), the succinat-ubiquinone oxidoreductase (complex II), the ubiquinone-cytochrome c oxidoreductase (complex III), the cytochrome c – O_2 oxidoreductase (complex IV) and the ATP synthase (complex V). The first four protein complexes together constitute the respiratory chain. They facilitate the transfer of electrons from organic compounds to molecular oxygen and hereby are involved in the generation of a proton gradient across the membrane. ATP synthase in contrast is the pass by which the protons flow back. Driven by the energy of this back flow ATP synthase phosphorylates ADP to form ATP. The transport of electrons is facilitated by a path of metallo proteins which are part of each protein complex.

The entry point for electrons that derive from NADH is complex I. Complex I has an L-shape and can be divided into a “membrane arm” and a “peripheral arm” which protrudes into the mitochondrial matrix (Friedrich et al. 2004). It is composed of more than 40 subunits (Carroll et al. 2003, Abdrakhmanova et al. 2004), but only a few subunits are relevant for electron transport. It is believed that all of them are located in the peripheral arm. Beginning with an iron sulfur cluster called N1a which is part of a 24 kDa subunit the electrons flow over a non

covalently bound flavin mononucleotide through three iron sulfur clusters N1b, N5 and N4 which belong to an adjacent 51 kDa subunit. Hereafter the electrons pass N6a and N6b the iron sulfur clusters of subunit TYKY. From here they finally are transferred to ubiquinone via the N2 iron sulfur cluster of subunit PSST. Ubiquinone in its reduced form ubiquinol is liberated readily to transfer electrons onto complex III via diffusion. While the electrons are passed from the matrix to the intermembrane space side protons are transferred in the opposite direction. It is generally accepted that this is done by the membrane part of complex I and that this part has at least seven essential subunits called ND1-4, ND4L and ND5-6. Complex I is the least understood complex and therefore the mechanism that couples proton transfer to electron transport is still unclear (for recent review see Brandt 2006).

Complex II is composed of 4 proteins, the flavoprotein subunit (SDH1), the iron-sulfur subunit (SDH2), and the so-called subunits III (SDH3) and IV (SDH4) which both constitute a hydrophobic membrane anchor (Yankovskaya et al. 2003). Complex II does not have the capability to transfer protons but facilitates the conversion of succinate into fumarate and thereby reduces FAD^+ to FADH_2 . Additionally, complex II is able to transfer electrons from FADH_2 to ubiquinone. Since one process is part of the citric acid cycle and the other part of the respiratory chain complex II plays an important role in two different processes.

Complex III is the receiver of electrons delivered by ubiquinol coming from complex I and II. Although this complex can have up to 11 subunits (Schägger et al. 1986) only three subunits, namely cytochrome b, cytochrome c₁ and the rieske protein, are of fundamental importance for its function. They contain the redox active prosthetic groups, haem b_L, Haem b_H, haem c₁ and an iron sulphur center which passes the electrons to the mobile electron carrier cytochrome c. Two electrons can enter the complex at a time. This takes place at the intermembrane side of complex III and therefore the corresponding protons are released into the intermembrane space. One electron is directly conducted to cytochrome c via the iron sulphur center of the rieske protein and haem c₁ of the cytochrome c₁ subunit. The second electron is directed to haem b_L and subsequently to haem b_H of subunit cytochrome b (for review see Rich 2003). The latter process is part of the so-called Q-cycle. During this cycle the electrons passed to haem b_H are transferred onto ubiquinone again to generate semi-ubiquinone and after transfer of another electron ubiquinol. Since haem b_H is located at the matrix side of complex III the protons taken up to form ubiquinol derive from the matrix. The matrix uptake and the intermembrane space release of protons together constitute the capability of complex III to

transfer protons across the inner mitochondrial membrane. This transfer is driven by the transport of electrons that in turn results in the release of reduced cytochrome c at the intermembrane space side of the complex.

Reduced cytochrome c can bind to complex IV. While about 13 subunits (Tsukihara et al. 1996) form part of this terminal complex of the respiratory chain its redox chain is constituted by only two subunits. The first subunit within this chain is subunit II, which represents the docking side for cytochrome c. With its Cu_A center it has the capability to conduct electrons from cytochrome c to the haem a of subunit I, the second subunit within the chain. Subunit I has a further redox center called haem a_3 which is associated with the copper center Cu_B . These two groups together represent a binuclear centre which is the terminal point within the redox chain of complex IV because oxygen can bind to this place to form water together with electrons and matrix protons. Unlike complex III complex IV performs real proton pumping through protein channels within subunit I, but the mechanism that couples proton transfer to electron transport so far is unclear (for review see Rich 2003).

The gate for proton backflow from the mitochondrial intermembrane space to the matrix is complex V. Complex V exhibits two distinct subcomplexes called F_0 and F_1 . While F_0 is strongly hydrophobic F_1 protrudes into the matrix and therefore is hydrophilic. Both subcomplexes are connected to each other by a central and by a peripheral stalk. The F_0 part is composed of at least three subunits namely subunit a, b, and c. Subunit c exists in 9-12 copies forming a protein ring to which subunits a and b are attached. The latter together with OSCP are part of the peripheral stalk. F_1 or the so called head piece of complex V comprises three copies of subunit α and three copies of subunit β . α and β are arranged in pairs and in an alternating manner around the central stalk (Abrahams et al. 1994), which is constituted by a protein called subunit γ . Subunit γ is associated to two smaller subunits namely δ and ϵ , whereby ϵ connects γ to the subunit c ring of F_0 . The subunit a mediated proton flow through F_0 induces a rotation of the subunit c ring within F_0 and the connected central stick. The rotary motion mechanically alters the spatial orientation of subunit α and β within a α - β pair of F_1 (Stock et al. 2000). This leads to periodical changes of their binding capabilities with respect to $\text{ADP} + \text{Pi}$ and ATP respectively allowing the uptake of $\text{ADP} + \text{Pi}$, their conversion to ATP and finally the release of ATP.

1.3 The Photophosphorylation System

1.3.1 Subcellular localization

ATP synthesis via photophosphorylation is a process exclusively found in chloroplasts. Chloroplasts are chlorophyll containing mostly disc like organelles, but in several organisms their shape is remarkably altered. With a size of up to 10 μm in length they are much bigger than mitochondria. Chloroplasts can be found only in eukaryotes able to carry out photosynthesis like algae or plants. As in the case of mitochondria the origin of chloroplasts is explained by an endosymbiosis event and like mitochondria chloroplasts are semi-autonomous organelles.

The basic structure of chloroplasts resembles the one of mitochondria. They have a permeable outer membrane followed by an intermembrane space and a much less permeable inner membrane. The inner membrane surrounds the lumen or stroma of the organelle and possess many pinches called thylakoids. They have lost their connection to the intermembrane space, but the lumens of all thylakoids are connected to each other. Most of the thylakoids are arranged into stacks named grana and are called grana thylakoids whereas the remaining unstacked thylakoids are termed stroma thylakoids.

While the stroma of chloroplasts is the place of CO_2 fixation and the formation of sugars via the Calvin cycle the thylakoid membranes with their Photophosphorylation System are the subcompartment which delivers the necessary reduction power as well as the energy to form the compounds of the Calvin cycle

1.3.2 Components of the Photophosphorylation System

Within the thylakoid membrane six major protein complexes are responsible for the capability mentioned above, light harvesting complex II (LHC II), photosystem II (PS II), the cytochrome b_6f complex (Cyt b_6f), light harvesting complex I (LHC I), photosystem I (PS I) and ATP synthase (CF_0F_1).

LHC II is a trimer that consists of three proteins called Lhcb1, Lhcb2 and Lhcb3 (Hobe et al. 1994). Each protein contains 5 chlorophyll b, 7 chlorophyll a and 2 lutein molecules. The

trimeric arrangement of the proteins makes sure that all chlorophyll b is adjusted in the periphery of the complex while chlorophyll a and the luteins are located in the centre of the complex. Because of the exact orientation to each other which is mediated by the protein scaffold the chlorophyll molecules are able to conduct light energy respectively excitons to an adjacent molecule (Heldt 2003). LHC II has the capability to transfer light energy from its chlorophyll molecules to PS II. The prerequisite for this process is the light induced excitation of chlorophyll electrons which are part of a conjugated π -electron system.

PS II is a protein complex that can be divided into three parts, a peripheral part, a central part and a domain called the oxygen evolving complex (OEC). The peripheral part or peripheral antenna has three subunits, namely CP24, CP26 and CP29. The central part of the core is made up of the subunits D1, D2, CP47, CP43 and two further subunits forming cytochrome b559. PS II has at least three further subunits (for recent review see Barber 2006). They are called PsbL, PsbK and PsbW but their possible functions are up to now subject to speculations. The oxygen evolving complex (OEC) harbors a manganese cluster that comprises 4 manganese atoms and one calcium atom (for recent review see Surosa 2007). The cluster is stabilized by the manganese stabilizing protein (MSP) which is accompanied by two further OEC proteins with a size of 23 and 17 kDa respectively. CP24-29 function as conductors for excitons coming from LHC II. CP47 and CP 43 constitute the internal antenna of PS II. This antenna harvests light energy and conducts excitons from LHC II to D1 and D2 (de Weerd et al. 2002), the reaction centre of PS II (Barber 1987). By incoming excitons the reaction centre can become ionized and liberated electrons are transferred to plastoquinone (PQ). The electron gap created continuously by the excitation of the reaction centre is filled up by the successive delivery of four electrons from the manganese cluster. When the most oxidized state is reached the cluster is able to facilitate the cleavage of water into molecular oxygen, electrons and protons in order to compensate its electron deficit. Since the protons are liberated at the lumen side of the complex they contribute to the generation of a proton gradient.

The cytochrome b_6f complex is composed of several subunits. The most important ones are cytochrome b_6 (cyt b_6), cytochrome f (cyt f) and the Rieske FeS protein due to the fact that they can facilitate the transport of electrons coming from PS II via plastoquinol to plastocyanin and they couple this process with the translocation of protons across the thylakoid membrane. The luminal Rieske protein receives electrons from plastoquinol and transfers them to cytochrome f and finally to plastocyanin. Thereby protons are liberated into the thylakoid

lumen and semiquinones are generated which turn to plastoquinone again by the surrender of one electron to $\text{cyt } b_6$. One part of the plastoquinone molecules is successively reduced again on the stromal side which leads to the uptake of stromal protons and the generation of plastoquinol (Heldt 2003).

The LHC I complex is the external light harvesting apparatus that provides PS I with excitons. LHC I is constructed of two subcomplexes, LHC I-730 and LHC I-680. While the latter contains one copy of the proteins Lhca2 and Lhca3 LHC I-730 is a product of Lhca1 and Lhca4 (Croce et al. 2002). Since the components of LHC I are chlorophyll binding proteins it functions in a similar way like LHC II.

PS I, the receiver of excitons provided by LHC I, consists of a core of two proteins called PsaA and PsaB with masses of approximately 82 and 83 kDa respectively (for recent review see Nelson et al. 2006). They bind the chlorophyll pair of the photoreaction centre and the redox carriers involved in electron donation as well as about hundred chlorophyll molecules which function as internal antenna. Additionally, PS I includes several small subunits with molecular weights below 18 kDa such as the copper protein subunit F which is a part of the binding side for plastocyanin or subunit C with its Fe-S centers A and B which is the reduction side for ferredoxin. While subunit C together with subunits D and E can be found on the stroma side of the complex subunit F is located at the opposite side, the lumen side (Ben-Shem 2003). The function of PS I takes place when light energy liberates an electron of the chlorophyll pair within the reaction centre. This process leads to an electron transfer onto ferredoxin and simultaneously to a padding of the electron gap within the chlorophyll pair by plastocyanin. The oxidized form of plastocyanin afterwards is released while ferredoxin is oxidized via the ferredoxin-NADP-reductase to generate NADPH (Heldt 2003).

The chloroplast ATP synthase complex resembles the general model of F_1F_0 type ATP synthases with a hydrophilic $\alpha_3\beta_3\gamma\delta\varepsilon$ F_1 part and a hydrophobic $abb'c_{12}$ F_0 part. The complex uses the proton gradient generated by the light driven electron transport to build up ATP, but unlike the mitochondrial version it is insensitive to oligomycin and its activity is light regulated (Heldt 2003).

1.4. New insights into the supramolecular structure of the Oxidative Phosphorylation System and the Photophosphorylation System

1.4.1 The discovery of protein supercomplexes

The model of the respiratory chain described above is the result of one century of basic research. However, within the last few years many new results indicate that the model has to be modified because the protein complexes of the Oxidative Phosphorylation System were found to precisely interact forming large so-called respiratory supercomplexes. Their existents raised the demand to declare a new hierarchical level of protein organization, the quaternary structure of proteins. Representatives of OXPHOS supercomplexes were described for several groups of organisms, like archaeobacteria (Iwasaki et al. 1995), bacteria (Berry et al. 1985, Sone et al. 1987, Niebisch et al. 2003, Stroh et al. 2004), fungi (Arnold et al. 1998, Cruciat et al. 2000, Krause et al. 2004a) and mammalia (Schägger et al. 2000, Krause et al. 2005).

Like the OXPHOS system also the protein complexes of the PHOTPHOS system were shown to exist in supercomplexes. In the case of cyanobacteria it was revealed that PS I exist as a trimer (Kruip et al. 1993). Later on it was demonstrated that this trimeric configuration is enlarged by an antenna ring of 18 subunits related to CP43 under conditions of iron deficiency (Boekema et al. 2001a, Bibby et al. 2001). In contrast to cyanobacteria plants and green algae were found to contain PS I in a monomeric configuration but the monomers are in a supercomplex with LHC I (Boekema et al. 2001b, Germano et al. 2002, Kargul et al. 2003) or LHC II (Kouril et al. 2005). Like PS I also the PS II forms a supramolecular structure since it forms dimers in cyanobacteria as well as in eukaryotes (Boekema et al. 1995). Further investigations revealed that the dimers represent cores of even larger supercomplexes with varying numbers of LHC II complexes (Boekema et al. 1998, Yakushevskaya et al. 2001).

1.4.2 New results obtained by Blue-native PAGE

By a closer view on the methods involved in the isolation and identification of OXPHOS supercomplexes the most powerful appears to be a rarely known technique called Blue-native PAGE (Schägger et al. 1991). Unlike the popular SDS PAGE this approach tries not to denature proteins in order to produce one protein band per protein species, but tries to separate the protein structures in the presence of more or less native conditions. This implies that one pro-

tein band on a Blue-native gel can comprise several proteins, if they are *in vivo* structurally associated. The most striking feature of this technique compared to the SDS-PAGE is the substitution of SDS by the wool dye Coomassie blue. Like SDS, Coomassie blue is negatively charged, binds to proteins and introduces negative charges necessary for protein mobility in the electric field. However, in contrast to SDS, Coomassie does not denature proteins or disassembles protein complexes. Coomassie blue treatment is combined with treatment by a non-ionic detergent if membrane proteins have to be analysed. Non-ionic detergents are known to be comparable mild detergents and therefore often allow the native solubilization of membrane proteins. With respect to respiratory supercomplexes the ones most frequently used are Dodecylmaltoside (DDM), Digitonin and Triton X 100. In many cases Digitonin treatment provides the best results.

The convincing capabilities of Blue-native PAGE in combination with Digitonin led to the usage of this technique to answer the question whether the respiratory chain of plants is also organized in supercomplexes or not. While Eubel and co-workers (Eubel et al. 2003) described the discovery of an I+III₂ supercomplex in Arabidopsis, potato, bean and barley, chapter 2 of this work shows that even larger structures composed of the complexes I, III and IV can be found in potato. Since these structures are termed “respirasomes” the publication represented by chapter 2 demonstrates that respirasomes are a feature that can be found not only in animals but also in plants. These findings later on were underlined by the work of Krause and co-workers (Krause et al. 2004b).

In contrast to its dominant role in the course of investigations made on the OXPHOS system, Blue-native PAGE played nearly no role within the field of photosynthesis research. In this field merely a few research projects were carried out applying Blue-native PAGE. However these investigations were either carried out with detergents different from Digitonin (Kügler et al. 1997, 1998, Singh et al. 2000, Thidholm et al. 2002, Surosa et al. 2004) or they were focused on cyanobacteria or green algae (Rexroth et al. 2003, 2004). This encouraged the work presented in this thesis to systematically investigate the Photophosphorylation System using this experimental strategy in order to search for novel so far unknown supercomplexes. Since PS I and PS II need to be located in different sections of the thylakoid membranes in order to avoid a competition about excitons, primarily associations of the Cyt b₆f complex with either PS I or PS II are conceivable. New results on the Photophosphorylation System obtained by Blue-native PAGE are presented in chapter 3.

1.4.3 New results obtained by single particle electron microscopy

While Blue-native PAGE was utilized in research on OXPHOS supercomplexes the efforts to examine the supramolecular organization of the Photophosphorylation System were mainly based on the usage of electron microscopy in combination with single particle analysis. A prerequisite for this approach is a high quality sample enriched in the protein supercomplex of interest. Such a sample is then negatively stained by the use of uranyl acetate. This step introduces an increased electron density to the protein structure and allows detecting the particle by electron microscopy. The features of the structure are resolved due to the varying amounts of uranyl acetate at different places of the structure which in turn depend on their amount of protein. The investigation of a stained sample by electron microscopy ends up with an electron micrograph, but in general the particles on such an electron micrograph are of varying shapes. Although they are of the same sort this happens due to their different possible orientations on the carbon support film. Furthermore, the resolution of a single particle is not sufficient to recognize details that allow interpretations on its configuration. To overcome these problems investigation of protein supercomplexes by electron microscopy is accompanied by single particle analysis. Single particle analysis is a semiautomatic computer based method that tries to find particles of the same orientation within electron micrographs. This leads to the definition of different particle classes representing the most dominant orientations of the supercomplex on the carbon support film.

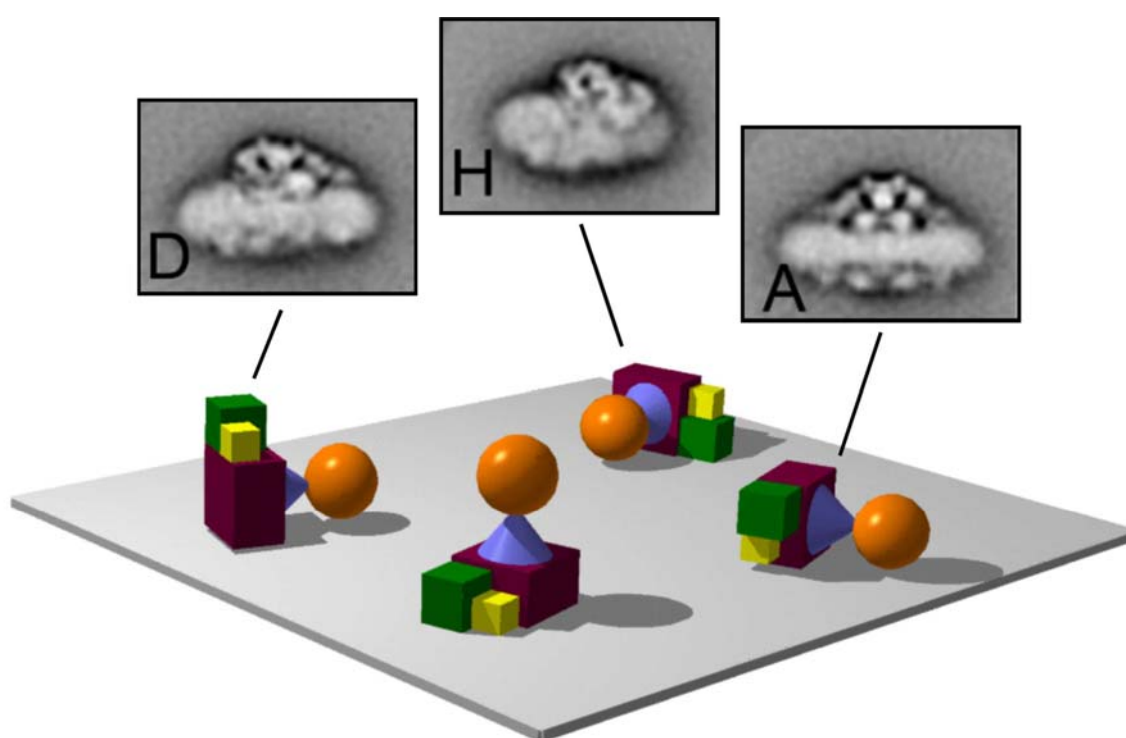


Figure 1: A model of different possible orientations of a supercomplex on a carbon support film. A-D: Images of different particle classes, representing different views onto the supercomplex.

In a further step the images of the particles within one class are averaged. Hereby features which are present in most of the images are sharpened whereas rare features which might represent artifacts are eliminated. The result is a sharpened and noise-reduced image representing a view onto a certain side of the supercomplex. This often allows addressing the sites of the single protein complexes involved in the formation of a supercomplex. Furthermore, if the number of different views respectively class images is sufficient, if the perspectives they represent is known and if the corresponding three dimensional crystal structures of the participating protein complexes are available the supercomplex can be depicted as a pseudoatomic model.

As a matter of fact, EM together with single particle analysis offers the opportunity to get quite detailed information on the shape of a supercomplex and the spatial orientation of its protein complexes. However as in the case of Blue-native PAGE, EM combined with single particle analysis so far mainly was applied in the field of chloroplasts. As a consequence the spatial information on OXPHOS supercomplexes for a long time were unavailable. Chapter 5 and 6 demonstrate the fruitfulness of transferring this experimental strategy to the field of research on OXPHOS supercomplexes. While chapter 5 gives information on the structure of dimeric ATP synthase of mitochondria from *polytomella*, chapter 6 reports details on the association of complex III and IV in yeast mitochondria. Since the structures of both assemblies were solved with a high degree of details they give direct hints to the relevance of supramolecular structures. Additionally, both works represent addenda to the works of Dudkina et al. (2005, 2006), Minauro-Sanmiguel et al. (2005) and Schäfer et al. (2006) which already provided information about the spatial configuration of OXPHOS supercomplexes.

Despite the fact that since today many striking evidences point toward the *in vivo* existents of protein supercomplexes the supramolecular architecture of the OXPHOS system still is a matter of debate. Chapter 7 and 8 of this work were contributed to deepen this debate. In this respect chapter 7 reports a summary of the different known supercomplexes and proposes a model on there possible distribution in a tubular cristae membrane while chapter 8 mainly discusses pros and cons for the occurrence of protein supercomplexes and suggests possible functions.

1.5. Literature cited

Abdrakhmanova A., Zickermann V., Bostina M., Radermacher M., Schägger H., Kerscher S., Brandt U. (2004)

Subunit composition of mitochondrial Complex I from the yeast *Yarrowia lipolytica*.

Biochim. Biophys. Acta. 1658: 148–156

Abrahams JP., Leslie AG., Lutter R., Walker J. (1994)

Structure at 2.8 Å resolution of F₁-ATPase from bovine heart mitochondria.

Nature 370: 621–628

Arnold I., Pfeiffer K., Neupert W., Stuart RA., Schägger H. (1998)

Yeast mitochondrial F₁F₀-ATP synthase exists as a dimer: identification of three dimer-specific subunits.

EMBO J. 17(24): 7170-7178.

Barber J. (1987)

Photosynthetic reaction centres: a common link.

Trends Biochem. Sci. 12: 321–326

Barber J. (2006)

Photosystem II: an enzyme of global significance.

Biochem. Soc. Trans. 34: 619-631

Ben-Shem A., Frolov F., Nelson N. (2003)

Crystal structure of plant photosystem I.

Nature 426(6967): 630-635

Bereiter-Hahn J. (1990)

Behavior of mitochondria in the living cell.

Int. Rev. Cytol. 122: 1-63

Berry EA., Trumpower BL. (1985)

Isolation of ubiquinol oxidase from *Paracoccus denitrificans* and resolution into cytochrome bc₁ and cytochrome c-aa₃ complexes.

J. Biol. Chem. 260(4): 2458-2467

Bibby TS., Nield J., Barber J. (2001)

Iron deficiency induces the formation of an antenna ring around trimeric photosystem I in cyanobacteria.

Nature 412(6848): 743-745

Boekema EJ., Hankamer B., Bald D., Kruip J., Nield J., Boonstra AF., Barber J., Rogner M. (1995)

Supramolecular structure of the photosystem II complex from green plants and cyanobacteria.

Proc. Natl. Acad. Sci. U S A. 92(1): 175-179

Boekema EJ., van Roon H., Dekker JP. (1998)

Specific association of photosystem II and light-harvesting complex II in partially solubilized photosystem II membranes.

FEBS Lett. 424(1-2): 95-99

Boekema EJ., Hifney A., Yakushevskaya AE., Piotrowski M., Keegstra W., Berry S., Michel KP., Pistorius EK., Kruip J. (2001a)

A giant chlorophyll-protein complex induced by iron deficiency in cyanobacteria.

Nature 412(6848): 745-748

Boekema EJ., Jensen PE., Schlodder E., van Breemen JF., van Roon H., Scheller HV., Dekker JP. (2001b)

Green plant photosystem I binds light-harvesting complex I on one side of the complex.

Biochemistry 40(4): 1029-1036

Brandt U. (2006)

Energy converting NADH:quinone oxidoreductase (complex I).

Annu. Rev. Biochem. 75: 69-92

Carroll J., Fearnley IM., Shannon RJ., Hirst J., Walker JE. (2003)

Analysis of the subunit composition of Complex I from bovine heart mitochondria.

Mol. Cell. Proteomics 2: 117–126

Croce R., Morosinotto T., Castelletti S., Breton J., Bassi R. (2002)

The Lhca antenna complexes of higher plants photosystem I.

Biochim. Biophys. Acta. 1556: 29-40

Cruciat CM., Brunner S., Baumann F., Neupert W., Stuart RA. (2000)

The cytochrome bc₁ and cytochrome c oxidase complexes associate to form a single supra-complex in yeast mitochondria.

J. Biol. Chem. 275(24): 18093-18098

De Duve C. (2007)

The origin of eukaryotes: a reappraisal.

Nat. Rev. Genet. 5: 395-403

De Weerd FL., van Stokkum IH., van Amerongen H., Dekker JP., van Grondelle R. (2002)

Pathways for energy transfer in the core light-harvesting complexes CP43 and CP47 of photosystem II.

Biophys. J. 82(3): 1586-1597

Dudkina NV., Eubel H., Keegstra W., Boekema EJ., Braun HP. (2005)

Structure of a mitochondrial supercomplex formed by respiratory-chain complexes I and III.

Proc. Natl. Acad. Sci. U S A 102: 3225–3229

Dudkina NV., Sunderhaus S., Braun HP., Boekema EJ. (2006)

Characterization of dimeric ATP synthase and cristae membrane ultrastructure from *Saccharomyces* and *Polytomella* mitochondria.

FEBS Lett. 580(14): 3427-3432

Eubel H., Jansch L., Braun HP. (2003)

New insights into the respiratory chain of plant mitochondria. Supercomplexes and a unique composition of complex II.

Plant Physiol. 133(1): 274-286

Friedrich T., Böttcher B. (2004)

The gross structure of the respiratory Complex I: a Lego system.

Biochim. Biophys. Acta. 1608 :1-9

Germano M., Yakushevskaya AE., Keegstra W., van Gorkom HJ., Dekker JP., Boekema EJ. (2002)

Supramolecular organization of photosystem I and light-harvesting complex I in *Chlamydomonas reinhardtii*.

FEBS Lett. 525(1-3): 121-125

Gray MW., Burger G., Lang BF. (2001)

The origin and early evolution of mitochondria.

Genome Biol. 2: Reviews 1018.1-1018.5

Heldt HW. (2003)

Pflanzenbiochemie.

Spektrum Akad. Verlag, 3. Auflage

Hobe S., Prytulla S., Kühlbrandt W., Paulsen H. (1994)

Trimerization and crystallization of reconstituted light-harvesting chlorophyll a/b complex.

EMBO J. 13(15): 3423-3429

Iwasaki T., Matsuura K., Oshima T. (1995)

Resolution of the aerobic respiratory system of the thermoacidophilic archaeon, *Sulfolobus* sp. strain 7. I. The archaeal terminal oxidase supercomplex is a functional fusion of respiratory complexes III and IV with no c-type cytochromes

J. Biol. Chem. 270(52): 30881-30892

Kargul J., Nield J., Barber J. (2003)

Three-dimensional reconstruction of a light-harvesting complex I-photosystem I (LHCI-PSI) supercomplex from the green alga *Chlamydomonas reinhardtii*. Insights into light harvesting for PSI.

J. Biol. Chem. 278(18): 16135-16141

Kouril R., Zygadlo A., Arteni AA., de Wit CD., Dekker JP., Jensen PE., Scheller HV., Boekema EJ. (2005)

Structural characterization of a complex of photosystem I and light-harvesting complex II of *Arabidopsis thaliana*.

Biochemistry. 44(33): 10935-10940

Krause F., Scheckhuber CQ., Werner A., Rexroth S., Reifschneider NH., Dencher NA., Osiewacz HD. (2004a)

Supramolecular organization of cytochrome c oxidase- and alternative oxidase-dependent respiratory chains in the filamentous fungus *Podospora anserina*.

J. Biol. Chem. 279(25): 26453-26461

Krause F., Reifschneider NH., Vocke D., Seelert H., Rexroth S., Dencher NA. (2004b)

"Respirasome"-like supercomplexes in green leaf mitochondria of spinach.

J. Biol. Chem. 279(46): 48369-48375

Krause F., Reifschneider NH., Goto S., Dencher NA. (2005)

Active oligomeric ATP synthases in mammalian mitochondria.

Biochem. Biophys. Res. Commun. 329(2): 583-590

Kruip J., Boekema EJ., Bald D., Boonstra AF., Rogner M. (1993)

Isolation and structural characterization of monomeric and trimeric photosystem I complexes (P700.FA/FB and P700.FX) from the cyanobacterium *Synechocystis* PCC 6803.

J. Biol. Chem. 268(31): 23353-23360

Kügler M., Kruft V., Schmitz UK., Braun HP. (1997)

Analysis of the chloroplast protein complexes by blue-native–polyacrylamide gel electrophoresis BN–PAGE.

Photosynth. Res. 53: 35–44

Kügler M., Kruft V., Schmitz UK., Braun HP. (1998)

Characterization of the PetM subunit of the b6f complex from higher plants.

J. Plant Physiol. 153: 581–586

Mannella CA. (2006)

Structure and dynamics of the mitochondrial inner membrane cristae.

Biochim. Biophys. Acta. 1763: 542-548

Minauro-Sanmiguel F., Wilkens S., Garcia JJ. (2005)

Structure of dimeric mitochondrial ATP synthase: novel F₀ bridging features and the structural basis of mitochondrial cristae biogenesis.

Proc. Natl. Acad. Sci. U S A 102: 12356–12358

Mitchell P. (1961)

Coupling of phosphorylation to electron and hydrogen transfer by a chemi-osmotic type of mechanism.

Nature 191: 144-148

Nelson N., Yocum CF. (2006)

Structure and function of photosystems I and II.

Annu. Rev. Plant Biol. 57: 521-65

Niebisch A., Bott M. (2003)

Purification of a cytochrome bc-aa₃ supercomplex with quinol oxidase activity from *Corynebacterium glutamicum*. Identification of a fourth subunit of cytochrome aa₃ oxidase and mutational analysis of diheme cytochrome c₁.

J. Biol. Chem. 278(6): 4339-4346

Rexroth S., Meyer zu Tittingdorf JM., Krause F., Dencher NA., Seelert H. (2003)

Thylakoid membrane at altered metabolic state: challenging the forgotten realms of the proteome.

Electrophoresis. 24(16): 2814-2823

Rexroth S., Meyer zu Tittingdorf JM., Schwassmann HJ., Krause F., Seelert H., Dencher NA. (2004)

Dimeric H⁺-ATP synthase in the chloroplast of *Chlamydomonas reinhardtii*.

Biochim. Biophys. Acta. 1658(3): 202-211

Rich PR. (2003)

The molecular machinery of Keilin's respiratory chain.

Biochem. Soc. Trans. 31: 1095-105

Sagan L. (1967)

On the origin of mitosing cells.

J. Theor. Biol. 14: 255-274

Schäfer E., Seelert H., Reifschneider NH., Krause F., Dencher NA., Vonck J. (2006)

Architecture of active mammalian respiratory chain supercomplexes.

J. Biol. Chem. 281(22): 15370-15375

Schägger H., Link TA., Engel WD., von Jagow G. (1986)

Isolation of the eleven protein subunits of the bc₁ complex from beef heart.

Methods Enzymol. 126: 224-237

Schägger H., von Jagow G. (1991)

Blue native electrophoresis for isolation of membrane protein complexes in enzymatically active form.

Anal. Biochem. 199(2): 223-231

Schägger H., Pfeiffer K. (2000)

Supercomplexes in the respiratory chains of yeast and mammalian mitochondria.

EMBO J. 19(8): 1777-1783

Singh P., Jänsch L., Braun HP., Schmitz UK. (2000)

Resolution of mitochondrial and chloroplast membrane protein complexes from green leaves of potato on Blue-Native–polyacrylamide gels.

Indian J. Biochem. Biophys. 37: 59–66

Sone N., Sekimachi M., Kutoh E. (1987)

Identification and properties of a quinol oxidase super-complex composed of a bc₁ complex and cytochrome oxidase in the thermophilic bacterium PS3.

J. Biol. Chem. 262(32): 15386-15391

Stock D., Gibbons C., Arechaga I., Leslie AG., Walker JE. (2000)

Rotary mechanism of ATP synthase.

Curr. Opin. Struct. Biol. 10: 672–679

Stroh A., Anderka O., Pfeiffer K., Yagi T., Finel M., Ludwig B., Schägger H. (2004)

Assembly of respiratory complexes I, III, and IV into NADH oxidase supercomplex stabilizes complex I in *Paracoccus denitrificans*.

J. Biol. Chem. 279(6): 5000-5007

Surosa M., Regel PE., Paakkarinen V., Battchikova N., Herrmann RG., Aro EM. (2004)

Protein assembly of photosystem II and accumulation of subcomplexes in the absence of low molecular mass subunits PsbL and PsbJ.

Eur. J. Biochem. 271: 96–107

Suorsa M., Aro EM. (2007)

Expression, assembly and auxiliary functions of photosystem II oxygen-evolving proteins in higher plants.

Photosynth. Res. in press

Thidholm E., Lindström V., Tissier C., Robinson C., Schröder WP., Funk C. (2002)

Novel approach reveals localisation and assembly pathway of the PsbS and PsbW proteins into the photosystem II dimer.

FEBS Lett. 513: 217–222

Tsukihara T., Aoyama H., Yamashita E., Tomizaki T., Yamaguchi H., Shinzawa-Itoh K., Nakashima R., Yaono R., Yoshikawa S. (1996)

The whole structure of the 13-subunit oxidized cytochrome c oxidase at 2.8Å.

Science 272: 1136–1144

Yakushevskaya AE., Jensen PE., Keegstra W., van Roon H., Scheller HV., Boekema EJ., Dekker JP. (2001)

Supramolecular organization of photosystem II and its associated light-harvesting antenna in *Arabidopsis thaliana*.

Eur. J. Biochem. 268(23): 6020-6028

Yankovskaya V., Horsefield R., Tornroth S., Luna-Chavez C., Miyoshi H., Leger C., Byrne B., Cecchini G., Iwata S. (2003)

Architecture of succinate dehydrogenase and reactive oxygen species generation.

Science 299: 700–704

Identification and Characterization of Respirasomes in Potato Mitochondria¹

Holger Eubel, Jesco Heinemeyer, and Hans-Peter Braun*

Institut für Angewandte Genetik, Universität Hannover, D-30419 Hannover, Germany

Plant mitochondria were previously shown to comprise respiratory supercomplexes containing cytochrome c reductase (complex III) and NADH dehydrogenase (complex I) of I₁III₂ and I₂III₄ composition. Here we report the discovery of additional supercomplexes in potato (*Solanum tuberosum*) mitochondria, which are of lower abundance and include cytochrome c oxidase (complex IV). Highly active mitochondria were isolated from potato tubers and stems, solubilized by digitonin, and subsequently analyzed by Blue-native (BN) polyacrylamide gel electrophoresis (PAGE). Visualization of supercomplexes by in-gel activity stains for complex IV revealed five novel supercomplexes of 850, 1,200, 1,850, 2,200, and 3,000 kD in potato tuber mitochondria. These supercomplexes have III₂IV₁, III₂IV₂, I₁III₂IV₁, I₁III₂IV₂, and I₁III₂IV₄ compositions as shown by two-dimensional BN/sodium dodecyl sulfate (SDS)-PAGE and BN/BN-PAGE in combination with activity stains for cytochrome c oxidase. Potato stem mitochondria include similar supercomplexes, but complex IV is partially present in a smaller version that lacks the Cox6b protein and possibly other subunits. However, in mitochondria from potato tubers and stems, about 90% of complex IV was present in monomeric form. It was suggested that the I₁III₂IV₄ supercomplex represents a basic unit for respiration in mammalian mitochondria termed respirasome. Respirasomes also occur in potato mitochondria but were of low concentrations under all conditions applied. We speculate that respirasomes are more abundant under in vivo conditions.

Prerequisite for oxidative phosphorylation (OXPHOS) in mitochondria are five protein complexes termed NADH dehydrogenase (complex I), succinate dehydrogenase (complex II), cytochrome c reductase (complex III), cytochrome c oxidase (complex IV), and ATP synthase (complex V). These protein complexes can be separated by biochemical procedures and are well characterized for several organisms. However, there is mounting evidence that in vivo these protein complexes specifically interact forming supermolecular structures called supercomplexes: (1) purification protocols for individual OXPHOS complexes sometimes lead to the isolation of stoichiometric assemblies of two or more complexes which are functionally active (Hatefi et al., 1961; Hatefi and Rieske, 1967); (2) stable and enzymatically active supercomplexes can be reconstituted upon mixture of complexes I and III (Fowler and Hatefi, 1961; Fowler and Richardson, 1963; Hatefi, 1978; Ragan and Heron, 1978); (3) respiratory protein complexes from several bacteria were found to form specific supermolecular structures (Berry and Trumpower, 1985; Sone et al., 1987; Iwasaki et al., 1995; Niebisch and Bott, 2003); (4) inhibitor titration experiments reveal that the respiratory chain of yeast (*Saccharomyces cerevisiae*) behaves like a single functional unit (Boumans et al., 1998); and (5) flux control experiments indicate specific interac-

tions of respiratory protein complexes (Genova et al., 2003). Several physiological roles were proposed for these respiratory supercomplexes, like substrate channeling, catalytic enhancement, protection of reactive reaction intermediates, and stabilization of individual protein complexes (Schägger and Pfeiffer, 2000; Genova et al., 2003).

Recently, characterization of mitochondrial supercomplexes was very much facilitated by the introduction of a novel experimental strategy which is based on protein solubilizations using mild nonionic detergents and separation of the solubilized protein complexes by Blue-native (BN) gel electrophoresis or gel chromatography (Arnold et al., 1998, 1999; Cruciat et al., 2000; Schägger and Pfeiffer, 2000; Zhang et al., 2002; Pfeiffer et al., 2003). Using this approach, several distinct supercomplexes could be described for mitochondria from different organisms (for review, see Schägger, 2001a, 2002).

In yeast, dimeric complex III (this protein complex always is dimeric for functional reasons) forms supercomplexes with one or two copies of complex IV. Furthermore, complex V was shown to partially occur in a dimeric state, which includes some dimer-specific subunits. In contrast, complex II from yeast does not form part of supermolecular structures under all experimental conditions applied. In beef, the complexes III₂ and I form a supercomplex. Additionally, this supercomplex can include one to four copies of complex IV. The resulting large structures are called respirasomes, because they can autonomously carry out respiration in the presence of cytochrome c and ubiquinone (Schägger and Pfeiffer, 2000). Like in yeast, ATP synthase partially forms dimers, and complex II does not form part of supercomplexes.

¹ This work was supported by the Fonds der Chemischen Industrie and the Deutsche Forschungsgemeinschaft (grant BR 1829-7/1).

* Corresponding author; e-mail braun@genetik.uni-hannover.de; fax 49511-7623608.

Article, publication date, and citation information can be found at www.plantphysiol.org/cgi/doi/10.1104/pp.103.038018.

Meanwhile, protein solubilizations using nonionic detergents and separations of solubilized protein complexes by BN-PAGE were used to systematically investigate the structure of the OXPHOS system of plants (Eubel et al., 2003). Three different supercomplexes were found in digitonin-solubilized mitochondrial fractions of *Arabidopsis*, potato (*Solanum tuberosum*), barley (*Hordeum vulgare*), and bean (*Phaseolus vulgaris*): (1) a 1,500-kD I_1III_2 supercomplex; (2) a 3,000-kD I_2III_4 supercomplex; and (3) a 1,100-kD dimeric ATP synthase complex. Depending on the plant investigated, the percentage of complex I integrated into the I_1III_2 supercomplex varies between 50% and 90%. The I_2III_4 supercomplex is of lower abundance and only becomes visible upon prolonged staining of BN gels. While the I_1III_2 and I_2III_4 supercomplexes are stable at high detergent to protein ratios, dimeric ATP synthase proved to be only stable at very low detergent concentrations. In contrast to yeast and mammals, cytochrome c oxidase (complex IV) of plant mitochondria did not form part of supercomplexes under all conditions applied. Instead, two different forms of monomeric complex IV are visible on BN gels, which are termed complex IVa and IVb (about 300 and 220 kD in *Arabidopsis*). Complex IVa includes at least one additional subunit, which is homologous to the Cox6b protein from mammals and yeast (Eubel et al., 2003).

Here we report a continuation of our efforts to carefully characterize the supermolecular structure of the OXPHOS system of plant mitochondria. Using highly active mitochondria isolated from freshly harvested potato tubers, five additional supercomplexes of about 850, 1,150, 1,850, 2,200, and 3,000 kD are visible on BN gels. All five protein complexes include complex IVa as shown by one-dimensional (1D) BN-PAGE, two-dimensional (2D) BN/SDS-PAGE, and 2D BN/BN-PAGE in combination with in-gel activity measurements for cytochrome c oxidase. The novel supercomplexes are of comparatively low abundance and have III_2IV_1 , III_2IV_2 , $I_1III_2IV_1$, $I_1III_2IV_2$, and $I_1III_2IV_4$ compositions. Slightly smaller versions of these protein complexes occur in potato stem mitochondria, which include complex IVb instead of complex IVa. Hence, the OXPHOS complexes of plant mitochondria partially form respirasomes, which most likely have important physiological and/or regulatory functions.

RESULTS

Identification of Novel Supercomplexes in Potato Mitochondrial Fractions

Previous investigations of digitonin-solubilized mitochondrial fractions from *Arabidopsis*, potato, bean, and barley by BN-PAGE led to the identification of I_1III_2 and I_2III_4 supercomplexes and dimeric ATP syn-

thase (Eubel et al., 2003) but did not reveal hints on complex IV-containing supercomplexes which were described for yeast and mammalian mitochondria (Schägger and Pfeiffer, 2000). However, these findings were based on mitochondrial isolations from etiolated seedlings (bean and barley), aged storage organs (potato), and suspension cell cultures (*Arabidopsis*), and it so far cannot be ruled out that mitochondrial preparations from other tissues or organs might allow the discovery of further supercomplexes. In an attempt to re-examine our previous findings, freshly harvested potato tubers were used for mitochondrial isolations and subsequent characterizations of digitonin-solubilized protein extracts on 1D BN gels (Fig. 1A). In parallel, mitochondrial preparations from 20-d-old etiolated potato stems were analyzed by this procedure (Fig. 1B).

All molecular masses of protein complexes given in this publication represent apparent molecular masses as deduced from separations on BN gels. These values should be considered with caution, because protein separations on BN gels do not exactly reflect calculated molecular masses. Some values for apparent molecular masses in this publication were corrected in comparison to the values given in Eubel et al. (2003): 600 kD for complex V (previously 550 kD), 350 kD for complex IVa (previously 300 kD), and 270 kD for complex IVb (previously 220 kD).

As expected, all known protein complexes of the OXPHOS system are visible on our gels (Fig. 1): complex I (approximately 1,000 kD), complex V (approximately 600 kD), and dimeric complex III (approximately 500 kD). Complex IVa (approximately 350 kD), complex IVb (approximately 270 kD), and complex II result in diffuse bands on the 1D gels but were clearly identified upon resolution of their subunits on second gel dimensions, which were carried out in the presence of SDS (data not shown). Finally, the I_1III_2 and I_2III_4 supercomplexes are visible. However, the occurrence of the I_2III_4 supercomplex and complex IVb was restricted to potato stem mitochondria. Dimeric ATP synthase could not be detected in both fractions, most likely because digitonin concentrations were too high.

Besides the known mitochondrial protein complexes and supercomplexes, additional complexes of low abundance showed up on our gels at approximately 850 kD and above 1,500 kD in both mitochondrial fractions (Fig. 1). To test if these protein supercomplexes include complex IV, in-gel activity measurements for cytochrome c oxidase were carried out. Indeed, five novel bands of approximately 850, 1,200, 1,850, 2,200, and 3,000 kD specifically were labeled in the potato tuber mitochondrial fraction (Fig. 1A). The 850- and 1,850-kD bands also are present in potato stem mitochondria and additionally two bands at approximately 770 and approximately 1,770 kD (Fig. 1). Identities of the newly discovered protein complexes were analyzed by 2D gel electrophoresis systems and are given below.

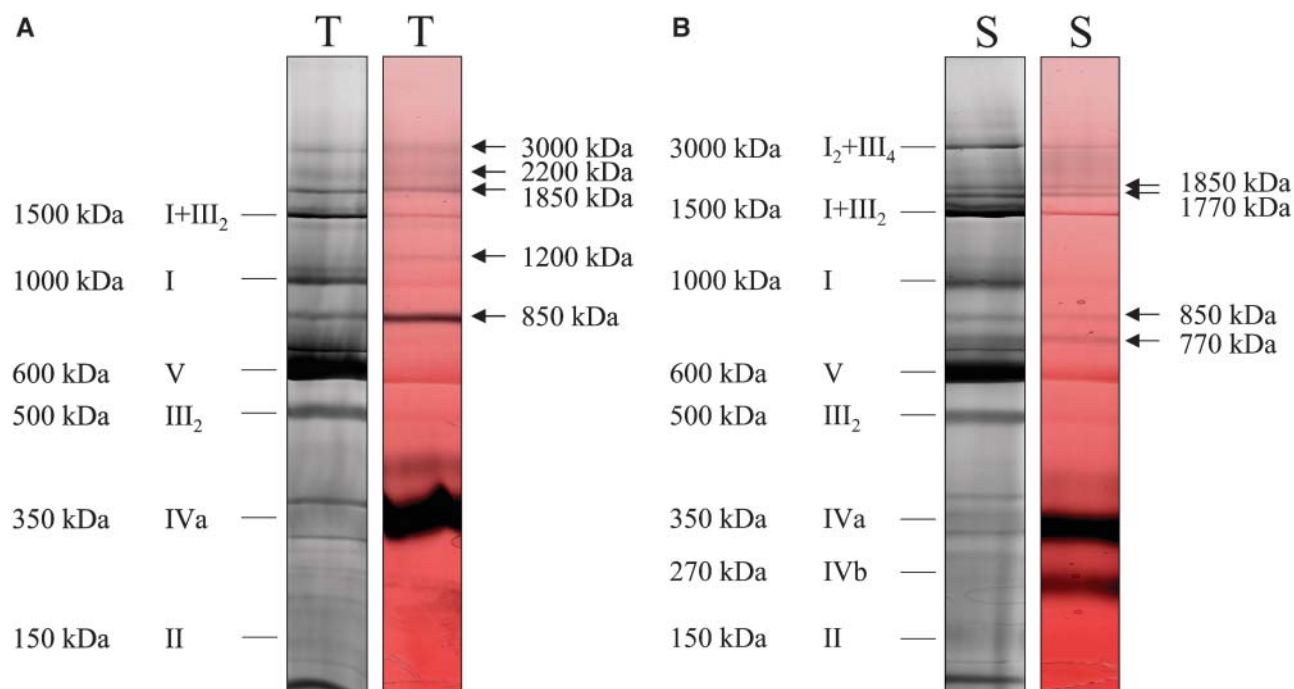


Figure 1. Identification of complex IV-containing supercomplexes in potato tuber (T) and stem (S) mitochondria. Protein complexes were solubilized by 5 g digitonin per g protein, separated by 1D BN-PAGE and either visualized by Coomassie staining (left gel strips) or by in-gel activity staining for cytochrome c oxidase (right gel strips). Activity stains are given in false-color mode to increase color contrast (red, Coomassie; black, enzyme activity). Molecular masses and identities of known protein complexes are indicated on the left side of the gels in Roman numerals (I, NADH dehydrogenase; II, succinate dehydrogenase; III, cytochrome c reductase; IVa and IVb, large and small form of cytochrome c oxidase; V, ATP synthase; I + III₂ and I₂ + III₄, supercomplexes of complexes I and III). Additional supercomplexes exhibiting cytochrome c oxidase activity are indicated by arrows.

Physiological State of Mitochondrial Fractions Used for Supercomplex Characterizations

Oxygen uptake measurements were carried out using a Clark-type oxygen electrode to ensure that mitochondria used for the characterization of the novel supercomplexes are intact and physiologically active (Fig. 2). Organelles prepared from freshly harvested potato tubers exhibited high oxygen consumption rates (on average 155 nmol O₂ min⁻¹ mg⁻¹ mitochondrial protein under state III conditions). In contrast, activity of potato stem mitochondria reproducibly was 40% to 50% lower under the same conditions. Mitochondria prepared from both organs had comparable state II respiration. Alternative respiration was low in mitochondrial isolations from potato stems and even lower in tuber mitochondria. We conclude that all mitochondrial fractions contained highly active organelles, but that mitochondria prepared from freshly harvested potato tubers exhibited highest state III respiration.

Optimization of Protein Solubilizations for Supercomplex Characterizations

To allow optimal visualization of the novel mitochondrial supercomplexes, isolated mitochondria

from potato tubers and stems were solubilized by varying concentrations of digitonin (Fig. 3). As previously reported (Eubel et al., 2003), 1 g digitonin per g mitochondrial protein only partially allowed solubilization of membrane-bound protein complexes as shown by resolutions on 1D BN gels. In contrast,

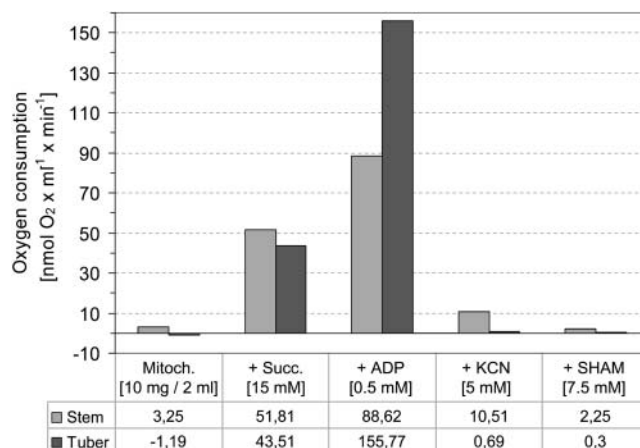


Figure 2. Oxygen consumption of isolated mitochondria from potato tubers and stems. Values are based on three independent mitochondrial preparations.

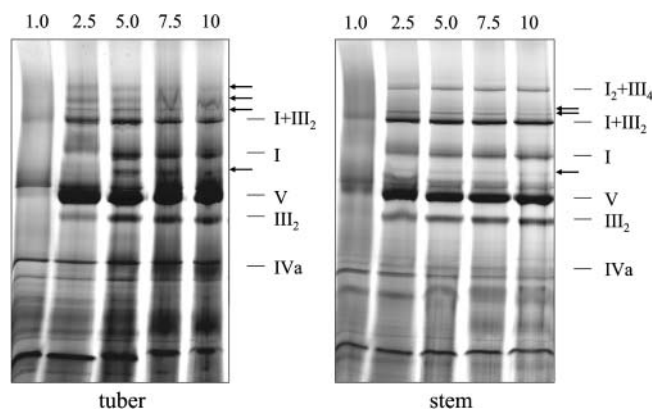


Figure 3. Resolution of mitochondrial protein complexes from potato mitochondria after solubilization using varying digitonin to protein ratios. Protein complexes were separated by 1D BN-PAGE and visualized by Coomassie staining. Detergent to protein ratios are given in g detergent per g mitochondrial protein. The OXPHOS complexes are designated by Roman numerals (see legend of Fig. 1). Unknown protein complexes are indicated by arrows.

solubilization of protein complexes and supercomplexes was very efficient between 2.5 and 10 g digitonin per g mitochondrial protein. Under these conditions, all known protein complexes and the newly discovered complexes of low abundance could be resolved. However, abundance of some supercomplexes decreased slightly in the presence of higher detergent to protein ratios. All further experiments were carried out with digitonin:protein ratios of 5 g/g.

Compositions of Newly Discovered Mitochondrial Supercomplexes

Two-dimensional BN/SDS-PAGE was carried out to characterize the subunit compositions of the novel mitochondrial protein supercomplexes (Fig. 4). High protein amounts had to be loaded onto the gels to overcome their low abundance and to obtain information on subunits of these supercomplexes. The 850-kD complex of potato tuber mitochondria contains subunits of complexes III and IV and most likely has III₂IV composition (Fig. 4A). The 1,200-kD complex could not be detected on our 2D gels. The 1,850-, 2,200-, and 3,000-kD complexes of potato tuber mitochondria all contain the subunits of the I₁III₂ supercomplex and additionally the Cox2 protein, which is the most dominant subunit of complex IV on BN gels (Fig. 4A). Further subunits of complex IV probably are present but could not be detected because they overlap with subunits of the complexes I and III on our gels. Due to low abundance, densitometric measurements of individual protein spots did not allow resolution of the stoichiometry of the protein complexes within these supercomplexes. However, based on the apparent molecular masses on the BN gels, the 1,850-, 2,200-, and 3,000-kD supercomplexes probably have I₁III₂IV₁, I₁III₂IV₂, and I₁III₂IV₄ compositions, which would be in

accordance with findings on respiratory supercomplexes in mammalian mitochondria (Schägger and Pfeiffer, 2000). We conclude that complex IV forms part of supercomplexes in potato tuber mitochondria. However, about 90% of complex IV was in monomeric state under the conditions applied (Fig. 4A).

Slightly different results were obtained upon resolution of mitochondrial protein complexes from potato stems by 2D BN/SDS-PAGE (Fig. 4B). First of all, about 50% of monomeric complex IV was not in the larger IVa (350 kD) but in the IVb form (270 kD), which could not be detected in the potato tuber mitochondrial fraction. Since the mitochondrial fractions from tubers and stems were treated equally, artificial generation of this smaller version of monomeric complex IV during mitochondrial isolations and/or BN-PAGE seems unlikely. As reported previously for Arabidopsis and bean, complex IVb lacks at least one 30-kD subunit, which was identified as being homologous to Cox6b proteins from yeast and mammals (Eubel et al., 2003). The 850- and 1,850-kD supercomplexes containing complex IV are also present in potato stem mitochondria and additionally two slightly smaller supercomplexes of 770 and 1,770 kD, which probably include complex IVb instead of complex IVa. The complex IV-containing 2,200- and 3,000-kD supercomplexes could not be found in mitochondrial isolations from potato stems. Instead, the 3,000-kD I₂III₄ supercomplex is present, which previously was described for Arabidopsis (Eubel et al., 2003).

Analysis of the Newly Discovered Supercomplexes by 2D BN/BN-PAGE

To further investigate the structure of the newly discovered complex IV-containing supercomplexes from potato, 2D gel electrophoreses were repeated using 2D BN/BN-PAGE (Schägger and Pfeiffer, 2000). This procedure is based on the separation of digitonin-solubilized protein complexes and supercomplexes on a first dimension BN-PAGE and subsequently a resolution of the separated supercomplexes on a second dimension BN-PAGE in the presence of dodecylmaltoside. Dodecylmaltoside is known to destabilize supercomplexes. Protein complexes and supercomplexes likewise stable in the presence of digitonin and dodecylmaltoside form a diagonal line on the resulting 2D gels, whereas supercomplexes destabilized by dodecylmaltoside dissociate into protein complexes of higher electrophoretic mobility.

2D BN/BN-PAGE of mitochondrial fractions from potato tuber (Fig. 5A) confirmed all results obtained by 2D BN/SDS-PAGE: the 850-kD supercomplex consists of complexes III and IV and the 1,850-, 2,200-, and 3,000-kD supercomplexes of complexes I, III, and IV. Separation of all these supercomplexes not only revealed occurrence of complex IVa but also presence of the smaller complex IVb. However, since monomeric complex IVb is absent in potato tuber mitochondrial fractions after digitonin solubilizations (Figs. 1A and

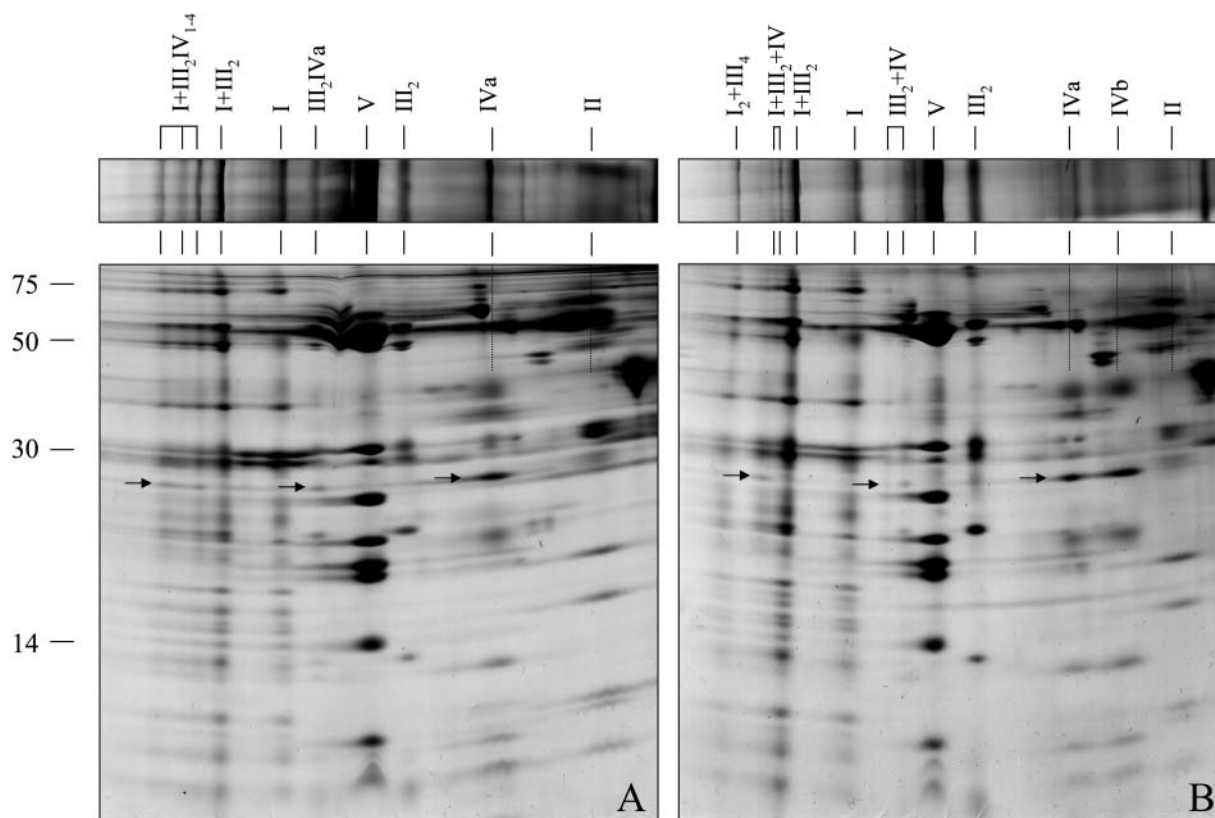


Figure 4. Two-dimensional resolution of mitochondrial protein complexes from potato tubers (A) and potato stems (B) by BN/SDS-PAGE. Mitochondrial proteins were solubilized by 5 g digitonin per g protein. Gels were Coomassie stained. Strips of corresponding 1D BN gels and identities of protein complexes and supercomplexes are given above the 2D gels. The numbers on the left indicate the molecular masses of standard proteins. Subunit II of cytochrome c oxidase is marked by arrows.

4A) but present after additional dodecylmaltoside treatment (Fig. 5A), this version of complex IV most likely is artificially generated during BN/BN-PAGE under the conditions applied. In contrast to 2D BN/SDS-PAGE, 2D BN/BN-PAGE allowed the analysis of the 1,200-kD supercomplex present in potato tuber mitochondria. Like the 850-kD complex, this supercomplex only contains the complexes III and IV and probably has a III_2IV_2 composition.

Analysis of mitochondrial fractions from potato stems by BN/BN-PAGE (Fig. 5B) also confirmed the findings obtained by 2D BN/SDS-PAGE: the 850- and 1,850-kD complexes include complexes III + IVa and I + III + IVa (complex IVa is partially converted into complex IVb as reported for mitochondria from potato tubers). The 770- and 1,770-kD complexes seem to have the same composition but most likely include complex IVb instead of complex IVa. The complex IV-containing 1,200-, 2,200-, and 3,000-kD supercomplexes of potato tuber mitochondria are absent, but a 3,000-kD I_2III_4 complex is present.

Interestingly, destabilization of the large complex IV-containing supercomplexes partially results in generation of the I_1III_2 but not of the III_2IV_{1-2} super-

complexes (Fig. 5, A and B). We conclude that interactions between the complexes I and III are stronger than interactions between complexes III and IV.

In-Gel Activity Measurements for Cytochrome c Oxidase in 2D BN/BN Gels

To increase sensitivity, a 2D BN-BN gel for potato stem mitochondria was repeated and stained by in-gel activity measurements for cytochrome c oxidase. This measurement was not possible after polymerization of the 1D BN gel stripe into the sample gel of a second gel dimension, most likely because N,N,N',N' -tetramethylethylenediamine (TEMED) and ammonium persulfate (APS) diffused into the gel stripe and destroyed enzymatic activities. However, fixation of the first gel dimension with agarose onto the second gel dimension proved to be compatible with this experimental approach. As shown in Figure 6, all previously made conclusions on complex IV-containing supercomplexes could be confirmed. Indeed, the 850- and 1,850-kD complexes include complex IVa, which partially dissociates into complex IVb in the presence of dodecylmaltoside. In contrast, the 770- and 1,770-kD

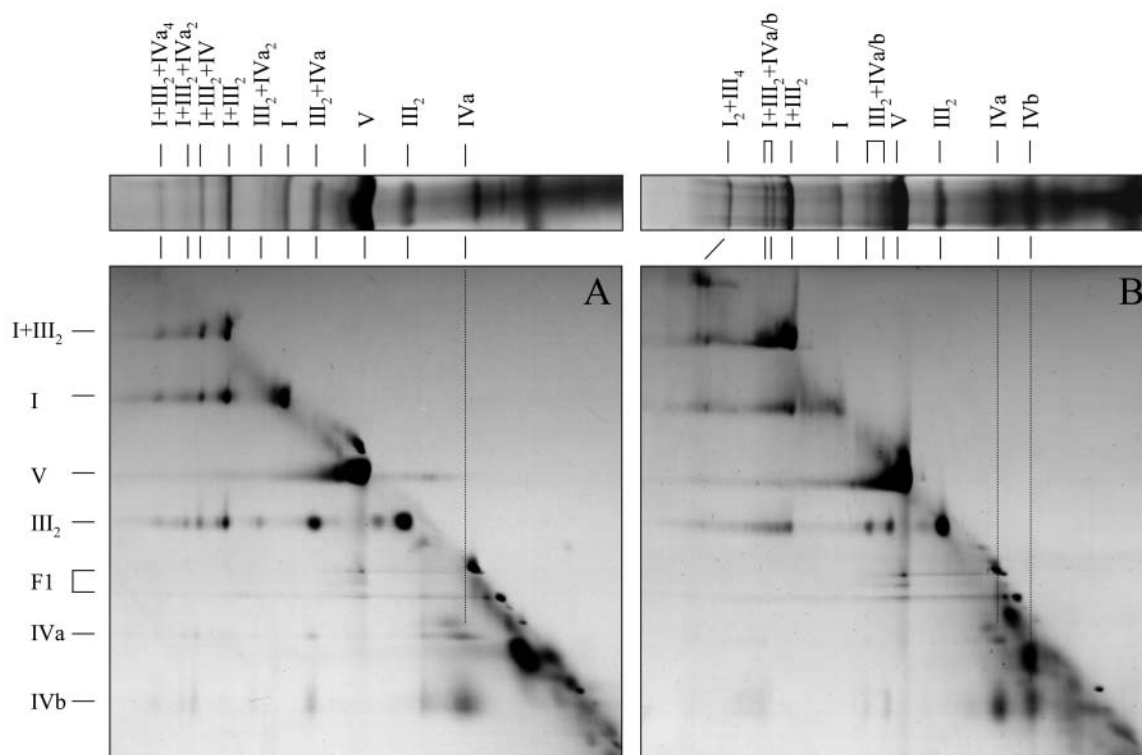


Figure 5. Two-dimensional resolution of mitochondrial protein complexes from potato tubers (A) and stems (B) by BN/PAGE. Mitochondrial proteins were solubilized by 5 g digitonin per g protein. Corresponding strips of 1D BN gels are shown above the 2D gels. Identities of the resolved protein complexes and supercomplexes are given above and to the left of the gels in Roman numerals.

complexes only contain the smaller IVb version of the cytochrome c oxidase complex (Fig. 6).

DISCUSSION

Structure of Respiratory Supercomplexes in Plants, Animals, and Fungi

Besides the previously described I_1III_2 and I_2III_4 supercomplexes and dimeric ATP synthase, potato tuber mitochondria contain five additional respiratory supercomplexes of about 850-, 1,200-, 1,850-, 2,200-, and 3,000-kD, which include complex IV. The 850- and 1,200-kD complexes only contain complexes III and IV and probably have III_2IV_1 and III_2IV_2 compositions; the other three complex IV-containing supercomplexes additionally include complex I and most likely have $I_1III_2IV_1$, $I_1III_2IV_2$, and $I_1III_2IV_4$ structures (Table I; Fig. 7). Similar supercomplexes were found in potato stem mitochondria. However, all newly described supercomplexes are of rather low abundance, because they only contain about 10% of total complex IV upon digitonin solubilizations and analysis on BN gels. Using comparable conditions, nearly 100% of yeast complex IV is associated with dimeric complex III (Cruciat et al., 2000; Schägger and Pfeiffer, 2000). In mammalian mitochondria—which include similar re-

spiratory supercomplexes than potato (Schägger and Pfeiffer, 2000)—most complex IV also is present in the monomeric form. However, there are some striking differences between mammalian and plant mitochondria with respect to respiratory supercomplexes: most complex I of bovine mitochondria forms part of the $I_1III_2IV_1$ complex, whereas in plants the I_1III_2 complex is of highest abundance. In fact the I_1III_2 complex seems to be of special stability in mitochondria from potato and other plants. Furthermore, a larger I_2III_4 supercomplex is present in plant mitochondria, which could not be described for mammalian mitochondria.

The $I_1III_2IV_4$ supercomplex was suggested to represent a basic unit for respiration in mammalian mitochondria termed respirasome (Schägger and Pfeiffer, 2000). Respirasomes are also present in plant mitochondria (Fig. 8). However, only very minor amounts of complex IV form part of respirasomes in mammals and plants (<5%). On the other hand, these structures might be much more abundant in vivo and only destabilized under the experimental conditions used for their characterization. Indeed, low digitonin to protein ratios seem to allow solubilization of higher quantities of respirasomes in potato (Fig. 3). Possibly in vivo even larger structures than respirasomes are formed by oligomerization of supercomplexes. In fact, some very weak protein bands can be seen above 3,000 kD on the gels shown in Figure 7. The I_2III_4 supercomplex of

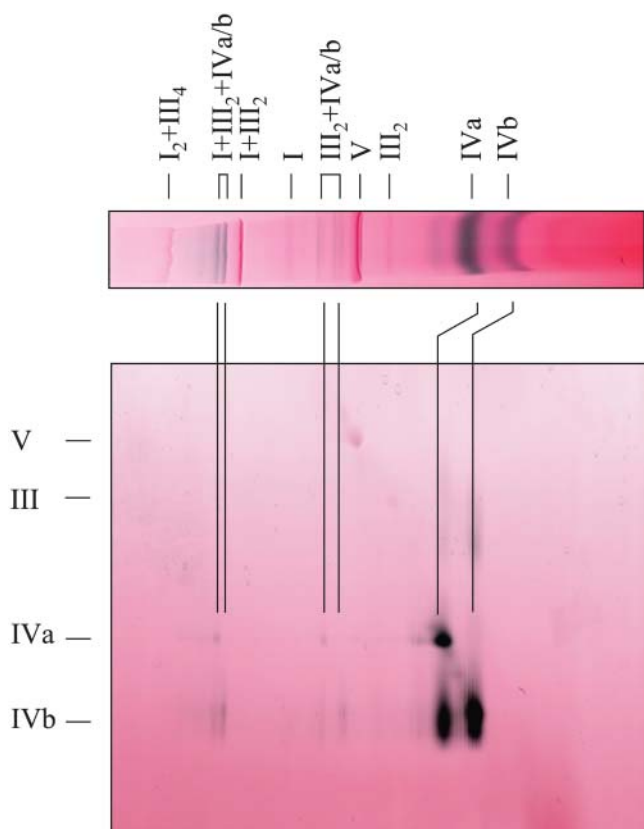


Figure 6. Identification of cytochrome c oxidase-containing supercomplexes of potato stem mitochondria by in-gel activity staining on 2D BN/BN gels. Mitochondrial proteins were solubilized by 5 g digitonin per g protein. A corresponding stripe of an activity-stained 1D BN gel is shown above the 2D gel. Identities of protein complexes and supercomplexes of the OXPHOS system from potato are given in Roman numerals. The activity stain is given in false-color mode to increase color-contrast (red, Coomassie; black, enzyme activity).

plant mitochondria could be a building block of these proposed oligomeric structures.

Are Some Supercomplexes Artificially Formed during Protein Solubilizations?

So far, formation of specific respiratory supercomplexes by artificial aggregation cannot be completely excluded but is highly unlikely for several reasons: (1) all complex IV-containing supercomplexes proved to be active by in-gel activity measurements for cytochrome c oxidase; (2) higher abundance of complex IV-containing supercomplexes in potato tuber mitochondria in comparison to potato stem mitochondria correlated with higher state III respiration; (3) the five OXPHOS complexes could theoretically form 10 different heterodimeric supercomplexes (composed of two different monomeric complexes); however, only heterodimeric I-III and III-IV complexes were observed, which represent the only meaningful associations with respect to the physiology of the

mitochondrial respiratory chain (besides II-III associations, which were not observed); and (4) several physiological data reviewed in the introduction section support specific supercomplex formations, like reconstitution, inhibitor titration, and flux control experiments (Hatefi and Rieske, 1967; Ragan and Heron, 1978; Boumans et al., 1998; Genova et al., 2003).

Assembly of Mitochondrial Supercomplexes

Currently the mechanisms for supercomplex formation in mitochondria are only poorly understood. In yeast cardiolipin proved to be essential for supercomplex stability. Based on studies with yeast mutants deficient in individual subunits of OXPHOS complexes, some proteins possibly forming part of supercomplex interphases could be defined (Pfeiffer et al., 2003). In potato the $I_1III_2IV_{1-4}$ complexes partly dissociate into the I_1III_2 supercomplex and monomeric complex VI, indicating that the complex I-III association is much stronger than the interaction between these complexes and complex IV. This disassembly order might represent reverse assembly stages.

Experimental Conditions for Supercomplex Characterizations in Plants

Digitonin solubilization and BN-PAGE proved to be a powerful tool for the investigation of mitochondrial supercomplexes from plants. However, visualization of individual supercomplexes in mitochondrial fractions of plants very much depends on various factors:

1. The digitonin to protein ratio. Five grams detergent per g protein proved to be optimal for the quantitative solubilization of most supercomplexes (Fig. 3). However, lower detergent to protein ratios significantly increase the amounts of some supercomplexes on BN gels. In fact, solubilization using 1 g digitonin per g protein seems to mainly

Table 1. Protein complexes and supercomplexes of the OXPHOS system in potato tuber and stem mitochondria

| Molecular Mass [kD] | Components | Proposed Composition | Occurrence | |
|---------------------|-------------|-----------------------|------------|------|
| | | | Tuber | Stem |
| 3,000 | I, III | $I_2 + III_4$ | — | x |
| 3,000 | I, III, IVa | $I_1 + III_2 + IVa_4$ | x | — |
| 2,200 | I, III, IVa | $I_1 + III_2 + IVa_2$ | x | — |
| 1,850 | I, III, IVa | $I_1 + III_2 + IVa_1$ | x | x |
| 1,770 | I, III, IVb | $I_1 + III_2 + IVb_1$ | — | x |
| 1,500 | I, III | $I_1 + III_2$ | x | x |
| 1,200 | III, IVa | $III_2 + IVa_2$ | x | — |
| 1,000 | I | I_1 | x | x |
| 850 | III, IVa | $III_2 + IVa_1$ | x | x |
| 770 | III, IVb | $III_2 + IVb_1$ | — | x |
| 600 | V | V_1 | x | x |
| 500 | III | III_2 | x | x |
| 350 | IVa | IVa_1 | x | x |
| 270 | IVb | IVb_1 | — | x |

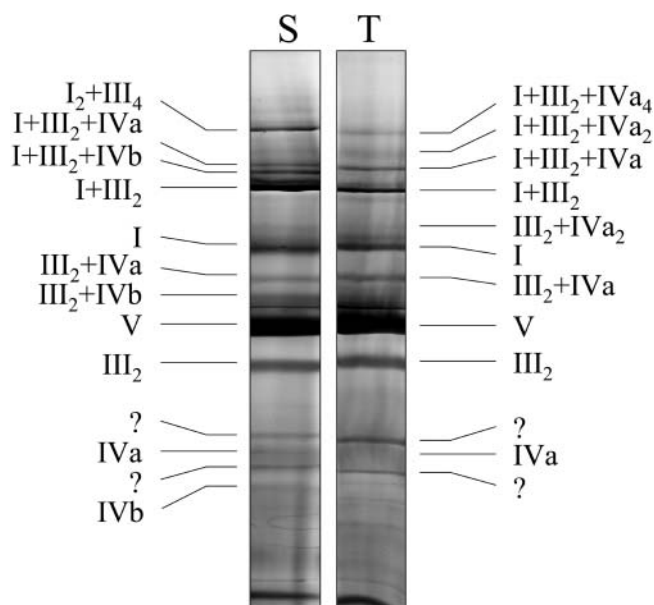


Figure 7. Identities of protein complexes and supercomplexes of the OXPHOS system in potato tubers (T) and stems (S) after separation by 1D BN-PAGE. Proteins were solubilized by 5 g digitonin per g protein. The gels were Coomassie stained. Identities of the protein complexes and supercomplexes are given by Roman numerals.

solubilize I_1III_2 and $I_1III_2IV_4$ supercomplexes (lane 1 of the gels in Fig. 3).

- The physiological state of the starting material for mitochondrial isolations. Freshly harvested potato tubers gave much better results concerning supercomplex visualization on BN gels than potato tubers stored for some weeks (data not shown). This most likely explains the absence of complex IV-containing supercomplexes of potato tubers in our previous investigations (however, some low amounts of the 850-kD III_2IV_1 supercomplex of potato mitochondria were overseen on the gel in Figure 4 in Eubel et al., 2003).
- The plant organs selected for mitochondrial preparations. Potato tubers and stems slightly differ with respect to occurrence of individual supercomplexes. Overall, stem mitochondria contained less complex IV-containing respiratory supercomplexes. Furthermore, complex IV partially is present in the smaller IVb form in stem mitochondria. So far it cannot be distinguished whether these differences reflect tissue-specific variations or rather represent differences in physiological states of the organelles of these two tissues. Possibly etiolated seedlings or suspension cell cultures are not optimal as starting material for the characterization of labile interactions of mitochondrial protein complexes.

We speculate that complex IV-containing supercomplexes are present in other plants depending on the physiological state of the organs used for mitochondrial isolations but might be of low abun-

dance. Indeed, mitochondria prepared from Arabidopsis leaves revealed some very small amounts of complex IV-containing supercomplexes (H. Eubel and H.-P. Braun, data not shown).

Functional Relevance of the Monomeric Cytochrome c Oxidase Complexes IVa and IVb of Plant Mitochondria

Monomeric complex IV is represented by two different forms in plants (Jansch et al., 1996; Eubel et al., 2003; Sabar et al., 2003), the larger of which includes at least one additional protein subunit homologous to the Cox6b protein of fungi and mammals. The smaller complex IVb is generated by dissociation of the larger complex IVa in the presence of dodecylmaltoside. However, digitonin-solubilized mitochondrial fractions from potato tubers and stems differ considerably with respect to complex IVb, which is absent in digitonin extracts of potato tuber mitochondria (Fig. 4A) but represents about 50% of monomeric complex IV of stem mitochondria (Fig. 4B). Furthermore, supercomplexes of potato stem mitochondria seem to partially include the smaller IVb form of cytochrome c oxidase. Complex IVb is enzymatically active, but specific activity is significantly reduced in comparison to complex IVa (compare Figs. 1 and 4/5). At the same time, state III respiration of stem mitochondria is reduced as shown by oxygen consumption measurements of isolated mitochondria (Fig. 2). We therefore speculate that there might be distinct physiological roles of the two forms of cytochrome c oxidase in plants. Possibly plant mitochondria contain a pool of partially inactivated complex IV which rapidly can be activated upon association with the Cox6b protein.

An even larger probably monomeric form of complex IV can be seen by activity stainings of BN gels in the 400-kD range (Fig. 1). This version of complex IV is not visible on Coomassie-stained BN gels (Fig. 4), and its identity so far remains a mystery. Possibly this form of complex IV is a chaperone-bound assembly intermediate of cytochrome c oxidase. Similarly, a slightly larger form of complex III (550 instead of 500 kD) can be seen on the 2D BN/BN gel in Figure 5, which is invisible on the corresponding first gel dimension and

The respirasome

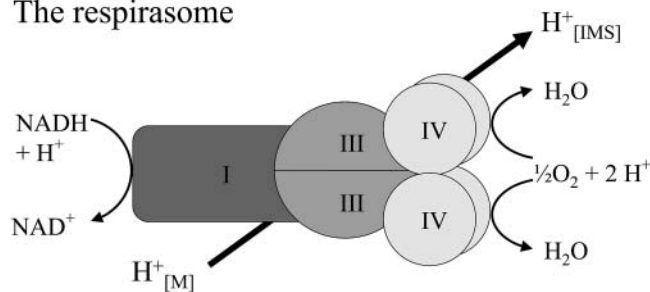


Figure 8. Structure and function of the respirasome in mitochondria. [M], Matrix; [IMS], mitochondrial intermembrane space.

might also represent a chaperone-bound form of this respiratory complex. Further experiments have to be carried out to explain these observations.

Outlook

Plant mitochondria exhibit several special features in comparison to mitochondria from heterotrophic eukaryotes. Due to the presence of numerous alternative oxidoreductases, the respiratory chain of plant mitochondria is very much branched (Vanlerberghe and McIntosh, 1997; Rasmusson et al., 1999; Moller, 2001; Moore et al., 2003). Furthermore, the protein complexes of the respiratory chain include plant-specific protein subunits (Braun and Schmitz, 1995; Eubel et al., 2003; Heazlewood et al., 2003a, 2003b; Millar et al., 2003). For instance, the two subunits of the mitochondrial processing peptidase form an integral part of complex III in plants (Braun et al., 1992b; Eriksson et al., 1994). As a consequence, respiratory supercomplexes most likely have special roles in plant mitochondria, e.g. in regulating access of alternative respiratory oxidoreductases to their substrates during respiration. Experiments to address these questions are under way in our laboratory.

MATERIALS AND METHODS

Isolation of Mitochondria from Potato Tubers and Stems

Freshly harvested potato (*Solanum tuberosum* var. *cilena*) tubers were purchased directly from a local farmer. Half of them were stored in the cold (4°C); the other half were planted into soil and grown in the dark at 20°C. Mitochondria were prepared from stored tubers and from etiolated potato stems after 20 d. Plant material (200 g) was homogenized at 4°C using a Waring blender for 3 × 5 s, filtrated through four layers of muslin, and subsequently organelles were purified by differential centrifugations and Percoll density gradient centrifugation as outlined previously (Braun et al., 1992a). Isolated mitochondria were either directly analyzed by gel electrophoresis or stored at -80°C.

Sample Preparation for Gel Electrophoresis

Mitochondrial samples of 500 µg (50 µg mitochondrial protein) were sedimented by centrifugation for 10 min at 14,000g, resuspended in 50 µL of digitonin solution (1%–10% digitonin/30 mM HEPES/150 mM potassium acetate/10% glycerol), and incubated for 20 min at 0°C. Afterwards samples were centrifuged for 10 min at 18,000g. Finally supernatants were supplemented with 5 µL of a Coomassie Blue solution (5% Coomassie Blue/750 mM aminocaproic acid) and directly loaded onto BN gels.

Gel Electrophoresis

BN-PAGE was carried out as described previously (Schägger, 2001b). Gels were destained by incubation in fixing solution (40% [v/v] methanol, 10% [v/v] acetic acid) overnight and subsequently stained with Coomassie colloidal (Neuhoff et al., 1985, 1990). Alternatively, strips of BN gels were transferred horizontally onto second gel dimensions. 2D BN/SDS-PAGE was carried out according to Schägger (2001b) and 2D BN/BN-PAGE according to Schägger and Pfeiffer et al. (2000). However, 1D gel strips for BN/BN-PAGE were fixed by 1.5% agarose onto the second gel dimension and not by direct polymerization into the stacking gel. This modification proved to be essential for subsequent in-gel activity measurements.

In-Gel Activity Stains for Cytochrome c Oxidase

In-gel activity of cytochrome c oxidase was measured according to Zerbetto et al. (1997) and Jung et al. (2000): 1D BN or 2D BN/BN gels were incubated in 20 mM phosphate buffer (pH 7.4), 1.0 mg/mL DAB (3,3'-diaminobenzidine), 24 units/mL catalase, 1 mg/mL cytochrome c, and 75 mg/mL sucrose. Reactions were carried out at room temperature for 1 h (1D gels) or overnight (2D gels). Staining was stopped by fixing the gels in 45% methanol/10% acetic acid. Finally, gels were scanned. To increase color contrast images were false-colored for Coomassie (red) and catalase activity (black) by Photoshop software (Adobe Systems, Mountain View, CA).

Oxygen Electrode Measurements

Oxidative phosphorylation of all mitochondrial preparations was analyzed using a Clark-type oxygen electrode with a reaction chamber of 2 mL (Oxygraph, Hansatech, Norfolk, England). Oxygen consumption of 10 mg mitochondria (1 mg mitochondrial protein) in reaction buffer (0.3 M mannitol, 10 mM K₂HPO₄ (pH 7.2), 10 mM KCl, 5 mM MgCl₂) was measured after supplementation of succinate (15 mM), ADP (5 mM), KCN (5 mM), and salicylhydroxamic acid (SHAM; 7.5 mM). Mitochondrial oxygen consumption was calculated in nmol ΔO₂ min⁻¹ mg protein⁻¹.

ACKNOWLEDGMENTS

We thank Dagmar Lewejohann for expert technical assistance and Leila Matter, Dennis Kahlisch, and Prof. Dr. Udo Schmitz for critical reading of the manuscript.

Received December 19, 2003; returned for revision January 13, 2004; accepted January 13, 2004.

LITERATURE CITED

- Arnold I, Pfeiffer K, Neupert W, Stuart RA, Schägger H (1998) Yeast mitochondrial F₁F₀-ATP synthase exists as a dimer: identification of three dimer-specific subunits. *EMBO J* **17**: 7170–7178
- Arnold I, Pfeiffer K, Neupert W, Stuart RA, Schägger H (1999) ATP synthase of yeast mitochondria: isolation of subunit j and disruption of the ATP18 gene. *J Biol Chem* **274**: 36–40
- Berry EA, Trumpower BL (1985) Isolation of ubiquinol oxidase from *Paracoccus denitrificans* and resolution into cytochrome bc₁ and cytochrome c-a₃ complexes. *J Biol Chem* **260**: 2458–2467
- Boumans H, Grivell LA, Berden JA (1998) The respiratory chain in yeast behaves as a single functional unit. *J Biol Chem* **273**: 4872–4877
- Braun HP, Emmermann M, Kruft V, Schmitz UK (1992a) Cytochrome c₁ from potato: a protein with a presequence for targeting to the mitochondrial intermembrane space. *Mol Gen Genet* **231**: 217–225
- Braun HP, Emmermann M, Kruft V, Schmitz UK (1992b) The general mitochondrial processing peptidase from potato is an integral part of cytochrome c reductase of the respiratory chain. *EMBO J* **11**: 3219–3227
- Braun HP, Schmitz UK (1995) The bifunctional cytochrome c reductase/processing peptidase complex from plant mitochondria. *J Bioenerg Biomembr* **27**: 423–436
- Cruciat CM, Brunner S, Baumann F, Neupert W, Stuart RA (2000) The cytochrome bc₁ and cytochrome c oxidase complexes associate to form a single supracomplex in yeast mitochondria. *J Biol Chem* **275**: 18093–18098
- Eriksson AC, Sjöling S, Glaser E (1994) The ubiquinol cytochrome c oxidoreductase complex of spinach leaf mitochondria is involved in both respiration and protein processing. *Biochim Biophys Acta* **1186**: 221–231
- Eubel H, Jänsch L, Braun HP (2003) New insights into the respiratory chain of plant mitochondria. Supercomplexes and a unique composition of complex II. *Plant Physiol* **133**: 274–286
- Fowler LR, Hatefi Y (1961) Reconstitution of the electron transport system III. Reconstitution of DPNH oxidase, succinic oxidase, and DPNH succinic oxidase. *Biochem Biophys Res Commun* **5**: 203–208
- Fowler LR, Richardson HS (1963) Studies on the electron transfer system. *J Biol Chem* **238**: 456–463

- Genova ML, Bianchi C, Lenaz G** (2003) Structural organization of the mitochondrial respiratory chain. *Ital J Biochem* **52**: 58–61
- Hatefi Y** (1978) Reconstitution of the electron-transport system of bovine heart mitochondria. *Methods Enzymol* **53**: 48–54
- Hatefi Y, Haavik AG, Jurtschuk P** (1961) Studies on the electron transport system. XXX. DPNH-cytochrome c reductase I. *Biochim Biophys Acta* **52**: 106–118
- Hatefi Y, Rieske JS** (1967) The preparation and properties of DPNH-cytochrome c reductase (complex I-III of the respiratory chain). *Methods Enzymol* **10**: 225–231
- Heazlewood JA, Howell KA, Millar AH** (2003b) Mitochondrial complex I from Arabidopsis and rice: orthologs of mammalian and yeast components coupled to plant-specific subunits. *Biochim Biophys Acta* **1604**: 159–169
- Heazlewood JL, Whelan J, Millar AH** (2003a) The products of the mitochondrial ORF25 and ORFB genes are F_0 components of the plant F_1F_0 ATP synthase. *FEBS Lett* **540**: 201–205
- Iwasaki T, Matsuura K, Oshima T** (1995) Resolution of the aerobic respiratory system of the thermoacidophilic archaeon, *Sulfolobus* sp. Strain 7. I. The archaeal terminal oxidase supercomplex is a functional fusion of respiratory complexes III and IV with no c-type cytochromes. *J Biol Chem* **270**: 30881–30892
- Jansch L, Kruff V, Schmitz UK, Braun HP** (1996) New insights into the composition, molecular mass and stoichiometry of the protein complexes of plant mitochondria. *Plant J* **9**: 357–368
- Jung C, Higgins CMJ, Xu Z** (2000) Measuring the quantity and activity of mitochondrial electron transport chain complexes in tissues of central nervous system using blue native polyacrylamide gel electrophoresis. *Anal Biochem* **286**: 214–223
- Millar AH, Mittova V, Kiddle G, Heazlewood JL, Bartoli CG, Theodoulou FL, Foyer CH** (2003) Control of ascorbate synthesis by respiration and its implications for stress responses. *Plant Physiol* **133**: 443–447
- Moller IM** (2001) Plant mitochondria and oxidative stress: electron transport, NADPH turnover, and metabolism of reactive oxygen species. *Annu Rev Plant Physiol Plant Mol Biol* **52**: 561–591
- Moore CS, Cook-Johnson RJ, Rudhe C, Whelan J, Day DA, Wiskich JT, Soole KL** (2003) Identification of AtNDI1, an internal non-phosphorylating NAD(P)H dehydrogenase in Arabidopsis mitochondria. *Plant Physiol* **133**: 1968–1978
- Neuhoff V, Stamm R, Eibl H** (1985) Clear background and highly sensitive protein staining with Coomassie Blue dyes in polyacrylamide gels: a systematic analysis. *Electrophoresis* **6**: 427–448
- Neuhoff V, Stamm R, Pardowitz I, Arold N, Ehrhardt W, Taube D** (1990) Essential problems in quantification of proteins following colloidal staining with Coomassie Brilliant Blue dyes in polyacrylamide gels, and their solution. *Electrophoresis* **11**: 101–117
- Niebisch A, Bott M** (2003) Purification of a cytochrome bc_1 - aa_3 supercomplex with quinol oxidase activity from *Corynebacterium glutamicum*. Identification of a fourth subunit of cytochrome aa_3 oxidase and mutational analysis of diheme cytochrome c_1 . *J Biol Chem* **278**: 4339–4346
- Pfeiffer K, Gohil V, Stuart RA, Hunte C, Brandt U, Greenberg ML, Schagger H** (2003) Cardiolipin stabilizes respiratory chain supercomplexes. *J Biol Chem* **278**: 52873–52880
- Ragan CI, Heron C** (1978) The interaction between mitochondrial NADH-ubiquinone oxidoreductase and ubiquinol-cytochrome c oxidoreductase. *Biochem J* **174**: 783–790
- Rasmusson AG, Svensson AS, Knoop V, Grohmann L, Brennicke A** (1999) Homologues of yeast and bacterial rotenone-insensitive NADH dehydrogenases in higher eukaryotes: two enzymes are present in potato mitochondria. *Plant J* **20**: 79–87
- Sabar M, Gagliardi D, Balk J, Leaver CJ** (2003) ORFB is a subunit of F(1)F(O)-ATP synthase: insight into the basis of cytoplasmic male sterility in sunflower. *EMBO Rep* **4**: 1–6
- Schagger H** (2001a) Respiratory chain supercomplexes. *IUBMB Life* **52**: 119–128
- Schagger H** (2001b) Blue-native gels to isolate protein complexes from mitochondria. *Methods Cell Biol* **65**: 231–244
- Schagger H** (2002) Respiratory supercomplexes of mitochondria and bacteria. *Biochim Biophys Acta* **1555**: 154–159
- Schagger H, Pfeiffer K** (2000) Supercomplexes in the respiratory chains of yeast and mammalian mitochondria. *EMBO J* **19**: 1777–1783
- Sone N, Sekimachi M, Kutoh E** (1987) Identification and properties of a quinol oxidase supercomplex composed of a bc_1 complex and cytochrome oxidase in the thermophilic bacterium PS3. *J Biol Chem* **262**: 15386–15391
- Vanlerberghe GC, McIntosh L** (1997) Alternative oxidase: from gene to function. *Annu Rev Plant Physiol Plant Mol Biol* **48**: 703–734
- Zerbetto E, Vergani L, Dabbeni-Sala F** (1997) Quantitation of muscle mitochondrial oxidative phosphorylation enzymes via histochemical staining of blue native polyacrylamide gels. *Electrophoresis* **18**: 2059–2064
- Zhang M, Mileykovskaya E, Dowhan W** (2002) Gluing the respiratory chain together. Cardiolipin is required for supercomplex formation in the inner mitochondrial membrane. *J Biol Chem* **277**: 43553–43556



Proteomic approach to characterize the supramolecular organization of photosystems in higher plants

Jesco Heinemeyer^a, Holger Eubel^a, Dirk Wehmhöner^b, Lothar Jänsch^b,
Hans-Peter Braun^{a,*}

^a *Institut für Angewandte Genetik, Universität Hannover, Herrenhäuser Str. 2, D-30419 Hannover, Germany*

^b *Gesellschaft für Biotechnologische Forschung, Mascheroder Weg 1, 38124 Braunschweig, Germany*

Received 11 January 2004; received in revised form 16 April 2004

Abstract

A project to investigate the supramolecular structure of photosystems was initiated, which is based on protein solubilizations by digitonin, protein separations by Blue native (BN)–polyacrylamide gel electrophoresis (PAGE) and protein identifications by mass spectrometry (MS). Under the conditions applied, nine photosystem supercomplexes could be described for chloroplasts of *Arabidopsis*, which have apparent molecular masses between 600 and 3200 kDa on BN gels. Identities of the supercomplexes were determined on the basis of their subunit compositions as documented by 2D BN/SDS–PAGE and BN/BN–PAGE. Two supercomplexes of 1060 and ~1600 kDa represent dimeric and trimeric forms of photosystem I (PSI), which include tightly bound LHCI proteins. Compared to monomeric PSI, these protein complexes are of low abundance. In contrast, photosystem II mainly forms part of dominant supercomplexes of 850, 1000, 1050 and 1300 kDa. According to our interpretation, these supercomplexes contain dimeric PSII, 1–4 LHCII trimers and additionally monomeric LHCII proteins. The 1300-kDa PSII supercomplex (containing four LHCII trimers) is partially converted into the 1000-kDa PSII supercomplex (containing two LHCII trimers) in the presence of dodecylmaltoside on 2D BN/BN gels. Analyses of peptides of the trypsinated 1300-kDa PSII supercomplex by mass spectrometry allowed to identify known subunits of the PSII core complex and additionally LHCII proteins encoded by eight different genes in *Arabidopsis*. Further application of this experimental approach will allow new insights into the supermolecular organization of photosystems in plants.

© 2004 Elsevier Ltd. All rights reserved.

Keywords: *Arabidopsis thaliana*; Proteomics; Blue-native polyacrylamide gel electrophoresis; Mass spectrometry; Chloroplasts; Supercomplexes; Photosystem I; Photosystem II; b₆f complex; Light harvesting complex

1. Introduction

The photosynthetic electron transport system in chloroplasts is based on the presence of three protein complexes termed photosystem I (PSI), photosystem II (PSII) and cytochrome b₆f complex (b₆f complex). Furthermore, light harvesting complexes (LHCI and LHCII) are associated with the two photosystems to increase the rates of their primary photoreactions. Linear photosynthetic electron transport involves PSII, the

b₆f complex and PSI, and catalyses reduction of ferredoxin, thioredoxin or NADP⁺ by water oxidation in the light. At the same time, linear electron transport causes formation of a proton gradient across the thylakoid membrane which is the prerequisite for “photophosphorylation”, the light-driven phosphorylation of ADP by the ATP synthase complex. Besides linear electron transport, PSI, the b₆f complex and possibly in addition a NADH dehydrogenase complex can carry out cyclic electron transport which only contributes to the proton gradient across the thylakoid membrane but does not lead to reduction or oxidation of external compounds.

Extensive knowledge is available on the structures of the two photosystems and the b₆f complex. Using X-ray

* Corresponding author. Tel.: +49-5117-622674; fax: +49-5117-623608.

E-mail address: braun@genetik.uni-hannover.de (H.-P. Braun).

crystallography, structures of PSI from *Synechococcus elongatus* and pea (Jordan et al., 2001; Ben-Shem et al., 2003), the structures of the b_6f complex from the cyanobacterium *Mastigocladus laminosus* and *Chlamydomonas* (Stroebel et al., 2003; Kurisu et al., 2003) and the structures of photosystem II from the cyanobacteria *Synechococcus elongates* and *Prochloron didemni* (Zouni et al., 2001; Bibby et al., 2003) were resolved. Furthermore, the structure of LHCII was solved by electron crystallography (Kühlbrandt et al., 1994; Liu et al., 2004).

In contrast, the supermolecular organization of protein complexes involved in photosynthesis is less understood. However, fascinating insights into supercomplexes formed by photosystems were obtained by electron microscopy combined with computer image analyses: in cyanobacteria, the photosystem I forms trimers (Kruip et al., 1993), which are surrounded by an antenna ring formed of 18 copies of the antenna protein CP43' under iron-deficiency conditions (Boekema et al., 2001a; Bibby et al., 2001). In contrast, PSI from *Chlamydomonas* and higher plants is monomeric and asymmetrically binds LHCI proteins on one side of the complex (Boekema et al., 2001b; Germano et al., 2002; Kargul et al., 2003). Four to 14 LHCI proteins are estimated to be associated with individual PSI complexes in plants. In contrast, photosystem II is dimeric in cyanobacteria and higher plants (Boekema et al., 1995). It is associated with monomeric and trimeric LHCII proteins. There are 2 × three binding sites for LHCII trimers at dimeric PSII, which are termed S-, M- and L-positions according to their binding strength for LHCII trimers (S, strong; M, moderate and L, loose) (Boekema et al., 1998a,b, 1999a,b; Yakushevskaya et al., 2001). According to a nomenclature proposed by Boekema et al. (1998a), which was extended by Yakushevskaya et al. (2001), the PSII supercomplexes are termed by the binding positions of dimeric PSII core complex (C_2) filled with LHCII trimers (C_2S_2 : dimeric PSII associated with two LHCII trimers at the S position, $C_2S_2M_2$: dimeric PSII associated with two LHCII trimers at the S position and two LHCII trimers at the M position, and so on). Additionally, monomeric LHCII proteins bind to the photosystem II supercomplexes (Boekema et al., 1999b). However, the structures of PSII supercomplexes in plants are still a matter of debate and possibly will not be precisely resolved until availability of X-ray crystallography data.

Recently, a novel electrophoretic strategy was developed to characterize supercomplexes of the respiratory chain in mitochondria, which is based on protein solubilization using mild non-ionic detergents and separation of the solubilized protein complexes by Blue-native (BN) gel electrophoresis (Schägger and Pfeiffer, 2000). Using this approach, distinct supercomplexes, formed of respiratory complexes I + III, III + IV and I + III + IV,

could be described for mitochondria from yeast, mammals and plants (Schägger and Pfeiffer, 2000; Schägger, 2001a, 2002; Zhang et al., 2002; Eubel et al., 2003, 2004; Pfeiffer et al., 2003).

BN-PAGE was previously employed to characterize photosystems in higher plants (Kügler et al., 1997). Using protein solubilizations with dodecylmaltoside, monomeric photosystems I and II, dimeric b_6f complex and trimeric LHCII complex from spinach, tobacco and potato chloroplasts were resolved by BN-PAGE (Kügler et al., 1997, 1998; Singh et al., 2000). Additionally, photosystem II supercomplexes could be described by this experimental approach in pea and tobacco (Thidholm et al., 2002; Surosa et al., 2004). Recently, protein solubilization by digitonin was combined with BN-PAGE and allowed to visualize supercomplexes of photosystems in *Chlamydomonas* (Rexroth et al., 2003).

Here, we describe a proteomic approach to characterize photosystem supercomplexes of *Arabidopsis* using digitonin solubilizations, BN-PAGE and mass spectrometry. Nine photosystem supercomplexes are visible in the molecular mass range between 600 and 3200 kDa. The identities of these supercomplexes were analysed by 2D BN/SDS-PAGE and 2D BN/BN-PAGE combined with mass spectrometry. Two supercomplexes of 1060 and ~1600 kDa represent dimeric and trimeric PSI. Four supercomplexes of 850, 1000, 1150 and 1300 kDa represent dimeric PSII, which are associated with a varying number of LHCII trimers and probably are of C_2S_1 (or C_2M_1), C_2S_2 (or $C_2S_1M_1$ or C_2M_2), $C_2S_2M_1$ (or $C_2S_1M_2$) and $C_2S_2M_2$ structures. Trypsination of the $C_2S_2M_2$ supercomplex, separation of the generated peptides by liquid chromatography (LC) and analysis of the separated peptides by electrospray tandem mass spectrometry (ESI-MS/MS) allowed to identify more than 20 different subunits of PSII, including eight different LHCII proteins. Applications of this experimental approach are discussed.

2. Results

2.1. Identification of chloroplast supercomplexes of *Arabidopsis* by 1D Blue-native PAGE

Digitonin proved to be a very suitable detergent for the solubilization and stabilization of supercomplexes of *Arabidopsis* mitochondria (Eubel et al., 2003, 2004). We therefore started a project to systematically investigate protein complexes of chloroplasts using this detergent. To determine the optimal detergent-protein ratio for supercomplex solubilization, isolated *Arabidopsis* chloroplasts were treated with different digitonin concentrations and subsequently analysed by 1D Blue-native PAGE. Detergent-protein ratios of 1 g/g or below only

allowed insufficient solubilization of chloroplast protein complexes, whereas ratios of 1.5 g/g or higher gave very good results (data not shown). Therefore, all further experiments were carried out using 1.5 g digitonin per g protein. Under these conditions, 14 protein complexes can be resolved on 1D Blue-native gels (Fig. 1). Due to the presence of Coomassie dyes during gel electrophoresis, protein bands become visible without staining (Fig. 1A). However, subsequent staining of 1D gels by Coomassie blue significantly increased the visibility of protein complexes (Fig. 1B).

To determine the apparent molecular masses of the resolved chloroplast protein complexes, mitochondrial protein complexes from *Arabidopsis* were separated in parallel by 1D BN-PAGE (Fig. 1). Five complexes could be detected, which were identified by comparison to gels published previously (Eubel et al., 2003): the F₁ part of the mitochondrial ATP synthase complex (390 kDa), dimeric complex III (500 kDa), monomeric complex V (600 kDa), monomeric complex I (1000 kDa) and a supercomplex formed of dimeric complex III and complex I (1500 kDa). Using these mitochondrial protein complexes as a molecular mass standard, the sizes of chloroplast complexes could be determined to lie in the molecular mass range between 110 and 3200 kDa (Table 1). [However, sizes above 1500 kDa and below 390 kDa

Table 1

Apparent molecular masses of digitonin solubilized mitochondrial and chloroplast protein complexes on BN gels^a

| Complex | Molecular mass (kDa) |
|-----------------------------------|----------------------|
| <i>Mitochondria</i> | |
| Supercomplex I + III ₂ | 1500 |
| Complex I | 1000 |
| Complex V | 600 |
| Complex III ₂ | 500 |
| mF ₁ -ATP synthase | 390 |
| <i>Chloroplasts</i> | |
| A | ~3200 |
| B | ~2200 |
| C | ~1600 |
| D | 300 |
| E | 1150 |
| F | 1060 |
| G | 1000 |
| H | 850 |
| I | 650 |
| PSI + LHCI | 530 |
| PSII | ~370 |
| cpF ₁ -ATP synthase | ~350 |
| Dimeric b ₆ f complex | ~300 |
| LHCII ₃ | ~110 |

^aThe designations of the complexes correspond to Fig. 1.

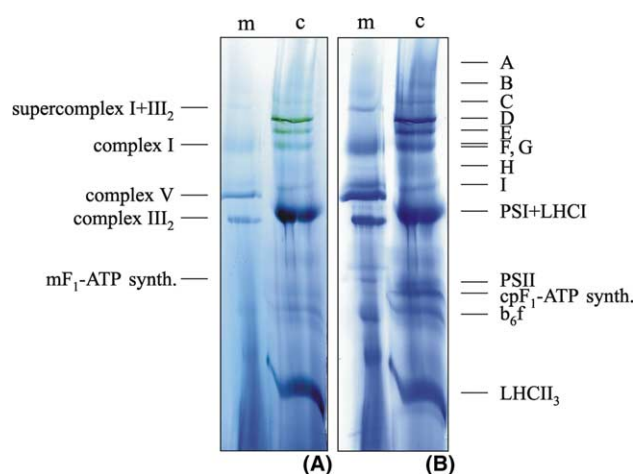


Fig. 1. Separation of mitochondrial (m) and chloroplast (c) protein complexes and supercomplexes of *Arabidopsis* by 1D BN-PAGE. Proteins were solubilized by 1.5 g/g digitonin. (A) Unstained gel; (B) Coomassie-stained gel. Identities of mitochondrial protein complexes are given to the left and identities of known chloroplast protein complexes to the right (mF₁-ATP synth., F₁ part of the mitochondrial ATP synthase complex; complex III₂, dimeric cytochrome *c* reductase; complex V, mitochondrial ATP synthase; complex I, NADH dehydrogenase; supercomplex I + III₂, supercomplex formed of dimeric cytochrome *c* reductase and NADH dehydrogenase; LHCII₃, trimeric light harvesting complex II; b₆f, cytochrome b₆f complex; cpF₁-ATP synth., F₁-part of plastidic ATP synthase; PSII, photosystem II; PSI, photosystem I; LHCI, light harvesting complex I). Unknown chloroplast protein complexes are designated by capital letters (A–I). Apparent molecular masses of all protein complexes are given in Table 1.

should be considered with caution, because they are not covered by the mitochondrial molecular mass standard. Furthermore, separations by Blue-native PAGE not necessarily reflect exactly calculated molecular masses as reported before (Schägger, 2001b).]

Identities of the chloroplast protein complexes smaller than 530 kDa can be predicted by comparison to previous separations of dodecylmaltoside solubilized chloroplast protein complexes from spinach and tobacco on the basis of 1D BN-PAGE (Kügler et al., 1997). In contrast, nine protein complexes between 650 and ~3200 kDa are of unknown identity (termed complexes A–I in Fig. 1).

2.2. Characterization of chloroplast supercomplexes by 2D BN/SDS-PAGE

One-dimensional Blue-native gels were combined with SDS-PAGE to elucidate identities of the resolved protein complexes on the basis of subunit compositions. For comparison, protein solubilizations were carried out with digitonin or dodecylmaltoside, because 2D BN/SDS gels of dodecylmaltoside-treated chloroplast protein complexes from spinach and tobacco were characterized previously in detail (Kügler et al., 1997). Indeed, 2D BN/SDS gels of dodecylmaltoside solubilized protein complexes of *Arabidopsis* chloroplasts very much resemble gels shown before for spinach and tobacco (Fig. 2A, Kügler et al., 1997). The largest protein

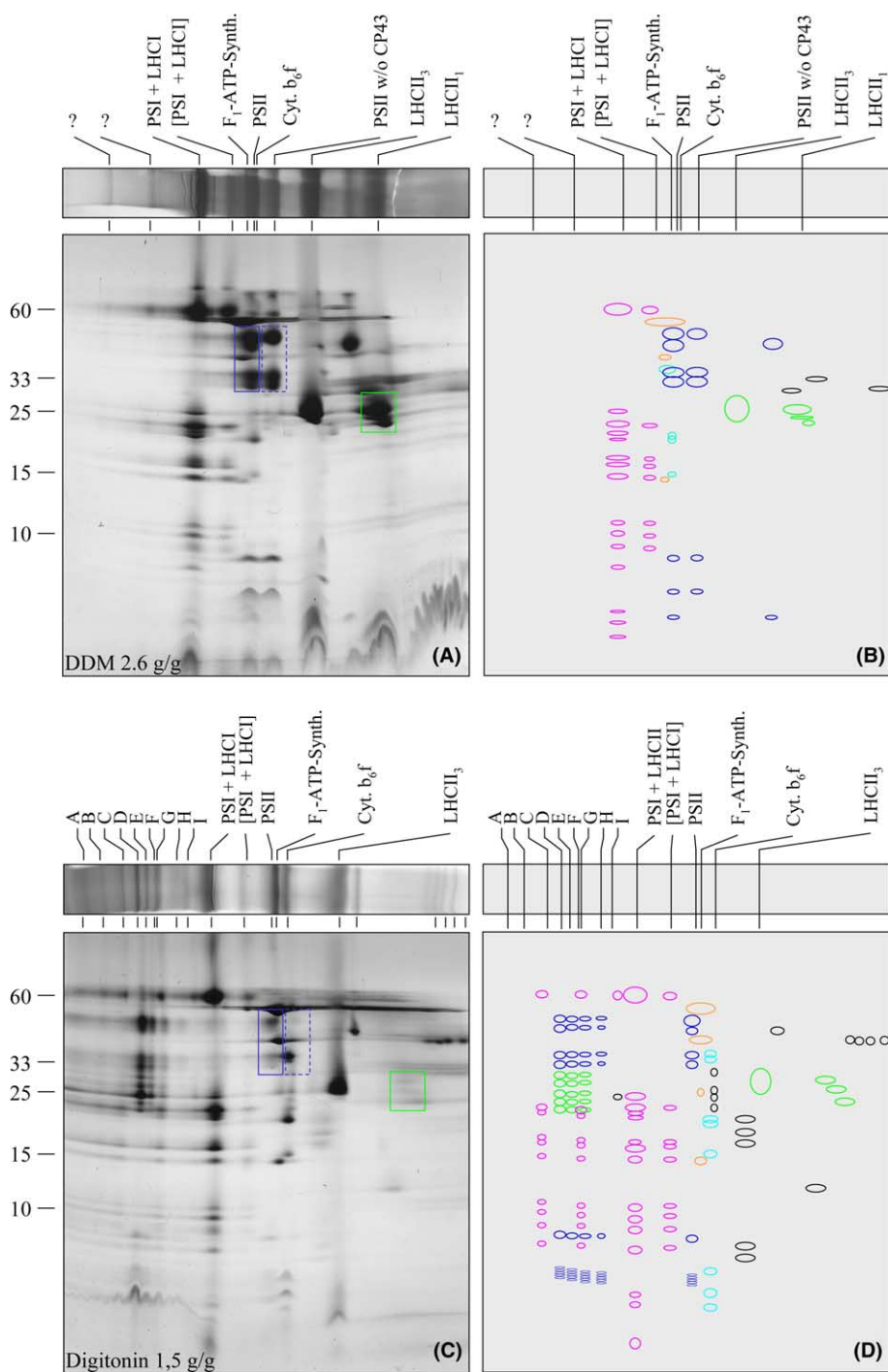


Fig. 2. Two-dimensional resolution of chloroplast protein complexes and supercomplexes of *Arabidopsis* by BN/SDS-PAGE. (A) Proteins were solubilized by 2.6 g/g dodecylmaltoside (B: scheme of the gel in A); (C) Proteins were solubilized by 1.5 g/g digitonin (D: scheme of the gel in C). Gels were Coomassie-stained. Identities of protein complexes are given above the gels (for designations see legend of Fig. 1; [PSI + LHCI], subcomplex of PSI + LHCI lacking some LHCI proteins). Subunits of individual protein complexes are given in colours on the scheme to facilitate recognition of protein complexes (purple: subunits of photosystem I or LHCI; blue: subunits of photosystem II; light blue: subunits of the b_6f complex; orange: subunits of F_1 -ATP synthase; green: subunits of LHCI; black: subunits of unknown protein complexes. The numbers to the right refer to molecular masses of standard proteins (in kDa). Proteins boxed in green on the gels in A and C indicate monomeric LHCI and proteins boxed in blue the CP47/CP43/D2 and D1 proteins of monomeric photosystem II, which are well visible upon dodecylmaltoside solubilization but hardly detectable upon digitonin solubilization.

complex represents photosystem I together with LHCI proteins (530 kDa). A smaller version of this complex, which lacks some LHCI proteins in the 20–25 kDa

range, has slightly higher electrophoretic mobility. The four protein complexes in the 250–400 kDa range represent the F_1 part of plastidic ATP synthase, monomeric

PSII, a subcomplex of monomeric PSII lacking the CP43 protein and dimeric b_6f complex. Furthermore, trimeric and monomeric LHCII are resolved at ~ 110 and ~ 30 kDa.

In contrast, 2D BN/SDS gels of digitonin solubilized chloroplast proteins from *Arabidopsis* considerably differ in comparison to gels of dodecylmaltoside solubilized proteins of the same fraction (Fig. 2C). Most strikingly, a significant amount of protein forms part of supercomplexes larger than 530 kDa. At the same time, proteins and protein complexes below 530 kDa are significantly reduced: (i) monomeric LHCI is hardly detectable, (ii) trimeric LHCII is reduced, (iii) the subcomplex of PSII lacking CP43 is absent, (iv) monomeric PSII is very much reduced and (v) the subcomplex of monomeric PSI lacking LHCI proteins is less abundant.

The subunit compositions on 2D BN/SDS gels allow to identify the newly described supercomplexes (Fig. 2C): The 1300-, 1150-, 1000- and 850-kDa complexes D, E, G and H represent PSII supercomplexes containing decreasing amounts of LHCII proteins and the ~ 1600 , 1060 and 650 kDa complexes C, F and I represent PSI supercomplexes associated with LHCI. PSII supercomplexes are very abundant, whereas the PSI supercomplexes are of lower abundance. Identity of the 3200 and 2200 kDa supercomplexes A and B is unclear, because their subunits are hardly detectable on the 2D gel in Fig. 2C, but more likely represent PSI supercomplexes than PSII supercomplexes.

2.3. Characterization of chloroplast supercomplexes by 2D BN/BN-PAGE

To better understand the composition of the supercomplexes A–I, a novel 2D gel electrophoresis procedure was applied, which employs BN-PAGE in the presence of digitonin in the first gel dimension and BN-PAGE in the presence of low dodecylmaltoside concentrations in the second dimension (Schägger and Pfeiffer, 2000). All protein complexes and supercomplexes likewise stable in the presence of both detergents are positioned on a diagonal line on the resulting 2D gels, whereas supercomplexes destabilized in the presence of dodecylmaltoside are dissected into protein complexes of higher electrophoretic mobility.

BN/BN-PAGE of digitonin solubilized chloroplast protein complexes from *Arabidopsis* (Fig. 3) supports the results obtained by BN/SDS-PAGE. Most PSI is present in a monomeric form which includes LHCI proteins (530 kDa). The PSI supercomplexes C and F (~ 1600 and 1060 kDa) are of low abundance and partially dissected into monomeric PSI on the BN/BN gels. Therefore, these complexes most likely represent trimeric and dimeric forms of PSI. The 650-kDa supercomplex of PSI seems to represent monomeric PSI associated with LHCII. In contrast to the three PSI supercomplexes, the 1000-kDa PSII supercomplex proved to be stable during BN/BN-PAGE. Furthermore, the 1300- and 1150-kDa supercomplexes of PSII are partially dissected into the 1000-kDa supercomplex and LHCII trimers on the

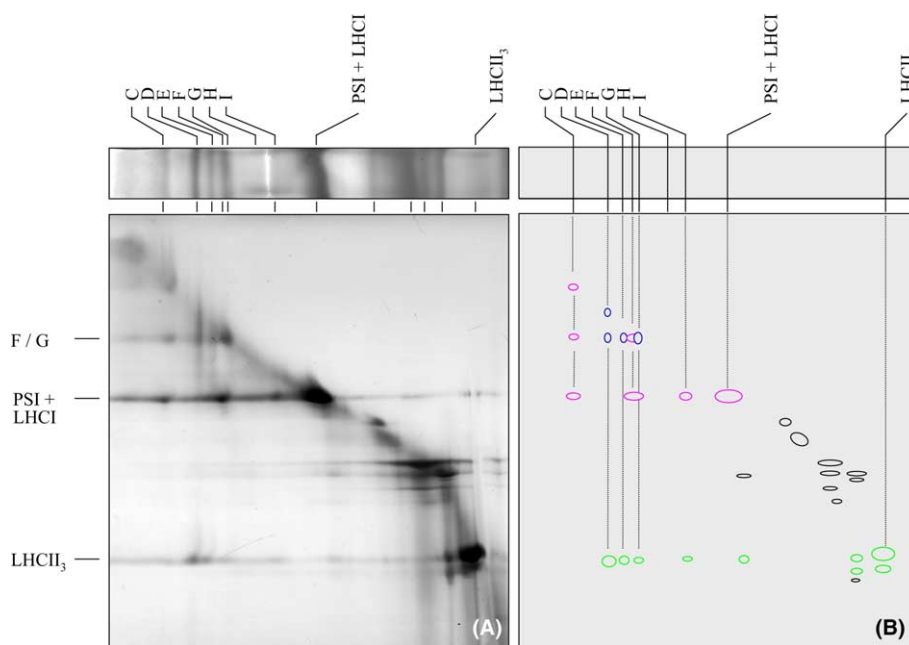


Fig. 3. Two-dimensional resolution of chloroplast protein complexes and supercomplexes of *Arabidopsis* by BN/BN-PAGE. Proteins were solubilized by 1.5 g/g digitonin. (A) Coomassie-stained gel; (B) scheme of the gel in (A). Identities of protein complexes are given above and to the left of the gel (for designations see legend of Fig. 1) and by a colour code (see legend of Fig. 2).

Table 2
Identified subunits of the 1300-kDa PSII supercomplex D^a

| No. | Gene | Identity | Score |
|-----|-----------|---------------------------------|-------|
| 1. | psbB | CP47 subunit of PSII | 509 |
| 2. | At4g10340 | CP26 subunit of PSII (Lhcb5) | 432 |
| 3. | At1g15820 | CP24 subunit of PSII (Lhcb6) | 348 |
| 4. | psbC | CP43 subunit of PSII | 262 |
| 5. | At5g66570 | 33 kDa subunit of OEC | 253 |
| 6. | At3g08940 | CP29 subunit of PSII (Lhcb4.1) | 244 |
| 7. | psbA | D1 subunit of PSII | 244 |
| 8. | At5g01530 | CP29 subunit of PSII (Lhcb4.2) | 240 |
| 9. | At2g05070 | LHCII antenna protein (Lhcb2.2) | 204 |
| 10. | At3g50820 | 33 kDa subunit of OEC | 201 |
| 11. | At1g29910 | LHCII antenna protein (Lhc1) | 199 |
| 12. | At2g34430 | LHCII antenna protein (Lhcb1) | 189 |
| 13. | At1g31330 | putative subunit III of PSI | 165 |
| 14. | At3g47470 | CP29 subunit of PSII (Lhcb4.3) | 150 |
| 15. | psbD | D2 subunit of PSII | 144 |

^a Identifications are based on LC–MS/MS.

second gel dimension (Fig. 3). The 850-kDa PSII supercomplex, which is of lower abundance (Fig. 1), was not detectable on the BN/BN gels.

2.4. Identification of the subunits of the 1300-kDa PSII supercomplex D by mass spectrometry

The 1300-kDa PSII supercomplex is of very high abundance, comprises more than 50% of total PSII and includes the largest amounts of LHCII proteins. In order to precisely define the subunits present in this supercomplex, a protein band representing this supercomplex was cut out of a 1D BN gel and analysed by mass spectrometry. Peptides generated by trypsination of the supercomplex were separated by LC and subsequently peptides were identified by tandem mass spectrometry as described in Section 4. Thirty different proteins could unambiguously be matched to specific gene products encoded by the *Arabidopsis* genome (The Arabidopsis Genome Initiative, 2000). Depending on the number of peptides identified per gene product, identified proteins have MASCOT scores between 35 and 509. At least 14 of the 15 identified proteins with the highest MASCOT scores (>150) encode subunits of PSII or LHCII (Table 2): the CP47, CP43, D1 and D2 proteins, two isoforms of the 33 kDa subunit of the oxygen evolving complex and eight different LHCII proteins. Further subunits of the PSII supercomplex were also unambiguously identified but have lower MASCOT scores (<100), e.g., the PsbL, PsbH proteins and the α - and β -subunit of cytochrome b_{559} (data not shown). The identified LHCII subunits exhibit sequence similarity to LHCII proteins from other organisms and can be assigned to five of the six subclasses which were defined for the LHCII protein family (termed Lhcb1–Lhcb6). However, assignments are partially difficult, because more than 30 genes of *Arabidopsis* encode LHC

proteins, which have very similar amino acid sequences (The Arabidopsis Genome Initiative, 2000).

3. Discussion

3.1. Protein supercomplexes in chloroplasts

Digitonin not only is a very suitable detergent for the solubilization and stabilization of supercomplexes from mitochondria, but also proved to be a powerful tool for supercomplex characterization in chloroplasts. In combination with BN–PAGE, nine photosystem supercomplexes can be resolved. Four of these represent PSII supercomplexes, three PSI supercomplexes and two are of so far unknown identity. Mitochondria were shown to contain heteromeric supercomplexes, which comprise more than one type of protein complex (Schägger and Pfeiffer, 2000; Eubel et al., 2003). In contrast, all described chloroplast protein supercomplexes contain only one type of photosystem, which is associated with light harvesting complexes. However, this result is not unexpected because the two photosystems are known to be localized in different areas of thylakoid membranes, PSI mainly in unstacked and PSII mainly in stacked membrane regions. The cytochrome b_6f complex, which always is dimeric for functional reasons, and the ATP synthase complex were not part of supercomplexes under all conditions applied. In contrast, mitochondrial ATP synthase forms dimers and the mitochondrial bc_1 complex forms supercomplexes with cytochrome c oxidase and/or NADH dehydrogenase.

3.2. PSI supercomplexes

About 90% of PSI is in monomeric state after solubilization using dodecylmaltoside or digitonin and sep-

aration by BN-PAGE (Figs. 1–3). In the presence of either detergent, it forms a band at 530 kDa and includes LHCI proteins. These data are very much in line with the results published for the crystallized PSI from pea, which has a molecular mass of 525 kDa and includes two tightly bound LHCI dimers (Ben-Shem et al., 2003). A minor form of PSI on the 1D BN gels is slightly smaller and seems to lack some LHCI proteins. This form of PSI is more abundant in the presence of dodecylmaltoside, indicating that it probably is formed by degradation of PSI + LHCI during solubilization. Furthermore, upon digitonin solubilization, about 10% of PSI forms part of three supercomplexes of 650, 1060, ~1600 kDa (Fig. 2C; very low amounts of the 1060- and 1600-kDa PSI supercomplexes are also visible upon dodecylmaltoside solubilization on BN gels; Fig. 2A). The two larger PSI supercomplexes most likely represent trimeric and dimeric forms of PSI + LHCI, because their molecular masses exceed the one of monomeric PSI by factor 2 or 3 and because they both are partially dissected into monomeric PSI complexes on 2D BN/BN gels (Fig. 3). Dimeric and trimeric PSI were previously described for higher plants, but found to be of low abundance (Boekema et al., 2001b). However, it is speculated that these supercomplexes possibly are artificially formed during solubilization, because image analyses of EM data revealed irregular interactions of the monomers and because of theoretical considerations on the basis of the crystal structure of pea PSI (Boekema et al., 2001b; Ben-Shem et al., 2003). On the other side, there are no hints for other artificial supercomplex formations on BN gels between any of the known chloroplast protein complexes under the conditions applied. Therefore, the occurrence of dimeric and trimeric PSI complexes in higher plants can currently not be excluded.

The 650 kDa complex includes PSI, LHCI proteins and additionally another protein component, which dissociates on the second dimension of BN/BN gels and co-migrates with trimeric LHCII (Fig. 3). It previously was reported that phosphorylated forms of LHCII are detached from PSII and transferred to PSI to regulate light distribution between the two photosystems in chloroplasts (Lunde et al., 2000).

3.3. PSII supercomplexes

Monomeric PSII is very abundant on BN gels upon dodecylmaltoside solubilization, but hardly detectable after treatment of chloroplast fractions with digitonin. Furthermore, monomeric LHCII is nearly absent after digitonin treatment, trimeric LHCII is reduced and a subcomplex of dimeric PSII lacking the CP43 protein, which clearly is visible after dodecylmaltoside solubilizations on BN gels, is absent. Instead, about 90% of PSII in digitonin treated fractions forms part of the four

supercomplexes of 850, 1000, 1150 and 1300 kDa, the latter of which is most abundant.

The apparent molecular mass of monomeric PSII on BN gels differs slightly upon dodecylmaltoside and digitonin solubilizations: in dodecylmaltoside fractions it migrates faster than the F_1 ATP synthase, whereas in digitonin fractions it migrates slower. Indeed, for unknown reasons, the apparent molecular mass of monomeric PSII is rather high in the presence of digitonin and lies in the range of 370 kDa. We speculate that the 850, 1000, 1150 and 1300 kDa supercomplexes represent dimeric PSII supercomplexes associated with one, two, three or four LHCII trimers and additional monomeric LHCII proteins. A dimeric structure of PSII was previously shown by EM (Boekema et al., 1995), X-ray crystallography (Zouni et al., 2001; Bibby et al., 2003) and genetic investigations (Swiatek et al., 2001). Furthermore, dimeric PSII was shown to be associated with 1–4 trimeric LHCII complexes and additional monomeric LHCII proteins by image analyses of EM data (Boekema et al., 1999b; Yakushevska et al., 2001). There are $2 \times$ three binding sites for LHCII trimers in higher plants, which differ with respect to their binding strength for LHCII trimers and which were designated S, M and L positions as given in Section 1. For *Arabidopsis*, C_2S , $C_2S_2/C_2S_1M_1/C_2M_2$, $C_2S_2M_1/C_2S_1M_2$ and $C_2S_2M_2$ complexes could be described (Yakushevska et al., 2001). The presence of 850, 1000, 1150 and 1300 kDa PSII supercomplexes on BN gels nicely corresponds to the EM data. In fact, these four supercomplexes comprise increasing amounts of chlorophyll, as visible in Fig. 1A. The size difference of 150 kDa between the individual PSII supercomplexes can be explained by one LHCII trimer (about 110 kDa) and additionally 1–2 monomeric LHCII proteins. Indeed it was reported previously that binding of LHCII trimers to dimeric PSII is preceded/accompanied by binding of distinct LHCII monomers (Boekema et al., 1999b).

Interestingly, the 1300-kDa supercomplex, which probably has $C_2S_2M_2$ composition, is the most abundant PSII supercomplex in digitonin solubilized fractions, whereas the 1000-kDa C_2S_2 (or $C_2S_1M_1/C_2M_2$) complex is the most stable PSII supercomplex which is not dissected during BN/BN-PAGE (Fig. 3).

PSII supercomplexes were not visible on BN gels upon dodecylmaltoside solubilizations under the conditions applied (Fig. 2B), most likely because this detergent destabilized these supramolecular structures. However, PSII supercomplexes could be described at lower dodecylmaltoside concentrations (Boekema et al., 1995). They also were detected previously on 1D BN gels representing minor forms of PSII complexes in pea (Thidholm et al., 2002). Furthermore, similar protein complexes are visible on 2D BN/SDS gels of digitonin solubilized chloroplast fractions from *Chlamydomonas* (Rexroth et al., 2003). Table 3 summarizes our data on

Table 3
Composition of digitonin solubilized chloroplast supercomplexes resolved on BN gels

| Supercomplex ^a | Apparent molecular mass (kDa) | Identity and proposed composition ^b |
|---------------------------|-------------------------------|--|
| A | ~3200 | ? |
| B | ~2200 | ? |
| C | ~1600 | [PSI + LHCI] ₃ |
| D | 1300 | [PSII] ₂ : C ₂ S ₂ M ₂ |
| E | 1150 | [PSII] ₂ : C ₂ S ₂ M ₁ or C ₂ S ₁ M ₂ |
| F | 1060 | [PSI + LHCI] ₂ |
| G | 1000 | [PSII] ₂ : C ₂ S ₂ or C ₂ S ₁ M ₁ or C ₂ M ₂ |
| H | 850 | [PSII] ₂ : C ₂ S ₁ or C ₂ M ₁ |
| I | 650 | [PSI + LHCI] ₁ + LHCI |
| | 530 | [PSI + LHCI] ₁ |

^a Designations of the supercomplexes corresponds to Figs. 1–3 and Table 1.

^b Nomenclature of PSII supercomplexes according to Boekema et al. (1998a) and Yakushevskaya et al. (2001).

the nine chloroplast supercomplexes from *Arabidopsis* visible on BN gels and their proposed composition.

3.4. Outlook

BN-PAGE originally was developed to characterize the protein complexes of the respiratory chain (Schägger and von Jagow, 1991) but also is a very powerful tool for investigations on chloroplast protein complexes (Kügler et al., 1997). In combination with digitonin solubilizations, supercomplexes can be stabilized for both cellular compartments. The availability of efficient protein identification procedures, which are based on mass spectrometry, now offers new strategies to characterize supercomplexes. So far, the exact composition of PSII supercomplexes with respect of LHCI proteins is largely unknown, because their structures are too labile to allow X-ray crystallography. Analysis by mass spectrometry now allowed to identify eight different LHCI proteins to be present in the 1300-kDa PSII supercomplex of *Arabidopsis*. The experimental strategy described in our study will allow to give new insights into the subunit compositions of labile supermolecular structures in plant organelles.

4. Experimental

4.1. Isolation of chloroplasts and mitochondria from *Arabidopsis*

Arabidopsis thaliana var. Columbia was grown for about 3 weeks at 24–26 °C/10,000 lux at long day conditions. Starting material for chloroplast preparations were about 200 g of plants (leaves and stems). Tissue was homogenized in extraction buffer (330 mM mannitol, 30 mM Hepes, 2 mM EDTA, 3 mM MgCl₂ and 0.1% (w/v) BSA, pH 7.8) by a Waring blender for 3 × 3 s and filtered through four layers of gaze. Subsequently, chloroplasts were sedimented by centrifugation for 3 min at 2000g/4 °C and purified by Percoll density gradient centrifugation

(40% [v/v] Percoll in extraction buffer) for 30 min at 30,000g/4 °C. Intact chloroplasts are represented by the lowest green band of the gradients. They are removed by a Pasteur pipette, supplemented with 4 volumes of extraction buffer without BSA and sedimented by centrifugation for 10 min at 2500g/4 °C. Finally chloroplasts are resuspended in extraction buffer without BSA at a protein concentration of 15 mg/ml, frozen by liquid nitrogen and stored at –80 °C. Mitochondria from *A. thaliana* cell suspension cultures were isolated as outlined previously (Werhahn et al., 2001).

4.2. Solubilization of membrane proteins

Purified organelles (750 µg protein) were sedimented by centrifugation for 10 min at 1250g (chloroplasts) or 14,300g (mitochondria) at 4 °C and resuspended in one of the two following buffers:

- 80 µl “digitonin solubilization buffer” (30 mM Hepes, pH 7.4, 150 mM potassium acetate, 10% glycerol, 2 mM PMSF and 1.5% [w/v] digitonin [Fluka, Buchs, Switzerland]);
- 95 µl “dodecylmaltoside solubilization buffer” (750 mM aminocaproic acid, 50 mM Bis-Tris, pH 7.0, 0.5 mM EDTA, 1 mM PMSF and 2% (w/v) dodecylmaltoside [Roche, Mannheim, Germany]).

Samples solubilized with digitonin were incubated for 20 min on ice and afterwards centrifuged for 30 min at 15,000g/4 °C, whereas samples solubilized with dodecylmaltoside were directly centrifuged at the same conditions. Supernatants were supplemented with 20 µl Coomassie-blue solution (5% [w/v] Coomassie-blue in 750 mM aminocaproic acid) and directly loaded onto Blue-native gels.

4.3. Gel electrophoresis

One-dimensional BN-PAGE and 2D BN/SDS-PAGE were carried out as described by Schägger (2001b) and 2D BN/BN-PAGE as outlined by Schägger and Pfeiffer (2000).

4.4. Protein identifications by mass spectrometry (LC–MS/MS)

A band of a 1D Blue-native gel containing the 1300-kDa PSII supercomplex D was excised, sliced in 1-mm³ cubes, and incubated once in 200 µl of 50 mM NH₄HCO₃ and twice in 200 µl of 50% acetonitril/25 mM NH₄HCO₃ for 30 min. Subsequently, the protein-containing gel pieces were dried in a SpeedVac concentrator, rehydrated in 2 µg/ml sequencing-grade modified porcine trypsin (Promega, Madison, WI) in 50 mM NH₄HCO₃ and incubated overnight at 37 °C. The resulting peptides were collected by two successive extractions with 50 mM NH₄HCO₃ and 50% acetonitrile/0.5% formic acid. Extracts were pooled in a microcentrifuge tube and lyophilized in a SpeedVac concentrator.

For LC–MS analysis the peptides were resuspended in 0.1% trifluoroacetic acid. About 10 µl of each sample was injected into the Ultimate Nano-HPLC (LC Packings/Dionex) and separated on a C₁₈ reversed-phase column (75 µm, 150 mm, PepMap, LC Packings), using a 120-min gradient (0–60% B (A = 0.1% formic acid; B = 60% acetonitrile/0.1% formic acid) and a flowrate of 200 nl/min. Doubly and triply charged peptide-ions were automatically selected by the MassLynx software and fragmented in a Q-TOF2 mass spectrometer (Micro-mass, Manchester, UK).

MS/MS-fragmentation data were analysed using an internal MASCOT-server (Matrix Science) (Perkins et al., 1999) searching against the NCBI-*A. thaliana* database. For the identification of proteins, the MASCOT default significance criteria were used, which means that if the score for a particular match exceeds the significance level, there is less than a 1 in 20 chance that the observed match is a random event. In the case of the *A. thaliana* database this significance threshold score was set to >34 by Mascot. The protein scores in the result table (Table 2) were generated cumulatively by the corresponding peptide scores.

It should be noted that not all proteins can be identified by this experimental approach, because some proteins lack basic amino acids and therefore are not fragmented by trypsin or because trypsin fragmentation in some cases only gives rise to hydrophobic peptides, which easily are lost during peptide purification prior to mass spectrometry.

Acknowledgements

We wish to thank Dagmar Lewejohann for the cultivation of *Arabidopsis* suspension cell cultures and expert technical assistance. The present work was supported by the Deutsche Forschungsgemeinschaft.

References

- Ben-Shem, A., Frolow, F., Nelson, N., 2003. Crystal structure of plant photosystem I. *Nature* 426, 630–635.
- Bibby, T.S., Nield, J., Barber, J., 2001. Iron deficiency induces the formation of an antenna ring around trimeric photosystem I in cyanobacteria. *Nature* 412, 743–744.
- Bibby, T.S., Nield, J., Chen, M., Larkum, A.W.D., Barber, J., 2003. Structure of a photosystem II supercomplex isolated from *Prochloron didemni* retaining its chlorophyll a/b light-harvesting system. *Proc. Natl. Acad. Sci. USA* 100, 9050–9054.
- Boekema, E.J., Hankamer, B., Bald, D., Kruij, J., Nield, J., Boonstra, A.F., Barber, J., Rögner, M., 1995. Supramolecular structure of the photosystem II complex from green plants and cyanobacteria. *Proc. Natl. Acad. Sci. USA* 92, 175–179.
- Boekema, E.J., van Roon, H., Dekker, J.P., 1998a. Specific association of photosystem II and light-harvesting complex II in partially solubilized photosystem II membranes. *FEBS Lett.* 424 (1–2), 95–99.
- Boekema, E.J., Nield, J., Hankamer, B., Barber, J., 1998b. Localization of the 23 kDa subunit of the oxygen-evolving complex of photosystem II by electron microscopy. *Eur. J. Biochem.* 252, 268–276.
- Boekema, E.J., van Roon, H., Calkoen, F., Bassi, R., Dekker, J.P., 1999a. Multiple types of association of photosystem II and its light-harvesting antenna in partially solubilized photosystem II membranes. *Biochemistry* 388, 2233–2239.
- Boekema, E.J., van Roon, H., van Breemen, J.F., Dekker, J.P., 1999b. Supramolecular organization of photosystem II and its light-harvesting antenna in partially solubilized photosystem II membranes. *Eur. J. Biochem.* 266, 444–452.
- Boekema, E.J., Hifney, A., Yakushevskaya, A.E., Piotrowski, M., Keegstra, W., Berry, S., Michel, K.P., Pistorius, E.K., Kruij, J., 2001a. A giant chlorophyll–protein complex induced by iron deficiency in cyanobacteria. *Nature* 412, 745–747.
- Boekema, E.J., Jensen, P.E., Schlodder, E., van Breemen, J.F., van Roon, H., Scheller, H.V., Dekker, J.P., 2001b. Green plant photosystem I binds light-harvesting complex I on one side of the complex. *Biochemistry* 40, 1029–1036.
- Eubel, H., Jaensch, L., Braun, H.P., 2003. New insights into the respiratory chain of plant mitochondria: supercomplexes and a unique composition of complex II. *Plant Physiol.* 133, 274–286.
- Eubel, H., Heinemeyer, J., Braun, H.P., 2004. Identification and characterization of respirasomes in potato mitochondria. *Plant Physiol.* 134, 1450–1459.
- Germano, M., Yakushevskaya, A.E., Keegstra, W., van Gorkom, H.J., Dekker, J.P., Boekema, E.J., 2002. Supramolecular organization of photosystem I and light-harvesting complex I in *Chlamydomonas reinhardtii*. *FEBS Lett.* 525, 121–125.
- Jordan, P., Fromme, P., Witt, H.T., Klukas, O., Saenger, W., Krauß, N., 2001. Three-dimensional structure of cyanobacterial photosystem I at 2.5 Å resolution. *Nature* 411, 909–917.
- Kargul, J., Nield, J., Barber, J., 2003. Three-dimensional reconstruction of a light-harvesting complex I–photosystem I LHCI–PSI supercomplex from the green alga *Chlamydomonas reinhardtii*. Insights into light harvesting for PSI. *J. Biol. Chem.* 278, 16135–16141.
- Kruij, J., Boekema, E.J., Bald, D., Boonstra, A.F., Rögner, M., 1993. Isolation and structural characterization of monomeric and trimeric photosystem I complexes P700-F_A/F_B and P700-F_X from the *Cyanobacterium synechocystis* PCC 6803*. *J. Biol. Chem.* 268, 23353–23360.
- Kügler, M., Kruff, V., Schmitz, U.K., Braun, H.P., 1997. Analysis of the chloroplast protein complexes by blue-native–polyacrylamide gel electrophoresis BN–PAGE. *Photosynth. Res.* 53, 35–44.

- Kügler, M., Kruff, V., Schmitz, U.K., Braun, H.P., 1998. Characterization of the PetM subunit of the b₆f complex from higher plants. *J. Plant Physiol.* 153, 581–586.
- Kühlbrandt, W., Wand, D.N., Fujiyoshi, Y., 1994. Atomic model of plant light-harvesting complex by electron crystallography. *Nature* 367, 614–621.
- Kurisu, G., Zhang, H., Smith, J.L., Cramer, W.A., 2003. Structure of the b₆f complex of oxygenic photosynthesis: tuning the cavity. *Science* 302, 1009–1014.
- Liu, Z., Yan, H., Wang, K., Kuang, T., Zhang, J., Gui, L., Chang, W., 2004. Crystal structure of spinach major light-harvesting complex at 2.72 Å resolution. *Nature* 428, 287–292.
- Lunde, C., Jensen, P.E., Haldrup, A., Knoetzel, J., Scheller, H.V., 2000. The PSI-H subunit of photosystem I is essential for state transitions in plant photosynthesis. *Nature* 408, 613–615.
- Perkins, D.N., Pappin, D.J., Creasy, D.M., Cottrell, J.S., 1999. Probability-based protein identification by searching sequence databases using mass spectrometry data. *Electrophoresis* 20, 3551–3567.
- Pfeiffer, K., Gohil, V., Stuart, R.A., Hunte, C., Brandt, U., Greenberg, M.L., Schägger, H., 2003. Cardiolipin stabilizes respiratory chain supercomplexes. *J. Biol. Chem.* 278, 52873–52880.
- Rexroth, S., Meyer zu Tittingdorf, J.M., Krause, F., Dencher, N.A., Seelert, H., 2003. Thylakoid membrane at altered metabolic state: challenging the forgotten realms of the proteome. *Electrophoresis* 2416, 2814–2823.
- Schägger, H., 2001a. Respiratory chain supercomplexes. *IUBMB Life* 52, 119–128.
- Schägger, H., 2001b. Blue-native gels to isolate protein complexes from mitochondria. *Methods Cell. Biol.* 65, 231–244.
- Schägger, H., 2002. Respiratory chain supercomplexes of mitochondria and bacteria. *Biochim. Biophys. Acta* 15551–3, 154–159.
- Schägger, H., von Jagow, G., 1991. Blue native electrophoresis for isolation of membrane protein complexes in enzymatically active form. *Anal. Biochem.* 199, 223–231.
- Schägger, H., Pfeiffer, K., 2000. Supercomplexes in the respiratory chains of yeast and mammalian mitochondria. *EMBO J.* 198, 1777–1783.
- Singh, P., Jänsch, L., Braun, H.P., Schmitz, U.K., 2000. Resolution of mitochondrial and chloroplast membrane protein complexes from green leaves of potato on Blue-Native-polyacrylamide gels. *Indian J. Biochem. Biophys.* 37, 59–66.
- Stroebel, D., Choquet, Y., Popot, J.L., Picot, D., 2003. An atypical haem in the cytochrome b₆f complex. *Nature* 426, 413–418.
- Surosa, M., Regel, P.E., Paakkarinen, V., Battchikova, N., Herrmann, R.G., Aro, E.M., 2004. Protein assembly of photosystem II and accumulation of subcomplexes in the absence of low molecular mass subunits PsbL and PsbJ. *Eur. J. Biochem.* 271, 96–107.
- Swiatek, M., Kuras, R., Sokolenko, A., Higgs, D., Olive, J., Cinque, G., Müller, B., Eichacker, L.A., Stern, D.B., Bassi, R., Herrmann, R.G., Wollman, F.A., 2001. The chloroplast gene ycf9 encodes a photosystem II (PSII) core subunit, PsbZ, that participates in PSII supramolecular architecture. *The Plant Cell* 13, 1347–1367.
- The *Arabidopsis* Genome Initiative, 2000. Analysis of the genome sequence of the flowering plant *Arabidopsis thaliana*. *Nature* 408, 796–815.
- Thidholm, E., Lindström, V., Tissier, C., Robinson, C., Schröder, W.P., Funk, C., 2002. Novel approach reveals localisation and assembly pathway of the PsbS and PsbW proteins into the photosystem II dimer. *FEBS Lett.* 513, 217–222.
- Werhahn, W., Niemeyer, A., Jänsch, L., Kruff, V., Schmitz, U.K., Braun, H.P., 2001. Purification and characterization of the preprotein translocase of the outer mitochondrial membrane from *Arabidopsis thaliana*: identification of multiple forms of TOM20. *Plant Physiol.* 125, 943–954.
- Yakushevskaya, A.E., Jensen, P.E., Keegstra, W., van Roon, H., Scheller, H.V., Boekema, E.J., Dekker, J.P., 2001. Supermolecular organization of photosystem II and its associated light-harvesting antenna in *Arabidopsis thaliana*. *Eur. J. Biochem.* 268, 6020–6028.
- Zhang, M., Mileykovskaya, E., Dowhan, W., 2002. Gluing the respiratory chain together. Cardiolipin is required for supercomplex formation in the inner mitochondrial membrane. *J. Biol. Chem.* 277, 43553–43556.
- Zouni, A., Witt, H.T., Kern, J., Fromme, P., Krauß, N., Saenger, W., Orth, P., 2001. Crystal structure of photosystem II from *Synechococcus elongatus* at 3.8 Å resolution. *Nature* 409, 739–743.

Structure of dimeric ATP synthase from mitochondria: An angular association of monomers induces the strong curvature of the inner membrane

Natalya V. Dudkina^a, Jesco Heinemeyer^b, Wilko Keegstra^a,
Egbert J. Boekema^{a,*}, Hans-Peter Braun^b

^a Department of Biophysical Chemistry, GBB, University of Groningen, Nijenborgh 4, 9747 AG Groningen, The Netherlands

^b Abteilung Angewandte Genetik, Universität Hannover, Herrenhäuser Str. 2, 30419 Hannover, Germany

Received 20 September 2005; accepted 27 September 2005

Available online 6 October 2005

Edited by Richard Cogdell

Abstract Respiration in all cells depends upon synthesis of ATP by the ATP synthase complex, a rotary motor enzyme. The structure of the catalytic moiety of ATP synthase, the so-called F₁ headpiece, is well established. F₁ is connected to the membrane-bound and ion translocating F₀ subcomplex by a central stalk. A peripheral stalk, or stator, prevents futile rotation of the headpiece during catalysis. Although the enzyme functions as a monomer, several lines of evidence have recently suggested that monomeric ATP synthase complexes might interact to form a dimeric supercomplex in mitochondria. However, due to its fragility, the structure of ATP synthase dimers has so far not been precisely defined for any organism. Here we report the purification of a stable dimeric ATP synthase supercomplex, using mitochondria of the alga *Polytomella*. Structural analysis by electron microscopy and single particle analysis revealed that dimer formation is based on specific interaction of the F₀ parts, not the F₁ headpieces which are not at all in close proximity. Remarkably, the angle between the two F₀ part is about 70°, which induces a strong local bending of the membrane. Hence, the function of ATP synthase dimerisation is to control the unique architecture of the mitochondrial inner membrane.

© 2005 Published by Elsevier B.V. on behalf of the Federation of European Biochemical Societies.

Keywords: ATP synthase; Dimer; Electron microscopy; *Polytomella*

1. Introduction

Mitochondrial F₁F₀ ATP synthase or ATPase is a complex of about 600 kDa formed by 15–18 distinct subunits. Five of these subunits (α , β , γ , δ , ϵ) constitute the F₁ headpiece, which has been resolved by X-ray crystallography [1,2]. In contrast, the F₀ part is structurally less well defined. It is composed of a ring of 9–12 copies of the lipoprotein “subunit c” attached to two larger subunits termed subunits a and b. A number of additional small subunits form part of F₀ and the peripheral stalk. In yeast, three of them, termed subunits e, g and k, only occur in a dimeric 1200 kDa ATP synthase supercomplex, which was described recently [3]. Yeast cells deficient in the di-

mer-specific subunits e or g lack dimeric ATP synthase [4,5]. Recent data also point to an involvement of subunit b in dimer formation [6]. Similar dimeric and oligomeric ATP synthase supercomplexes were also found in bovine heart [7], *Arabidopsis* [8] and *Chlamydomonas* [9]. However, so far knowledge on dimeric ATP synthase is limited due to the lack of structural data.

Dimeric ATP synthase from *Chlamydomonas* was found to be especially stable [9–11]. Compared to ATP synthase dimers from other organisms it includes an additional 60 kDa protein designated “mitochondrial ATP synthase associated protein” (MASAP), which is speculated to be involved in dimer formation [9]. A very similar ATP synthase supercomplex is present in the closely related non-green alga *Polytomella* [12]. Here we report purification and structural characterization of the ATP synthase supercomplex from *Polytomella*.

2. Materials and methods

2.1. Cultivation of *Polytomella*

Polytomella spp. (198.80, E.G. Pringsheim) was obtained from the “Sammlung von Algenkulturen der Universität Göttingen (SAG)” (<http://www.epsag.uni-goettingen.de/html/sag.html>). Cells were cultivated for 4–5 days in 2.5-liter culture flasks including 200 ml medium [0.2% (w/v) sodium acetate, 0.1% (w/v) yeast extract and 0.1% (w/v) tryptone] at 25 °C in the dark without shaking.

2.2. Preparation of mitochondria

For mitochondrial isolations, cells were sedimented by centrifugation at 2000 × g for 10 min, washed twice in 20 mM sodium phosphate buffer, pH 7.4 and finally re-suspended in 0.32 M sucrose, 4 mM EDTA, 20 mM Tris–HCl, pH 7.4. Disruption of cells was carried out using a “Dounce Homogenisator” (10 strokes). Organelles were enriched by differential centrifugation for 8 min at 1000 × g (mitochondria in supernatant), 8 min at 1000 × g (mitochondria in supernatant) and 15 min at 10000 × g (mitochondria in pellet). The resulting crude mitochondrial fraction was re-suspended in gradient buffer (0.4 M mannitol/0.1% BSA, 1 mM EGTA, 0.2 mM PMSF, 10 mM KH₂PO₄, pH 7.2) and organelles were purified by Percoll density gradient centrifugation (14%, 22%, 45% Percoll in gradient buffer) at 70000 × g for 45 min. Finally, *Polytomella mitochondria* were washed twice by centrifugation at 15000 × g at 10 min and re-suspended in gradient buffer at a protein concentration of 10 mg/ml.

2.3. Purification of dimeric ATP synthase

Isolated mitochondria were treated with solubilization buffer (30 mM HEPES, 150 mM K-acetate, 10% glycerol, 5% digitonin, pH 7.4) and solubilized protein complexes were separated by sucrose

*Corresponding author. Fax: +31 50 363 4800.

E-mail address: e.j.boekema@rug.nl (E.J. Boekema).

gradient ultracentrifugation (gradients of 0.3–1.5 M sucrose, 15 mM Tris base, pH 7.0, 20 mM KCl, 0.2% digitonin; centrifugation for 17 h at $150000 \times g/4^\circ\text{C}$). Afterwards, fractions were removed from the gradient from bottom to top. 1D Blue-native PAGE and 2D Blue-native/SDS-PAGE was carried out as described by Schagger [13].

2.4. Electron microscopy and single particle analysis

Electron microscopy and single particle analyses including alignments of projections with multi-reference and non-reference procedures, multivariate statistical analysis and classification, was carried out as outlined by Dudkina et al. [14].

3. Results and discussion

3.1. Purification of ATP synthase dimers

Total mitochondrial membranes from *Polytomella* were solubilized by digitonin and protein complexes were separated by sucrose gradient ultracentrifugation (Fig. 1). A 1D Blue-native PAGE was carried out to monitor the protein complex composition of the fractions of the sucrose gradient (Fig. 1, left gel). Identification of the protein complexes was based on their subunit composition by a parallel 2D Blue-native/SDS-PAGE of total mitochondrial protein from *Polytomella* (Fig. 1, right gel). On the 2D gels, dimeric ATP synthase migrates well above complex I and is resolved into the known subunits, including MASAP [9]. Monomeric ATP synthase was not detectable. The respiratory chain complexes I, III₂ and IV are present as monomeric complexes, but partially also form large supermolecular structures, which run on the top of the 2D gel. The highest concentration of dimeric ATP synthase was in fraction 5 of the sucrose gradient and this fraction

was used for a structural characterization by electron microscopy and single particle analysis [14].

3.2. Structural analysis by single particle electron microscopy

Projection maps were obtained after classification of large numbers of particles. The best classes have a resolution of about 17 Å, according to the Fourier-ring correlation criterion (see [14]). They show how the interaction of the F₁F₀ ATP synthase monomers occurs within the dimer (Fig. 2(a)). The projection map indicates that most if not all of the interaction is between the membrane-bound F₀ parts. Surprisingly, the F₁ headpieces are not at all in close proximity and the stator structures are much more substantial than in any other monomeric F- or V-ATPase [15], likely because of the special dimer-specific subunits such as the MASAP subunit of 60 kDa. The most remarkable feature is the angle of about 70° between the F₀ parts, which implies a strong local bending of the inner mitochondrial or cristae membrane around the dimers. This angle was found for the vast majority of the dimers and is even maintained in those particles in which one of the headpieces was dissected (Fig. 2(b) and (c)). The angle of 70° between the ATP synthase monomers deviates by up to $\pm 5^\circ$ in a small number of dimers only (results not shown), indicating a specific type of interaction.

4. Discussion

We have shown for the first time the projection structure of an ATP synthase dimer in which the F₁ and F₀ parts are well

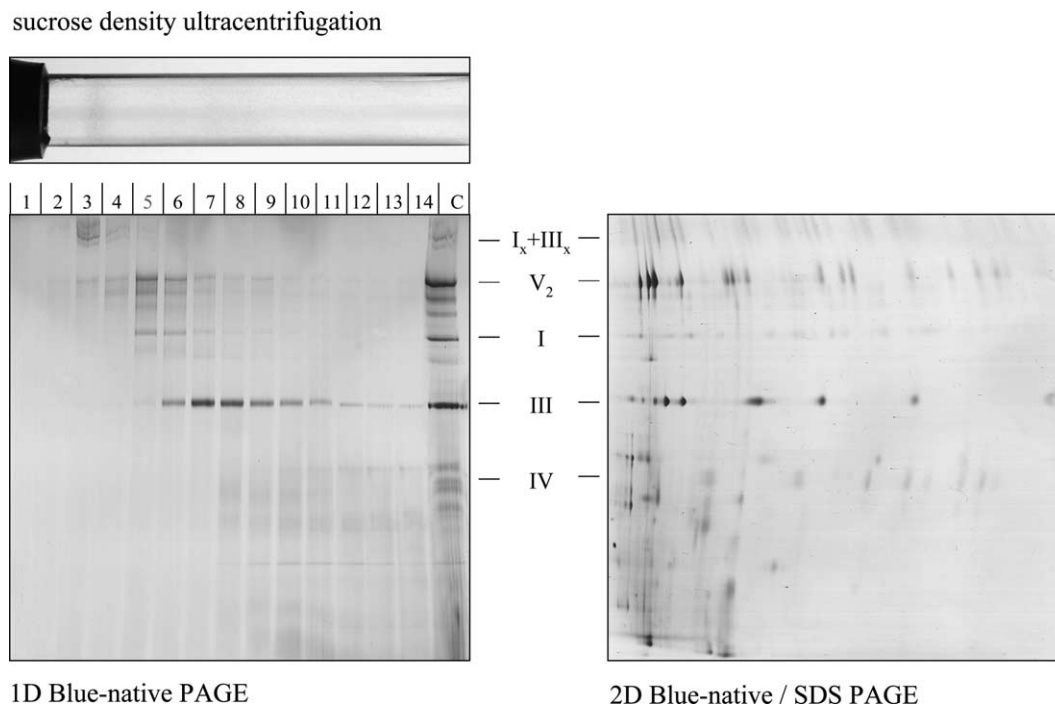


Fig. 1. Purification of dimeric ATP synthase of *Polytomella* by sucrose gradient ultracentrifugation. *Top*. Separation of mitochondrial protein complexes by ultracentrifugation. *Left gel*. 1D Blue-native PAGE of the fractions of the gradient. Numbers on top of the gel refer to the fractions of the sucrose gradient (from bottom to top as indicated); C; total mitochondrial protein. *Right gel*. 2D Blue-native/SDS-PAGE of total mitochondrial protein of *Polytomella*. Identities of protein complexes are indicated between the two gels: IV, complex IV; III₂, dimeric complex III; I, complex I; V₂, dimeric complex V; I_x + III_x, supercomplex including complexes I and III. Fraction 5 was selected for electron microscopy and single particle analysis.

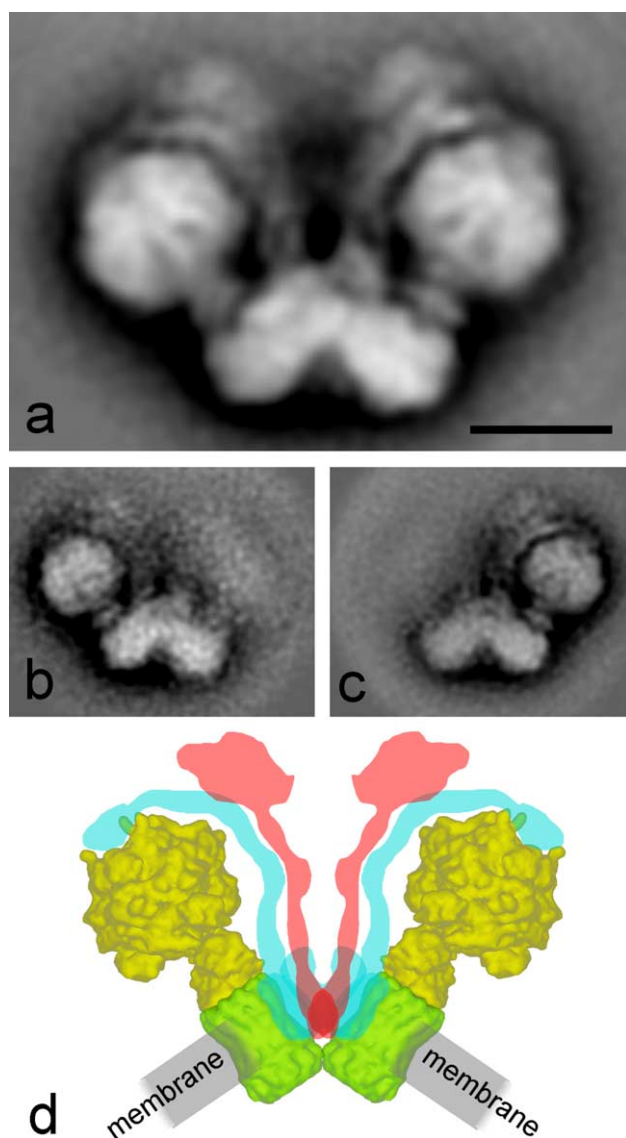


Fig. 2. Electron microscopy analysis and interpretation. (a) Projection map of dimeric ATPase. The average 2D projection is the sum of a homogeneous subset of 3000 projections out of 40000 projections found by statistical analysis and classification. Bar is 10 nm. (b,c) Dimeric ATP synthase fragments lacking one specific F_1 headpiece. The class-sums are comprised of about 500 projections each. (d) Interpretation. Yellow, F_1 headpiece and central stalk; green, c-subunit rotor component of F_0 ; blue, peripheral stalk and red, dimer-specific components, not present in monomeric ATPase.

resolved, including flanking peripheral stalks or stators. The projection maps of the complete dimers and the fragments missing one of the F_1 parts clearly indicate that the interaction between the monomers is within their F_0 parts. In parallel to our current investigation another dimeric ATP synthase was studied by Minnauro-Sanmiguel et al. [16]. Analysis of the dimer from beef heart mitochondria indicates that the monomers also make an angle. In comparison to the dimer from *Polytomella* the angle is substantially smaller and about 40° and the F_1 parts seem to be (almost) in contact. Although the authors present a scheme in which two peripheral stalks or stators should be in between the two F_1 parts the processed images do not show such peripheral stalks. Thus it

is likely that most of the dimers do not contain the peripheral stalk anymore. On the other hand it could be possible that this small and thin stator is difficult to see because of overlap in projection with other subunits or a limited resolution. However, the loss of a stator often co-insides with absence of the OSCP subunit, which is located at the top of the F_1 part. This position has been convincingly shown by immuno-labelling of the homologous δ subunit in *Escherichia coli* [17]. This investigation indicates that the presence of the δ subunit causes the F_1 part to end in a sharp tip, like OSCP in our images and in contrast to the blunt tip as presented in [16]. We therefore are not convinced about the intactness of the monomers in the ATP synthase dimer of beef. In contrast, the peripheral stalks are clearly visible in the *Polytomella* dimer.

Until now there is no emerging role for the dimeric ATPase, although it was speculated that the ATP synthase supercomplex formation might optimize energy transduction [3]. Alternatively, it has been proposed that dimers could be involved in the control of the biogenesis of the inner mitochondrial membrane [4,5]. The authors of the latter studies suggested that there should be a link between ATP synthase dimerization and the cristae morphology, because deletion of dimer-specific subunits changes the overall morphology of the membrane foldings. Yeast mutants unable to form dimeric ATP synthase comprise mitochondria with drastically changed morphology, which lack the characteristic highly folded inner membrane architecture, the cristae. Instead the membranes consist of atypical “onion-like” structures. A similar mitochondrial morphology was observed in yeast cells containing in vivo cross-linked F_1 -headpieces [18], providing further evidence for a role of dimerization of ATP synthase for cristae formation.

Our data provide a direct clue for the role of dimerization of ATP synthase monomers. It is proposed to be the driving force for cristae formation and overall mitochondrial morphology because the unique way of the out of plane association of the F_0 membrane domains will force a strong local curvature of the membrane (Fig. 2(d)). It should be realized that the bulk of the ATP synthase complexes is not part of a rather flat inner mitochondrial membrane, but present within curved invaginations known as cristae lamellae and tubules [19]. For tubular membranes, the diameter is often in the range 24–32 nm, if the width of the bilayer is included [19]. If the bent membrane in the region of the dimers is regarded as a 70° arc section of radius 16 nm, this configuration could by extrapolation induce a tubule with a diameter of about 25 nm. Such a diameter would fit the observed cristae dimensions nicely. Likely the ATP synthase dimers would associate in specific oligomers with the other respiratory chain supercomplexes such as the supercomplex formed by monomeric complex I and dimeric complex III [14] in between. Indeed oligomeric ATP synthase structures were previously described by rapid-freeze deep-etch EM [19,20] and by Blue-native PAGE [4,5,21,22]. We propose that dimeric ATP synthase supercomplexes represent basic building blocks of ATP synthase oligomers and that formation of these structures is the driving force for cristae formation and overall mitochondrial morphology. It should finally be remarked that a spectacular surface extension of the inner membrane is realized by multiple foldings of this membrane. It has for instance been estimated that the surface of the inner mitochondrial membrane in an average human would be around 14000 m^2 [23].

Acknowledgements: H.P.B. acknowledges a grant of the Deutsche Forschungsgemeinschaft (Br1829-7/1) and E.J.B. a grant of the Dutch science foundation NWO-CW.

References

- [1] Stock, D., Gibbons, C., Arechaga, I., Leslie, A.G.W. and Walker, J.E. (2000) Rotary mechanism of ATP synthase. *Curr. Opin. Struct. Biol.* 10, 672–679.
- [2] Abrahams, J.P., Leslie, A.G., Lutter, R. and Walker, J. (1994) Structure at 2.8 Å resolution of F₁-ATPase from bovine heart mitochondria. *Nature* 370, 621–628.
- [3] Arnold, I., Pfeiffer, K., Neupert, W., Stuart, R.A. and Schägger, H. (1998) Yeast mitochondrial F₁F₀-ATP synthase exists as a dimer: identification of three dimer-specific subunits. *EMBO J.* 17, 7170–7178.
- [4] Paumard, P., Vaillier, J., Coulary, B., Schaeffer, J., Soubannier, V., Mueller, D.M., Brèthes, D., di Rago, J.P. and Velours, J. (2002) The ATP synthase is involved in generating mitochondrial cristae morphology. *EMBO J.* 21, 221–230.
- [5] Giraud, M.F., Paumard, P., Soubannier, V., Vaillier, J., Arselin, G., Salin, B., Schaeffer, J., Brèthes, D., di Rago, P. and Velours, J. (2002) Is there a relationship between the supramolecular organization of the mitochondrial ATP synthase and the formation of cristae?. *Biochim. Biophys. Acta* 1555, 174–180.
- [6] Gavin, P.D., Prescott, M. and Devenish, R.J. (2005) Yeast F₁F₀-ATP synthase complex interactions in vivo can occur in the absence of the dimer specific subunit e. *J. Bioenerg. Biomem.* 37, 55–66.
- [7] Schägger, H. and Pfeiffer, K. (2000) supercomplexes in the respiratory chains of yeast and mammalian mitochondria. *EMBO J.* 19, 1777–1783.
- [8] Eubel, H., Heinemeyer, J., Sunderhaus, S. and Braun, H.P. (2004) Respiratory chain supercomplexes in plant mitochondria. *Plant Physiol. Biochem.* 42, 937–942.
- [9] Van Lis, R., Atteia, A., Mendoza-Hernandez, G. and Gonzalez-Halphen, D. (2003) Identification of novel mitochondrial protein components of *Chlamydomonas reinhardtii*. A proteomic approach. *Plant Physiol.* 132, 318–330.
- [10] Atteia, A., van Lis, R., Mendoza-Hernandez, G., Henze, K., Martin, W., Riveros-Rosas, H. and Gonzalez-Halphen, D. (2003) Bifunctional aldehyde/alcohol dehydrogenase (ADHE) in chlorophyte algal mitochondria. *Plant Mol. Biol.* 53, 175–188.
- [11] Rexroth, S., Meyer Zu Tittingdorf, J.M., Schwassmann, H.J., Krause, F., Seelert, H. and Dencher, N.A. (2004) Dimeric H⁺-ATP synthase in the chloroplast of *Chlamydomonas reinhardtii*. *Biochim. Biophys. Acta* 1658, 202–211.
- [12] Van Lis, R., Mendoza-Hernandez, G. and Gonzalez-Halphen, D. (2005) Divergence of the mitochondrial electron transport chains from the green alga *Chlamydomonas reinhardtii* and its colorless close relative *Polytomella* sp. *Biochim. Biophys. Acta* 1708, 23–34.
- [13] Schägger, H. (2001) Blue-native gels to isolate protein complexes from mitochondria. *Methods Cell Biol.* 65, 231–244.
- [14] Dudkina, N.V., Eubel, H., Keegstra, W., Boekema, E.J. and Braun, H.P. (2005) Structure of a mitochondrial supercomplex formed by respiratory-chain complexes I and III. *Proc. Natl. Acad. Sci. USA* 102, 3225–3229.
- [15] Boekema, E.J., Van Breemen, J.F.L., Brisson, A., Ubbink-Kok, T., Konings, W.N. and Lolkema, J.S. (1999) Connecting stalks in V-type ATPase. *Nature* 401, 37–38.
- [16] Minauro-Sanmiguel, F., Wilkens, S. and Garcia, J.J. (2005) Structure of dimeric mitochondrial ATP synthase: novel F₀ bridging features and the structural basis of mitochondrial cristae biogenesis. *Proc. Natl. Acad. Sci.* 102, 12356–12358.
- [17] Wilkens, D., Zhou, J., Nakayama, R., Dunn, S.D. and Capaldi, R.A. (2000) Localization of the δ subunit in the *Escherichia coli* F₁F₀-ATP synthase by immuno electron microscopy: the δ subunit binds on top of the F₁. *J. Mol. Biol.* 295, 387–391.
- [18] Gavin, P.D., Prescott, M., Luff, S.E. and Devenish, R.J. (2004) Cross-linking ATP synthase complexes in vivo eliminates mitochondrial cristae. *J. Cell Sci.* 117, 2233–2243.
- [19] Allen, R.D., Schroeder, C.C. and Fok, A.K. (1989) An Investigation of mitochondrial inner membranes by rapid-freeze deep-etch techniques. *J. Cell Biol.* 108, 2233–2240.
- [20] Allen, R.D. (1995) Membrane tubulation and proton pumps. *Protoplasma* 189, 1–8.
- [21] Arselin, G., Giraud, M.F., Dautant, A., Vaillier, J., Brèthes, D., Coulary-Salin, B., Schaeffer, J. and Velours, J. (2003) The GxxxG motif of the transmembrane domain of subunit e is involved in the dimerization/oligomerization of the yeast ATP synthase complex in the mitochondrial membrane. *Eur. J. Biochem.* 170, 1875–1884.
- [22] Everard-Gigot, V., Dunn, C.D., Dolan, B.M., Brunner, S., Jensen, R.E. and Stuart, R.A. (2005) Functional analysis of subunit e of the F₁F₀-ATP synthase of the yeast *Saccharomyces cerevisiae*: importance of the N-terminal membrane anchor region. *Eukaryotic Cell* 4, 346–355.
- [23] Rich, P. (2003) The cost of living. *Nature* 421, 583.

A Structural Model of the Cytochrome *c* Reductase/Oxidase Supercomplex from Yeast Mitochondria*

Received for publication, November 13, 2006, and in revised form, January 29, 2007. Published, JBC Papers in Press, February 23, 2007, DOI 10.1074/jbc.M610545200

Jesco Heinemeyer[†], Hans-Peter Braun^{†1}, Egbert J. Boekema^{§2}, and Roman Kouril^{§3}

From the [†]Institute for Plant Genetics, Faculty of Natural Sciences, Universität Hannover, Herrenhäuser Strasse 2, 30419 Hannover, Germany and the [§]Department of Biophysical Chemistry, GBB, University of Groningen, Nijenborgh 4, 9747 AG Groningen, The Netherlands

Mitochondrial respiratory chain complexes are arranged in supercomplexes within the inner membrane. Interaction of cytochrome *c* reductase (complex III) and cytochrome *c* oxidase (complex IV) was investigated in *Saccharomyces cerevisiae*. Projection maps at 15 Å resolution of supercomplexes III₂ + IV₁ and III₂ + IV₂ were obtained by electron microscopy. Based on a comparison of our maps with atomic x-ray structures for complexes III and IV we present a pseudo-atomic model of their precise interaction. Two complex IV monomers are specifically attached to dimeric complex III with their convex sides. The opposite sides, which represent the complex IV dimer interface in the x-ray structure, are open for complex IV-complex IV interactions. This could lead to oligomerization of III₂ + IV₂ supercomplexes, but this was not detected. Instead, binding of cytochrome *c* to the supercomplexes was revealed. It was calculated that cytochrome *c* has to move less than 40 Å at the surface of the supercomplex for electron transport between complex III₂ and complex IV. Hence, the prime function of the supercomplex III₂ + IV₂ is proposed to be a scaffold for effective electron transport between complexes III and IV.

On a global scale, aerobic respiration provides most of the energy for metabolism and cellular activity. In prokaryotes and mitochondria of eukaryotes it is based on the occurrence of membrane bound oxidoreductase complexes termed complex I (NADH-ubiquinone oxidoreductase), complex II (succinate-ubiquinone oxidoreductase), complex III (ubiquinol-cytochrome *c* oxidoreductase or cytochrome *bc*₁ complex), and complex IV (cytochrome *c*-O₂ oxidoreductase), which together constitute the respiratory chain. The main task of the respiratory chain is to generate the electrochemical proton gradient across the cytoplasmic membrane of prokaryotes or the inner mitochondrial membrane of eukaryotes, which is utilized by complex V (ATP synthase) to synthesize ATP (1, 2).

There is increasing evidence now that three of the respiratory chain complexes and the ATP synthase complex are part of defined supramolecular structures termed respiratory supercomplexes. Mainly due to employment of the detergent digitonin for mild solubilization and Blue native (BN)⁴-PAGE for purification, various supercomplexes were isolated and characterized in several organisms (see Refs. 2–4 for recent reviews). One main group of supercomplexes consists of combinations of complexes I, III, and IV; one other supercomplex is a homodimer of complex V. At least two forms of yeast III + IV supercomplexes were identified by two-dimensional BN-SDS-PAGE: a III₂ + IV₁ and a III₂ + IV₂ supercomplex (5, 6). Although structural evidence is so far lacking, inhibitor titration studies, gel filtrations, and immunoprecipitations further support the occurrence of III₂ + IV_{1–2} supercomplexes in yeast (5, 7). In bovine heart mitochondria, up to four copies of complex IV might be bound to dimeric complex III (6). In addition, mammalian I + III₂ + IV_{1–4} supercomplexes were described and named “respirasomes” because they are composed of three of the respiratory chain complexes, which deliver most of the proton motive force to yield ATP (6). Also in bacteria respiratory complexes were reported to form defined supercomplexes (8, 9).

In schematic “text book” representations of the respiratory chain its individual protein complexes are commonly depicted as single copies in a flat membrane, but this is actually an oversimplification of the overall membrane organization. The inner mitochondrial membrane is heavily folded into lamellar or tubular structures termed cristae. In addition, the cristae membrane morphology is dynamic and regulated, at least in part, by proteins that control inter-mitochondrial fission and fusion (10). Electron microscopy three-dimensional reconstructions of quickly frozen mitochondria give the impression of a dynamic interconnected membrane continuum. The lipid to protein ratio within the inner mitochondrial membrane is as low as 1:2–3 (11). There are many indications that this tight packing of proteins in a heavily folded membrane very much restricts the free movement of protein complexes (12). At the same time, the specific way of membrane protein packing most likely influences membrane morphology. Hence, for a closer understanding of respiration, it is necessary to characterize the supramolecular structure of the building blocks of the cristae membranes.

* The costs of publication of this article were defrayed in part by the payment of page charges. This article must therefore be hereby marked “advertisement” in accordance with 18 U.S.C. Section 1734 solely to indicate this fact.

¹ Supported by a grant from the Deutsche Forschungsgemeinschaft (Br1829-7/2).

² To whom correspondence may be addressed. Tel.: 31-50-3634225; Fax: 31-50-3634800; E-mail: e.j.boekema@rug.nl.

³ Supported by grants from the Dutch Science Foundation Netherlands Organization for Scientific Research, Council for Chemical Sciences (NWO-CW). To whom correspondence may be addressed. Tel.: 31-50-3634225; Fax: 31-50-3634800; E-mail: r.kouril@rug.nl.

⁴ The abbreviations used are: BN, Blue native; EM, electron microscopy; Tricine, *N*-[2-hydroxy-1,1-bis(hydroxymethyl)ethyl]glycine; BisTris, 2-[bis(2-hydroxyethyl)amino]-2-(hydroxymethyl)propane-1,3-diol.

Model of the Yeast Cytochrome Reductase/Oxidase Supercomplex

Recently, the first projection maps of respiratory supercomplexes were obtained by single particle electron microscopy. Characterization of a I + III₂ supercomplex of Arabidopsis revealed lateral association of dimeric complex III to the membrane arm of complex I (13). However, lack of a high-resolution structure of the membrane arm of complex I has so far prevented insight into the precise subunit interactions responsible for formation of this supercomplex. The structure of a dimeric ATP synthase supercomplex was characterized for bovine, *Polytomella*, and yeast (14–16). Interaction of the monomers takes place between their F₀ parts and the long axes of the monomers form angles of up to 90°, resulting in strong local bending of the inner mitochondrial membrane. This bending is believed to be a prerequisite for cristae formation, because yeast mutants lacking dimer-specific ATP synthase subunits lack ATP synthase dimers and at the same time have a flat inner membrane without the characteristic foldings (17, 18). A first projection map of the mammalian I₁ + III₂ + IV₁ supercomplex was also presented recently (19), but lack of detail prevents a consistent modeling of the individual complexes within it. So far, the interaction of complexes III and IV within respiratory supercomplexes is the least understood and therefore was addressed by our current investigation. The advantage of characterizing III–IV supercomplexes is that high resolution structures of the individual complexes III and IV are available.

We have chosen to work on the III₂ + IV_{1–2} supercomplexes from the yeast *Saccharomyces cerevisiae* because they were previously shown to be rather stable (5). The tightly associated lipid cardiolipin was found to stabilize this supercomplex (20, 21). Moreover, *S. cerevisiae* does not possess a respiratory chain complex I involved in proton translocation, which reduces the complexity of this supramolecular system. Here, we report projection maps of yeast III₂ + IV_{1–2} supercomplexes on the basis of single particle electron microscopy using a set of 86,000 single projections. Various side views and angled side views of particles could be assigned to the supercomplexes. Based on a comparison of our maps for the III₂ + IV_{1–2} supercomplexes with the existing atomic x-ray structures for the individual complexes III₂ (22) and IV (23), we present a model on their precise interaction. Within the III₂ + IV₂ supercomplex, complex IV is specifically attached to complex III₂ as a monomer on two opposite sides. Complex IV interacts with complex III₂ with its convex side which is opposite to the dimer interface within dimeric complex IV as revealed by x-ray crystallography. This supramolecular configuration most likely forms the basis for efficient electron transfer from complex III₂ to complex IV by cytochrome *c*, which is partially attached to the III₂ + IV₂ supercomplex.

EXPERIMENTAL PROCEDURES

Cultivation of *S. cerevisiae*—*S. cerevisiae* (strain Y187) was cultivated in YPD medium (1 liter of YPD medium contains: yeast extract (10 g), bacto-peptone (20 g), D(+)-glucose (20 g)). For mitochondrial isolations, cells were transferred into Lactate medium (2.6 mM glucose, 7.3 mM KH₂PO₄, 18.7 mM NH₄Cl, 4.5 mM CaCl₂, 8.6 mM NaCl, 2.9 mM MgCl, 2.2% lactate).

Preparation of Mitochondria—Isolation of yeast mitochondria was based on differential centrifugations and sucrose gra-

dient ultracentrifugation as described by (31). Mitochondria were shock-frozen using liquid nitrogen and stored at –80 °C until use.

Characterization of Mitochondrial Protein Complexes by Blue Native PAGE—Mitochondria from yeast were solubilized by digitonin solution (5% digitonin, 30 mM HEPES, 150 mM potassium acetate, 10% glycerine, pH 7.4), and protein complexes were separated by one-dimensional Blue native PAGE (32, 33). For subunit analysis, gel stripes including the resolved protein complexes were transferred horizontally onto a second gel dimension, which was carried out in the presence of SDS (two-dimensional Blue native/SDS-PAGE). For supercomplex analysis, gel stripes of the Blue native gel were incubated in transfer solution (0.03% dodecyl maltoside, 50 mM Tricine, 15 mM BisTris, 0.02% Coomassie 250G, pH 7.0) and resolved by another Blue native PAGE (6, 34). Gels were either Coomassie-stained (35) or stained by an in-gel activity assay for cytochrome *c* oxidase (36).

Purification of Supercomplexes III₂ + IV₂—The membrane-bound protein complexes of yeast were solubilized using digitonin solution (5% digitonin, 30 mM HEPES, 150 mM potassium acetate, 10% glycerol, pH 7.4) and separated by sucrose gradient ultracentrifugation (gradients of 0.3–1.5 M sucrose, 15 mM Tris base, pH 7.0, 20 mM KCl, 0.2% digitonin; centrifugation for 17 h at 150,000 × *g* at 4 °C). Afterward, the gradients were fractionated and the protein complex compositions of the fractions analyzed by one-dimensional Blue native PAGE.

Electron Microscopy—Selected fractions of the gradients including supercomplexes of complex III and complex IV were directly used for electron microscopy and single particle analyses. Samples of purified complexes were negatively stained by using the droplet method with 2% uranyl acetate on glow-discharged, carbon-coated copper grids. Electron microscopy was performed on a CM120 electron microscope (FEI, Eindhoven, The Netherlands) operated at 120 kV. Images were recorded under low dose conditions (a total dose ~25 e[–]/Å²) with a 4000 SP 4K slow-scan CCD camera (Gatan, Pleasanton, CA) at –340 nm defocus and at the final magnification of 80,000 at the level of the CCD camera with GRACE software for semi-automated specimen selection and data acquisition (37). The pixel size (after binning the images) was 3.75 Å at the specimen level. In total, about 4,300 images were recorded and over 86,000 single particle projections were selected for image analysis. A major part of the projections was selected using Boxer, a graphical program for semiautomatic particle selection from EMAN software package (38). Single-particle analysis was performed with the Groningen Image Processing (GRIP) software package on a PC cluster. Selected single-particle projections were aligned by multireference and reference-free alignment procedures (37, 39). Particles were then subjected to multivariate statistical analysis followed by hierarchical classification (39). From the whole data set, almost 85% of single particles were assigned to specific supercomplexes, of which the III₂ + IV₂ and III₂ + IV₁ supercomplexes were present in almost equal amount (about 44 and 41%, respectively). Final two-dimensional projection maps of different angular views of the III₂ + IV₂ and III₂ + IV₁ supercomplexes were calculated from the best resolved classes, which represented about 20% of whole data set. The remaining

Model of the Yeast Cytochrome Reductase/Oxidase Supercomplex

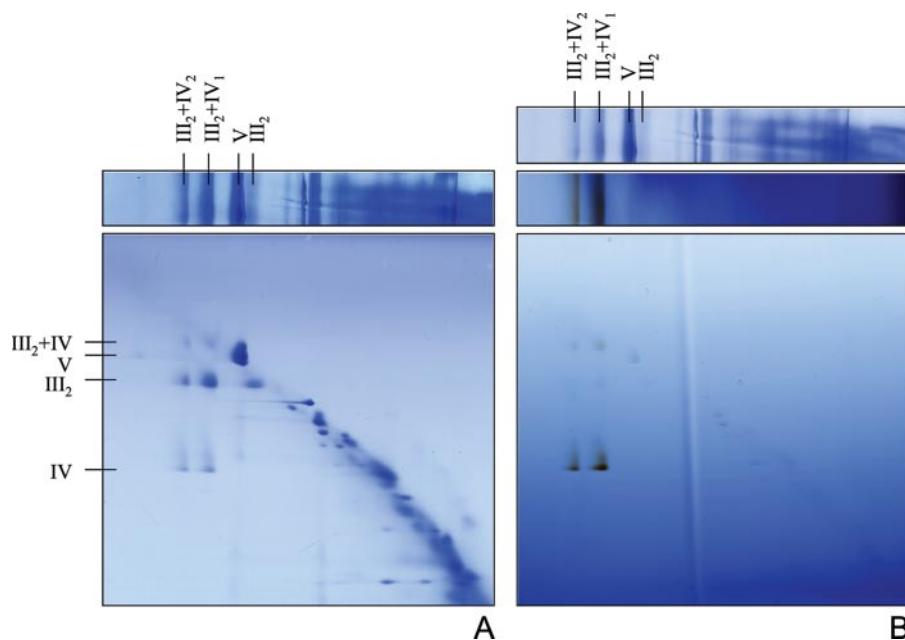


FIGURE 1. **Characterization of the $III_2 + IV_2$ and $III_2 + IV_1$ supercomplexes.** Mitochondrial proteins from yeast (1 mg) were separated by two-dimensional Blue native/Blue native PAGE. Gels were stained by Coomassie Blue (A) or by an in-gel activity assay for complex IV (B). Under the applied conditions, the supercomplexes are dissected into dimeric complex III and monomeric complex IV. Monomeric complex IV was absent on the first gel dimension, indicating that it is exclusively present as part of the supercomplexes.

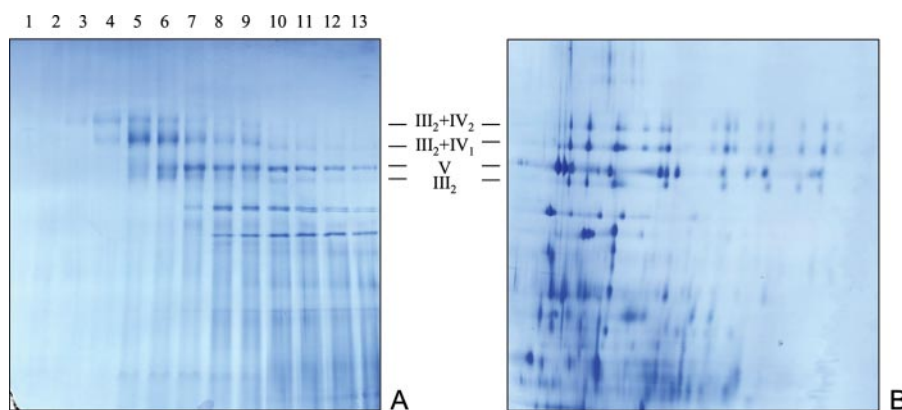


FIGURE 2. **Purification of the $III_2 + IV_2$ and $III_2 + IV_1$ supercomplexes by sucrose gradient ultracentrifugation.** Mitochondrial membrane proteins from yeast were solubilized by digitonin (5 g detergent per g protein) and resolved by ultracentrifugation as described under "Experimental Procedures." The sucrose gradient was fractionated into 13 fractions from bottom to top. All fractions were analyzed by one-dimensional Blue native-PAGE (A) to monitor their protein complex content. Protein complexes were identified by a parallel two-dimensional Blue native-SDS-PAGE of a mitochondrial fraction of yeast (B). Fractions 4 and 5 of the sucrose gradient contain the $III_2 + IV_2$ and $III_2 + IV_1$ supercomplexes and were used for EM and single particle analysis. III_2 : dimeric complex III; V, monomeric complex V; $III_2 + IV_1$, supercomplex composed of dimeric complex III and monomeric complex IV; $III_2 + IV_2$, supercomplex composed of dimeric complex III and two copies of monomeric complex IV.

classes represented the same views of supercomplexes, however, with less resolved features. Resolution was measured using Fourier-ring correlation and the 3σ criterion (40).

X-ray structures of the yeast cytochrome *c* reductase (22) and the bovine heart cytochrome *c* oxidase (23) were used for generating the pseudo-atomic model of the $III_2 + IV_2$ and $III_2 + IV_1$ supercomplexes (the Protein Data Bank accession numbers 1KB9 and 1OCC, respectively). Mammalian subunits Cox VIIb and Cox VIII, which are not present in the yeast cytochrome *c* oxidase, were removed from the x-ray data file. Atomic coordinates of cytochrome *c* were obtained from (22) (the Protein Data Bank accession number 1KY0). Pseudo-atomic models of

the $III_2 + IV_2$ and $III_2 + IV_1$ supercomplexes were constructed manually using Swiss Protein Data Bank viewer (41). First, a starting model of the most symmetrical view of the $III_2 + IV_2$ supercomplex (Fig. 5A) was constructed. Importantly, a contact (or a distance) between the complexes III and IV in the starting model was such that there were no clashes detected between transmembrane helices of the complexes III and IV within 2 \AA . Afterward, the model of the $III_2 + IV_2$ supercomplex was closely fitted into the EM averaged projection. Subsequently, the tilted views of the $III_2 + IV_2$ and $III_2 + IV_1$ supercomplexes (coordinates of one complex IV monomer were deleted from the Protein Data Bank file) were generated solely by a rotation of the whole starting model and manually fitted into the tilted EM projections. If structural inconsistencies were found, the starting model was modified. The position of complex IV with respect to complex III was repeatedly changed by a rotational increment of about 20° followed by fine shifts and rotations until all generated models of the $III_2 + IV_2$ and $III_2 + IV_1$ supercomplexes closely matched the EM maps. Different views of the $III_2 + IV_2$ and $III_2 + IV_1$ supercomplexes were finally displayed using PyMOL software (42). Truncated versions and two-dimensional projection maps of the generated models for the $III_2 + IV_2$ and $III_2 + IV_1$ supercomplexes at 15 \AA resolution were generated using routines from the EMAN package (38).

RESULTS

All Complex IV Is Bound to a Dimeric Complex III_2 Scaffold—The presence and composition of complex $III_2 + IV_{1-2}$ supercomplexes after membrane solubilization with the detergent digitonin was first explored by BN-PAGE (Fig. 1). Using one-dimensional native gels, $III_2 + IV_{1-2}$ supercomplexes are visible at ~ 650 and ~ 850 kDa in accordance with previous investigations (6). A two-dimensional BN/BN-PAGE system, which is carried out in the presence of digitonin for the first gel dimension and in the presence of dodecylmaltosid for the second, was employed to investigate the protein complex composition of the two supercomplexes. Under the conditions applied, both supercomplexes are dissected into monomeric complex IV (~ 200 kDa) and dimeric

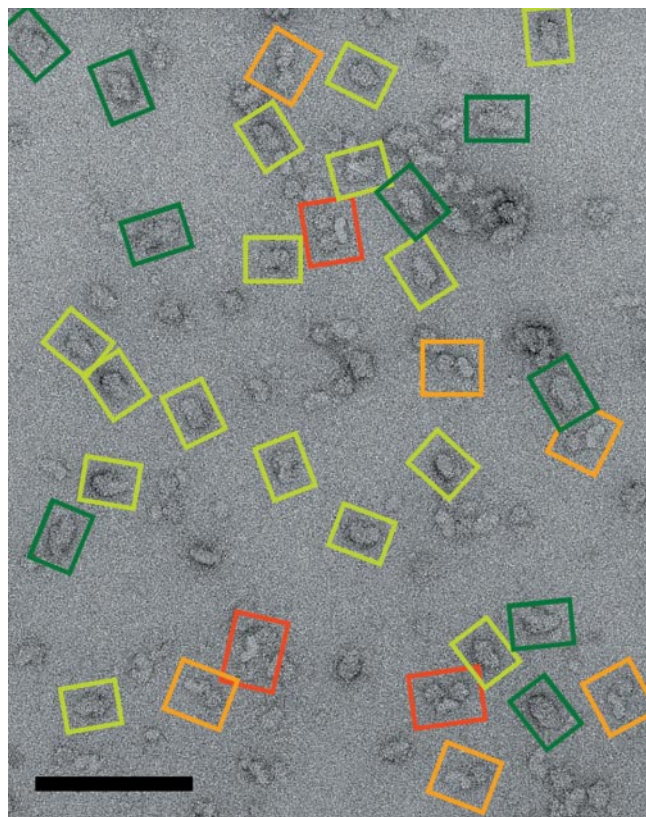


FIGURE 3. Part of an electron micrograph of membrane proteins from the fraction 5 obtained by sucrose gradient centrifugation. Dark green and light green boxes indicate $\text{III}_2 + \text{IV}_2$ and $\text{III}_2 + \text{IV}_1$ supercomplexes, respectively. Intact complex V_2 and fragments of complex V_2 are indicated by red and orange boxes, respectively. The space bar is 100 nm.

complex III (~ 450 kDa) as reported previously (6). The ratio of complex IV to complex III_2 clearly differs within the supercomplexes, with complex IV being relatively less abundant within the smaller supercomplex. The two supercomplexes were interpreted as supercomplex $\text{III}_2 + \text{IV}_1$ (650 kDa) and $\text{III}_2 + \text{IV}_2$ (850 kDa). In-gel complex IV activity staining reveals that complex IV of the supercomplex is active (Fig. 1B). Furthermore, activity staining reveals that all complex IV is present within the two supercomplexes. No free monomeric (~ 200 kDa) or dimeric (~ 400 kDa) forms of complex IV were detected upon detergent solubilization, indicating that complex IV is completely bound to dimeric complex III within the yeast mitochondrial membrane.

Multiple Projection Views of the $\text{III}_2 + \text{IV}_2$ and $\text{III}_2 + \text{IV}_1$ Supercomplexes—To obtain $\text{III}_2 + \text{IV}_{1-2}$ supercomplexes free of Coomassie Blue, which might alter supercomplex structure due to the introduction of negative charge, proteins of digitonin-treated mitochondrial fractions were resolved by sucrose gradient ultracentrifugation (Fig. 2A). The protein complex content of the fractions of the gradient was subsequently analyzed by one-dimensional BN-PAGE. Sucrose gradient fractions 4 and 5 were found to include the 650- and 850-kDa supercomplexes in the purest form. Separation of the subunits of the two supercomplexes by two-dimensional BN-SDS-PAGE revealed the known subunits of the complexes III and IV, which previously were identified by cyclic Edman degradation (6) (Fig. 2B).

Electron microscopy of negatively stained specimens of the sucrose gradient fractions 4 and 5 revealed the presence of complexes with variable size and shape, which could potentially represent views of the $\text{III}_2 + \text{IV}_1$ and $\text{III}_2 + \text{IV}_2$ supercomplexes with varying orientations on the carbon support film (Fig. 3).

From about 4300 electron micrographs, all plausible projections of the $\text{III}_2 + \text{IV}_2$ and $\text{III}_2 + \text{IV}_1$ supercomplexes were selected and a data set of over 86,000 single particle projections was subjected to image analysis. The analysis revealed that fraction 4 was almost free of other supercomplexes, whereas fraction 5 (Fig. 3) also contained dimeric ATP synthase particles, which have a very different shape. (An analysis of 20,000 supercomplex V_2 projections is presented in (16)). Fig. 4 shows the gallery of the best resolved two-dimensional projection maps obtained by statistical analysis and classification. Fig. 4A represents the most symmetrical view of the supercomplex. As the central part of the supercomplex exhibits the characteristic shape and features of the x-ray structure of dimeric complex III and the dimensions of the two additional densities are similar to the dimensions of the x-ray model of complex IV, the

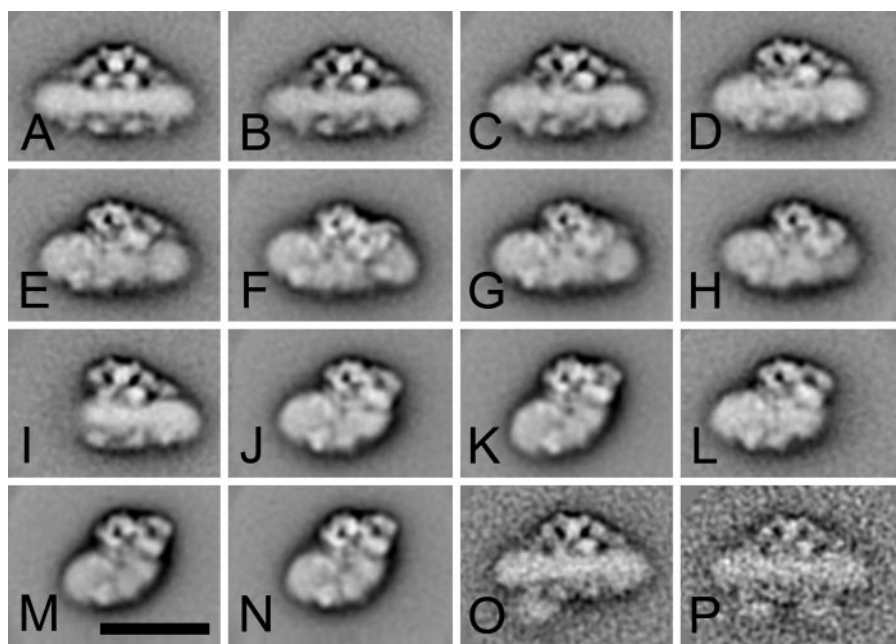


FIGURE 4. Single particle electron microscopy of the $\text{III}_2 + \text{IV}_2$ and $\text{III}_2 + \text{IV}_1$ supercomplexes purified from the yeast *S. cerevisiae*. Projection maps (A–H) represent class sums of 832 (A), 768 (B), 962 (C), 743 (D), 1000 (E), 1024 (F), 2440 (G), and 1648 (H) aligned projections of the $\text{III}_2 + \text{IV}_2$ supercomplex with different orientations on the support carbon film, respectively. I–N represent class sums of 768 (I), 2048 (J), 2048 (K), 717 (L), 1765 (M), and 2048 (N) aligned projections of the $\text{III}_2 + \text{IV}_1$ supercomplex. Projection maps (O, P) represent class sums of 75 and 16 aligned particles of the $\text{III}_2 + \text{IV}_2$ supercomplex with either one or two additional densities in the lower part of the projections, respectively. The scale bar equals 20 nm.

Model of the Yeast Cytochrome Reductase/Oxidase Supercomplex

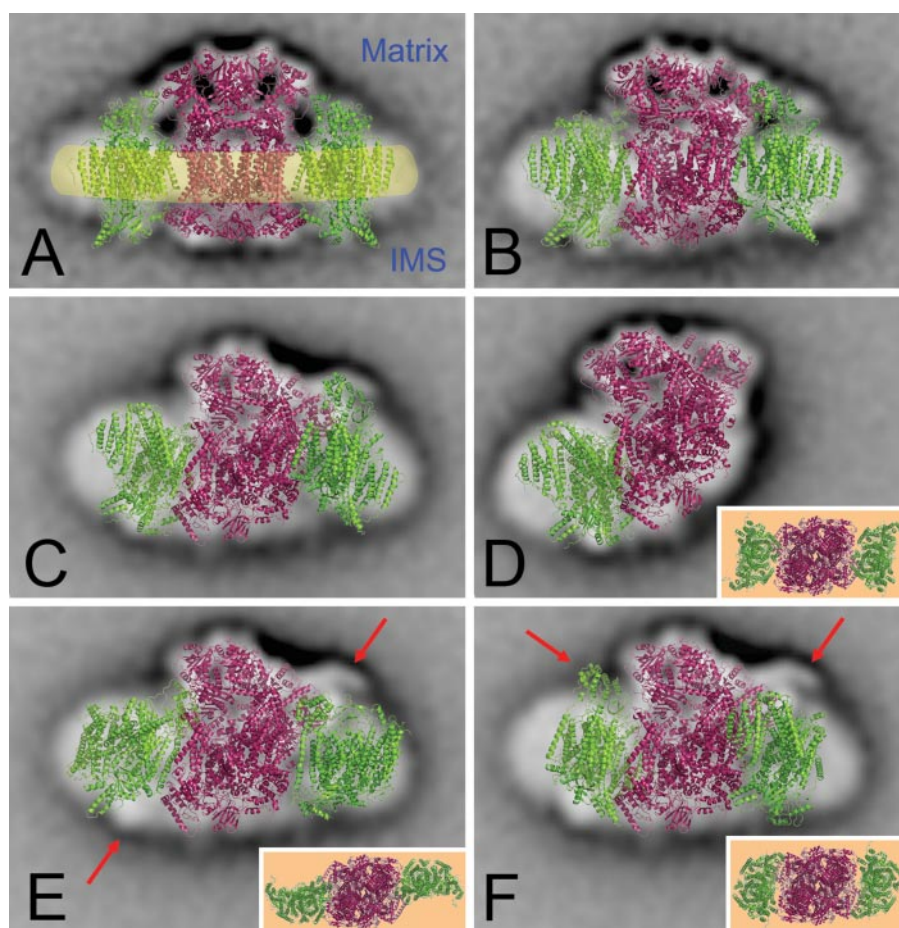


FIGURE 5. Fitting of atomic structures of the yeast cytochrome bc_1 complex (red) and the bovine heart cytochrome c oxidase or complex IV (green) into selected EM projection maps for assignment of the arrangement of the $III_2 + IV_2$ and $III_2 + IV_1$ supercomplexes. One common pseudo-atomic model was constructed (presented in the membrane plane in the inset of *D*) and used for generating different overlays closely matching the $III_2 + IV_2$ (*A–C*) and $III_2 + IV_1$ (*D*) supercomplex maps, respectively. The membrane is depicted in yellow in *A*. The extended length of the $III_2 + IV_2$ average structures obtained by EM compared with the pseudo-atomic structure most likely is due to the presence of both detergent and membrane lipids bound to the membrane-spanning regions of the supercomplex. *E* and *F*, examples of alternative fitting models in which the position of the complex IV monomers was changed by a 90° and 180° rotation in the membrane plane (see insets of *E* and *F*). Red arrows indicate the most pronounced mismatches between these alternative models and corresponding EM maps.

averaged projection in Fig. 4*A* could be unambiguously assigned to the side view of the $III_2 + IV_2$ supercomplex (see below). Fig. 4, *B–H*, represents averaged projections of slightly tilted views of the $III_2 + IV_2$ supercomplex. In addition to the $III_2 + IV_2$ supercomplex, different projections of a smaller supercomplex containing only one copy of complex IV were also found (Fig. 4, *I–N*). Interestingly, extensive analysis of the whole data set revealed about 100 particles which show characteristic features of the $III_2 + IV_2$ supercomplex, and one or two additional densities on the intermembrane-space-exposed side of the supercomplex (Fig. 4, *O* and *P*, respectively). This additional density is attached to complex III_2 at the position of the mobile electron transporter cytochrome *c*, as present in the x-ray structure of the complex III_2 +cytochrome *c* particle of yeast (22).

Fitting of X-ray Models of Complexes III and IV to Averaged EM Projections—To interpret the EM projection maps of the $III_2 + IV_2$ and $III_2 + IV_1$ supercomplexes, they were compared with atomic x-ray structures of yeast complex III (22) and

bovine heart complex IV (23), as the x-ray structure of the yeast complex IV has not been solved yet. Although the bovine heart complex IV contains two additional subunits (Cox7b and Cox8) compared with yeast complex IV, the overall structure of the yeast complex IV can be considered to be similar to its mammalian counterpart (24). First, the largest core subunits Cox1, Cox2, and Cox3, which represent the major part and active core of the complex, are highly conserved in eukaryotes. Second, the other subunits are less conserved, however, they are smaller than the core subunits and several of them, including Cox7b and Cox8, are represented merely by a single transmembrane helix. As the resolution in the best EM projections was about 15 Å, we assume that the x-ray structure of the bovine complex with excluded Cox7b and Cox8 subunits can be substituted for the structure of the yeast complex IV.

Unambiguous assignment of the complex III dimer to the central part of the supercomplex is facilitated by the characteristic shape and well resolved features of the almost 100-kDa membrane-protruding core 1 and 2 subunit moieties (Fig. 4). This implies that complex IV is peripherally located. One copy is flanking each side of the complex III dimer in the $III_2 + IV_2$ supercomplex, which means that complex IV

is not present as a dimer in the supercomplex, although it is present as a dimer in the crystals used for structure determination (23). It is also obvious that one copy of complex IV is lacking in a substantial number of particles (Fig. 4, *I–N*). Determination of the exact orientation of complex IV was more difficult due to the presence of a detergent shell and less resolved features of the complex IV in the projection maps. The availability of various angular projections of the $III_2 + IV_2$ and $III_2 + IV_1$ supercomplexes turned out to be crucial for an unambiguous assignment of the complex IV orientation and its interaction with the complex III_2 within the supercomplex. A pseudo-atomic model of the whole supercomplex was constructed (see “Experimental Procedures”) and compared with different angular projection maps of the $III_2 + IV_2$ and $III_2 + IV_1$ supercomplexes (Fig. 4, *A*, *D*, *F*, and *J*).

Fig. 5*A* shows the side view of the pseudo-atomic model, which unambiguously matches the EM averaged projection of the $III_2 + IV_2$ supercomplex presented in Fig. 4*A*. In the model, membrane-protruding parts of both complex III_2 and complex

IV closely fit the densities of our EM projection. Furthermore, the stain accumulated areas in the EM projection correspond to low density areas in the model of the supercomplex. The extended width of the EM projection at the membrane plane compared with the atomic model can be explained by the presence of a negative stain-excluding detergent shell. However, molecular flattening of a partially stained membrane part upon air drying cannot be fully excluded and also could explain the observed lateral extensions (43). Fig. 5, *B* and *C*, show that computer generated tilted views of the atomic model closely match the tilted EM projections of the III₂ + IV₂ supercomplex. Finally, Fig. 5*D* shows a close matching of the atomic model of the III₂ + IV₁ supercomplex over the averaged EM projection. Importantly, a close match of the complex IV in our pseudo-atomic model with angular projection maps of the III₂ + IV₂ and III₂ + IV₁ supercomplexes (Fig. 4, *F* and *J*) was exclusively obtained when the complex IV faces the complex III₂ with its convex side which is the opposite of the dimer interface in the x-ray structure of dimeric complex IV (Fig. 5*D*, *inset*). Any other orientation of the complex IV with respect to the complex III₂ did not lead to a consistent fitting into our EM projection maps; there was always at least one map, which did not match with such models. This is exemplified by Fig. 5, *E* and *F*, which show two extreme positions of complex IV that differ by 90 and 180°. These models, depicted as *insets* of Fig. 5, *E* and *F*, clearly do not lead to a close match with one specific tilted view of the III₂ + IV₂ supercomplex. In particular, the matrix exposed part of the complex IV does not fit with resolved EM densities of the III₂ + IV₂ supercomplex (see *red arrows* in Fig. 5, *E* and *F*), which rules out these hypothetical associations of the complex IV to the complex III₂.

Once pseudo-atomic models of the III₂ + IV₂ and III₂ + IV₁ were constructed, truncated two-dimensional projection maps of x-ray models could be generated and compared with EM projection maps (Fig. 6). Visual comparison indicates that the overall shape of generated two-dimensional projection maps is similar to the shape of supercomplexes revealed by single particle EM. Particularly, characteristic features of the complex III₂ revealed in the EM projections are well recognizable in generated two-dimensional projection maps too. Stain accumulated areas in the EM projections of the complex III₂ correspond well to the low density areas in the generated two-dimensional projection maps. Although the presence of detergent reduces resolution of the complex IV in EM projection maps, it is evident that the overall shape and the position of the complex IV in the generated two-dimensional projections are consistent with experimental data.

DISCUSSION

Structural characterization of the individual respiratory chain complexes and their interactions within the inner mitochondrial membrane are of prime importance for a better understanding of oxidative phosphorylation, the major function of mitochondria. Furthermore, recent investigations indicate that respiratory supercomplexes are the building blocks of the higher order structure of the mitochondrial membranes. This publication reports a structural characterization of the yeast III₂ + IV₁₋₂ supercomplexes by single particle electron

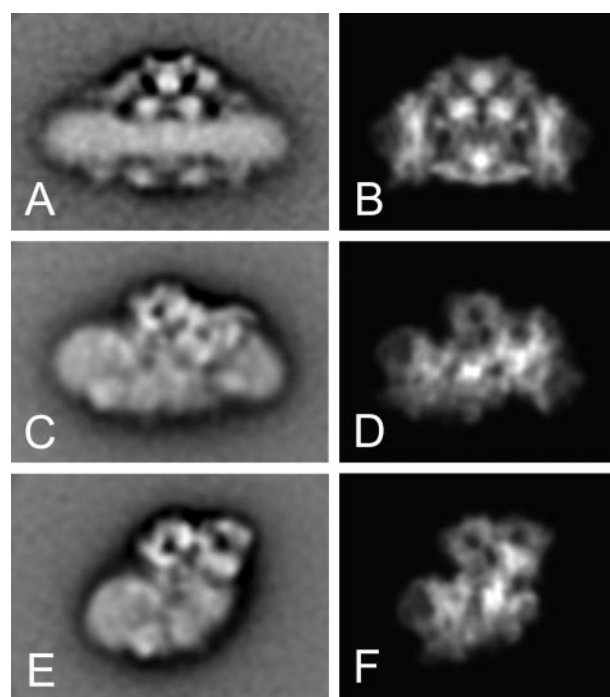


FIGURE 6. Comparison of selected EM projection maps of the III₂ + IV₂ (*A*, *C*) and III₂ + IV₁ (*E*) supercomplexes with two-dimensional projection maps generated from the proposed pseudo-atomic models of the III₂ + IV₂ (*B*, *D*) and III₂ + IV₁ (*F*) supercomplexes at 15 Å resolution.

microscopy. In principle, the optimal way to do such a structural investigation is to perform a three-dimensional reconstruction from low contrast ice-embedded unstained samples. However, this is often not feasible because such labile supercomplexes cannot be purified to homogeneity at a high concentration and need to be kept in the presence of detergent to maintain covering of their hydrophobic surface parts. A good compromise is to perform EM investigations in a classical high-contrast medium, such as the negative stain uranyl acetate. Analysis of a large data set of over 86,000 particle projections revealed various angular two-dimensional projection maps of the III₂ + IV₂ and III₂ + IV₁ supercomplexes at 15 Å resolution in the best classes (Fig. 4), which enabled us to compare our two-dimensional projections with x-ray structures of the yeast complex III and bovine heart complex IV and construct a pseudo-atomic model of the III₂ + IV₂ supercomplex (Fig. 5). Given the resolution of 15 Å for the projection maps, the estimated precision of the fitting is at best at 10 Å, which means that it is not possible to indicate particular amino acid residues involved in the interaction, but valid to indicate subunit interactions that are within 20 Å range of each other. Resolution of different angular EM projections of the III₂ + IV₂ and III₂ + IV₁ supercomplexes was found to be essential for unambiguous determination of the complex IV position and orientation in a pseudo-atomic model. On the basis of simulations, we can conclude that complex IV has to interact with the complex III through its convex side, which is the opposite side of the complex IV dimer interface in the x-ray structure (Fig. 7*B*). Any other orientation of the complex IV within the pseudo-atomic model did not lead to a successful simulation of all resolved EM maps of the III₂ + IV₂ and III₂ + IV₁ supercomplexes (Fig. 5). Generation of trun-

Model of the Yeast Cytochrome Reductase/Oxidase Supercomplex

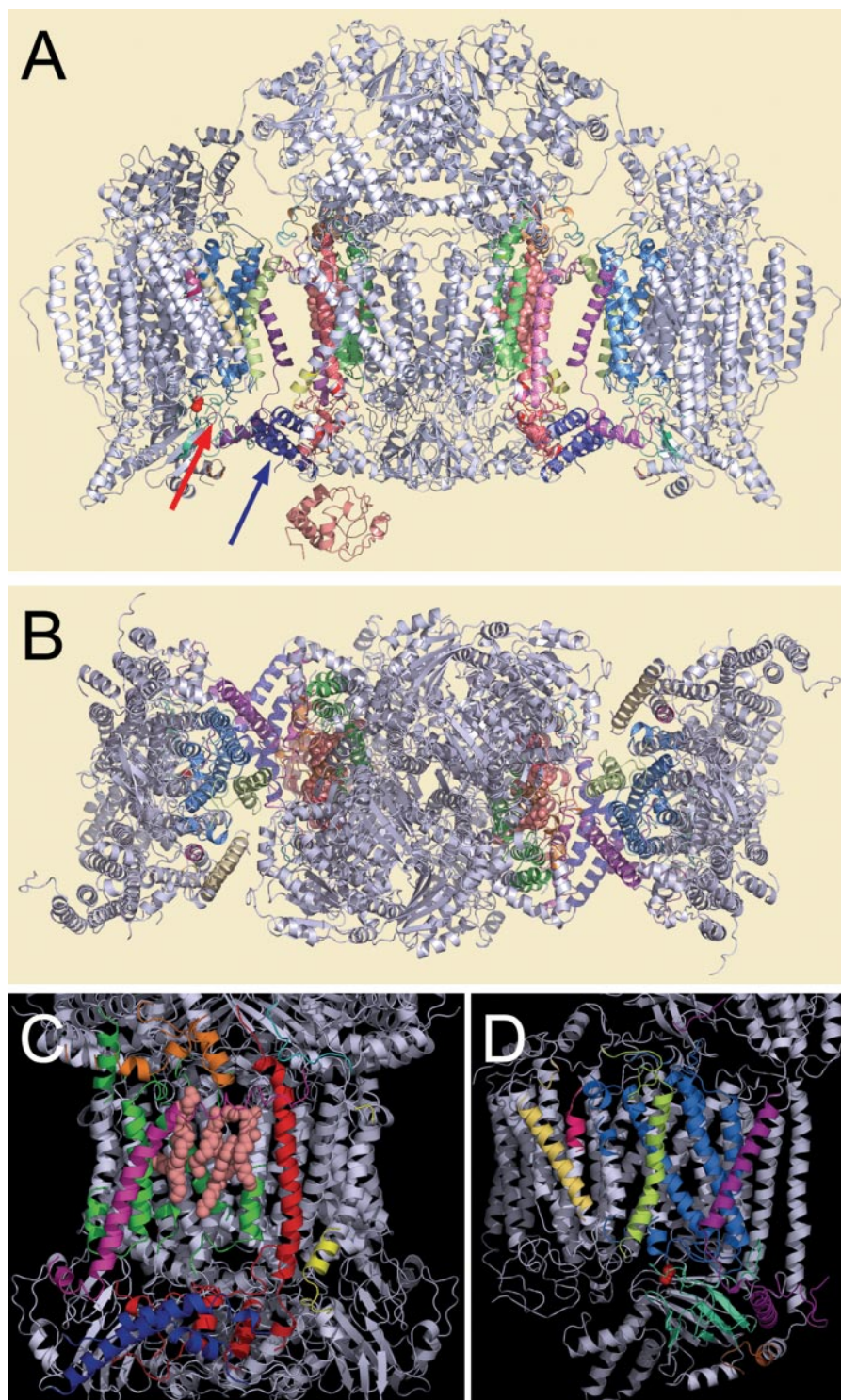


FIGURE 7. Pseudo-atomic model of the $III_2 + IV_2$ supercomplex with attached cytochrome *c*, showing the interactions between complexes III and IV. A, side view of the $III_2 + IV_2$ supercomplex with cytochrome *c*, bound to complex III. Blue and red arrows indicate the hinge protein (QCR6) of complex III and the cytochrome *c* binding pocket of complex IV, respectively. The first electron acceptors of complex IV, Cu_A atoms, are depicted as a red spheres. B, top view of the $III_2 + IV_2$ supercomplex from the matrix side of the membrane. C and D, detailed view on interaction sides of complex III or complex IV showing subunits involved in interaction with either complex IV or complex III, respectively. Helices and loops of the complex III and IV, which are within 20 Å distance of each other, are highlighted in colors: green, cytochrome *b*; red, cytochrome *c*₁; cyan, RIP1; blue, QCR6 (hinge protein); orange, subunit QCR7; light magenta, subunit QCR8; yellow, QCR9; salmon, cardiolipin and phosphatidyl ethanolamine molecules of the complex III and subunits Cox I (navy blue), Cox II (green cyan), Cox III (hot pink), Cox IV (purple), Cox VIc (brown), Cox VIIa (yellow orange), and Cox VIIc (green yellow) of the complex IV, respectively.

cated two-dimensional projection maps of x-ray models revealed similar density profiles observed in EM projection maps (Fig. 6), which further supports the correctness of our proposed model. Cox I, Cox II, Cox III, Cox IV, Cox VIc, Cox VIIa, and Cox VIIc subunits of complex IV were found to be involved in varying degrees in the interaction with complex III (Fig. 7D). Although involvement of Cox I, Cox II, and Cox III in interaction with complex III has been predicted previously by deletion studies, the exact orientation of the complex IV relative to complex III remained unclear (21, 25). It is important to realize that due to a different nomenclature Cox IV, CoxVIc, Cox VIIa, and Cox VIIc in mammals refer to CoxV, CoxVIIa, CoxVII, and CoxVIII in yeast, respectively. On the complex III_2 side, cytochrome *b*, cytochrome *c*₁, QCR6 (hinge protein), QCR7, QCR8, QCR9, cardiolipin, and phosphatidylethanolamine molecules were identified at the complex III_2 -IV interface (Fig. 7C). Although cytochrome *b* and cytochrome *c*₁ were considered as the most likely candidates for a direct link between complexes III and IV (5, 25, 21), direct evidence supporting their gluing function was missing so far. Similarly, there was no structural evidence proving a close position of QCR6, QCR7, QCR8, and QCR9 to the complex III-IV interaction side. Localization of cardiolipin at the complex III-IV interaction interface further supports its essential role in formation of yeast supercomplexes, as was recently reported (20, 21). In addition, the fitting of the complexes within the supercomplex was generally close for all parts, except for the Rieske FeS subunit of complex III. However, this subunit is known to undergo conformational changes of about 20 Å during catalysis (26).

Previous investigations have indicated that purified bovine heart complex IV is in either a monomeric or a dimeric state, depending on the presence of lipids and the type of

Model of the Yeast Cytochrome Reductase/Oxidase Supercomplex

detergent used for solubilization. In the three-dimensional crystals, which were used for x-ray crystallography, complex IV is dimeric (27). However, the nature and the physiological significance of the dimer is still a matter of debate. Intermonomer interactions are strong enough to prevent the dimer from spontaneous dissociation and thus the dimeric state could be dominant in the membrane (27). Surprisingly, BN-PAGE does not reveal complex IV forms outside the $\text{III}_2 + \text{IV}_{1-2}$ supercomplexes, neither in monomeric nor in dimeric form (Fig. 1 and 2). The supercomplex-bound form of complex IV is always a monomer. However, since the proposed interface important for complex IV dimerization is on the opposite side of the complex IV-complex III_2 interface, the $\text{III}_2 + \text{IV}_{1-2}$ supercomplex structures do not exclude the possibility of complex IV-complex IV interactions in *in vivo* conditions. Occurrence of these interactions would allow oligomerization of $\text{III}_2 + \text{IV}_2$ supercomplexes into long “string”-like structures, which previously were proposed for mammalian mitochondria (28). However, we found no direct evidence for the presence of such strings in yeast, e.g. particles of dimeric complex IV bound to dimeric complex III. In contrast a couple of dozen $\text{III}_2 + \text{IV}_2$ supercomplex particles were found, which include 1–2 copies of cytochrome *c* (see below). Therefore, complex IV-complex IV binding, if existing at all, seems to be at least weaker than binding of cytochrome *c* to the $\text{III}_2 + \text{IV}_2$ supercomplex in yeast. This does not necessarily imply that mitochondria from other organisms need to have the same type of membrane complex organization. In bovine mitochondria, the ratio of complex IV to III is two times higher than in yeast (2). Another difference is that complex I, which is absent in *S. cerevisiae*, is expected to interact with the $\text{III}_2 + \text{IV}_{1-2}$ supercomplexes in other organisms.

Single particle analysis indicated small numbers of an additional protein binding at the interface of complexes III and IV at one or two positions (Fig. 4, *O* and *P*). The fuzzy appearance in the average map of Fig. 4*O* indicates small flexibilities upon binding which results in a smeared-out projection density. It is interpreted as cytochrome *c*, because this protein is known to bind at this side of complexes III and IV. It was shown in yeast that cytochrome *c* is protected from degradation by interaction with both complex III and complex IV (29). We can suggest that some of the 75 particles, which were used for the class sum shown in Fig. 4*O*, represent situations in which cytochrome *c* is in an intermediate position between the two binding sites. Subunits like, e.g. the hinge protein of complex III, which was found to be essential for a binding of cytochrome *c* to complex III (44), can be important for transfer and channeling of cytochrome *c* from complex III to complex IV. The short distance between the cytochrome *c* binding sites on complexes III and IV can facilitate electron transfer mediated by cytochrome *c* within the supercomplex (Fig. 7*A*). Previous x-ray data and computing simulations indicated that the distance between the heme iron of cytochrome *c* and either the heme iron of the cytochrome c_1 (electron donor of the complex III) or the Cu_A atom (the first electron acceptor of the complex IV), is about 18 Å, which allows a direct electron transfer between appropriate redox pairs and cytochrome *c* (22, 30). Taking the above mentioned distances into account, our pseudo-atomic model of the supercomplex shows that cytochrome *c* has to move and rotate

within 40 Å to be able to mediate electron transfer between the complexes III and IV.

In conclusion, our data indicate one single and specific type of interaction between complexes III and IV in yeast but no higher ordering of these supercomplexes into strings or other types of oligomers. This is in contrast to the V_2 supercomplex, which appears to form a defined type of oligomer in which dimeric ATP synthase supercomplexes associate in long rows (3, 15, 16). There is increasing evidence that this oligomer has a special function of inducing local membrane curvature, because the ATP synthase monomers within the oligomers make angles of 35–90° with their neighbors across and along the direction of the oligomers. In contrast the $\text{III}_2 + \text{IV}_2$ supercomplex is a flat structure embedded within the membrane plane. Because the membrane is strongly negative stain-excluding, the overall position of the lipid membrane can be fitted as indicated in Fig. 5*A*. The fitting is in agreement with the position of the membrane-spanning helices according to the atomic models (22, 23). The fitting shows that the membrane could be slightly curved (up to 4°), but certainly not very much kinked as it was found for the ATP synthase dimer (16). Hence we conclude that it does not have a defined role in folding of the inner mitochondrial membrane. However, formation of the $\text{III}_2 + \text{IV}_2$ supercomplex most likely has important physiological implications, because electron transport between complex III_2 and complex IV can be realized by a simple ping-pong movement of cytochrome *c* between the these two complexes. Indeed the cytochrome *c* binding sites on complex III_2 and complex IV within the supercomplex are in very close proximity. It was previously shown by inhibitor titration experiments that cytochrome *c* does not exhibit pool behavior in yeast and that the whole respiratory chain of yeast behaves like a single functional unit (7). Our structural data suggest that the $\text{III}_2 + \text{IV}_2$ supercomplex forms the core of this functional unit in yeast and probably in many other species.

Acknowledgment—We thank Jan Tiesinga (Department of Biophysical Chemistry, University of Groningen) for help with modeling.

REFERENCES

1. Saraste, M. (1999) *Science* **283**, 1488–1493
2. Schägger, H. (2002) *Biochim. Biophys. Acta* **1555**, 154–159
3. Dudkina, N. V., Heinemeyer, J., Sunderhaus, S., Boekema, E. J., and Braun, H. P. (2006a) *Trends Plant Sci.* **11**, 232–240
4. Heinemeyer, J., Dudkina, N. V., Boekema, E. J., and Braun, H. P. (2007) in *Plant Mitochondria, Annual Plant Reviews Series* (Logan, D. C., ed) Blackwell Publishing, Oxford, UK, in press
5. Cruciat, C. M., Brunner, S., Baumann, F., Neupert, W., and Stuart, R. A. (2000) *J. Biol. Chem.* **275**, 18093–18098
6. Schägger, H., and Pfeiffer, K. (2000) *EMBO J.* **19**, 1777–1783
7. Boumans, H., Grivell, L. A., and Berden, J. A. (1998) *J. Biol. Chem.* **273**, 4872–4877
8. Berry, E. A., and Trumpower, B. L. (1985) *J. Biol. Chem.* **260**, 2458–2467
9. Stroh, A., Anderka, O., Pfeiffer, K., Yagi, T., Finel, M., Ludwig, B., and Schägger, H. (2004) *J. Biol. Chem.* **279**, 5000–5007
10. Mannella, C. A. (2006) *Biochim. Biophys. Acta* **1763**, 542–548
11. Schwerzmann, K., Cruz-Orive, L. M., Eggman, R., Sängler, A., and Weibel, E. R. (1986) *J. Cell Biol.* **102**, 97–103
12. Allen, R. D., Schroeder, C. C., and Fok, A. K. (1989) *J. Cell Biol.* **108**, 2233–2240

Model of the Yeast Cytochrome Reductase/Oxidase Supercomplex

13. Dudkina, N. V., Eubel, H., Keegstra, W., Boekema, E. J., and Braun, H. P. (2005a) *Proc. Natl. Acad. Sci. U. S. A.* **102**, 3225–3229
14. Minauro-Sanmiguel, F., Wilkens, S., and Garcia, J. J. (2005) *Proc. Natl. Acad. Sci. U. S. A.* **102**, 12356–12358
15. Dudkina, N. V., Heinemeyer, J., Keegstra, W., Boekema, E. J., and Braun, H. P. (2005b) *FEBS Lett.* **579**, 5769–5772
16. Dudkina, N. V., Sunderhaus, S., Braun, H. P., and Boekema, E. J. (2006b) *FEBS Lett.* **580**, 3427–3432
17. Paumard, P., Vaillier, J., Couly, B., Schaeffer, J., Soubannier, V., Mueller, D. M., Brethes, D., di Rago, J. P., and Velours, J. (2002) *EMBO J.* **2**, 221–230
18. Giraud, M. F., Paumard, P., Soubannier, V., Vaillier, J., Arselin, G., Salin, B., Schaeffer, J., Brèthes, D., di Rago, P., and Velours, J. (2002) *Biochim. Biophys. Acta* **1555**, 174–180
19. Schäfer, E., Seelert, H., Reifschneider, N., Krause, F., Dencher, N. A., and Vonck, J. (2006) *J. Biol. Chem.* **281**, 15370–15375
20. Zhang, M., Mileykovskaya, E., and Dowhan, W. (2002) *J. Biol. Chem.* **277**, 43553–43556
21. Pfeiffer, K., Gohil, V., Stuart, R. A., Hunte, C., Brandt, U., Greenberg, M. L., and Schägger, H. (2003) *J. Biol. Chem.* **278**, 52873–52880
22. Lange, C., and Hunte, C. (2002) *Proc. Natl. Acad. Sci. U. S. A.* **99**, 2800–2805
23. Tsukihara, T., Aoyama, H., Yamashita, E., Tomizaki, T., Yamaguchi, H., Shinzawa-Itoh, K., Nakashima, R., Yaono, R., and Yoshikawa, S. (1996) *Science* **272**, 1136–1144
24. Khalimonchuk, O., and Rödel, G. (2005) *Mitochondrion* **5**, 363–388
25. Schägger, H. (2001) *IUBMB Life* **52**, 119–128
26. Zhang, Z., Huang, L., Shulmeister, V. M., Chi, Y. L., Kim, K. K., Hung, L. W., Crofts, A. R., Berry, E. A., and Kim, S. H. (1998) *Nature* **392**, 677–684
27. Lee, S. J., Yamashita, E., Abe, T., Fukumoto, Y., Tsukihara, T., Shinzawa-Itoh, K., Ueda, H., and Yoshikawa, S. (2001) *Acta Crystallogr. Sect. D Biol. Crystallogr.* **57**, 941–947
28. Wittig, I., Carrozzo, R., Santorelli, F. M., and Schägger, H. (2006) *Biochim. Biophys. Acta* **1757**, 1066–1072
29. Pearce, D. A., and Sherman, F. (1995) *Proc. Natl. Acad. Sci. U. S. A.* **92**, 3735–3739
30. Roberts, V. A., and Pique, M. E. (1999) *J. Biol. Chem.* **274**, 38051–38060
31. Meisinger, C., Pfanner, N., and Truscott, K. N. (2006) *Methods Mol. Biol.* **313**, 33–39
32. Schägger, H., and von Jagow, G. (1991) *Anal. Biochem.* **199**, 223–231
33. Wittig, I., Braun, H. P., and Schägger, H. (2006) *Nat. Protocols* **1**, 418–428
34. Sunderhaus, S., Eubel, H., and Braun, H. P. (2006) in *Mitochondrial Genomics and Proteomics Protocols, Methods in Molecular Biology Series* (Leister, D., and Herrmann, J., eds) Humana Press, Totowa, NJ, in press
35. Neuhoff, V., Arold, N., Taube, D., and Ehrhardt, W. (1988) *Electrophoresis* **9**, 255–262
36. Zerbetto, E., Vergani, L., and Dabbeni-Sala, F. (1997) *Electrophoresis* **18**, 2059–2064
37. Penczek, P., Radermacher, M., and Frank, J. (1992) *Ultramicroscopy* **40**, 33–53
38. Ludtke, S. J., Baldwin, P. R., and Chiu, W. (1999) *J. Struct. Biol.* **128**, 82–97
39. Van Heel, M., Gowen, B., Matadeen, R., Orlova, E. V., Finn, R., Pape, T., Cohen, D., Stark, H., Schmidt, R., Schatz, M., and Patwardhan, A. (2000) *Q. Rev. Biophys.* **33**, 307–369
40. Van Heel, M. (1987) *Ultramicroscopy* **21**, 95–100
41. Guex, N., and Peitsch, M. C. (1997) *Electrophoresis* **18**, 2714–2723
42. DeLano, W. L. (2002) *The PyMOL Molecular Graphics System*, DeLano Scientific, San Carlos, CA
43. Harris, J. R., and Horne, R. W. (1994) *Micron* **25**, 5–13
44. Kim, C. H., and King, T. E. (1983) *J. Biol. Chem.* **258**, 13543–13551



Respiratory chain supercomplexes in the plant mitochondrial membrane

Natalya V. Dudkina^{1,*}, Jesco Heinemeyer^{2,*}, Stephanie Sunderhaus², Egbert J. Boekema¹ and Hans-Peter Braun²

¹Department of Biophysical Chemistry, GBB, University of Groningen, Nijenborgh 4, 9747 AG Groningen, The Netherlands

²Institute for Plant Genetics, Faculty of Natural Sciences, Universität Hannover, Herrenhäuser Str. 2, 30419 Hannover, Germany

The intricate, heavily folded inner membrane of mitochondria houses the respiratory chain complexes. These complexes, together with the ATP synthase complex, are responsible for energy production, which is stored as ATP. The structure of the individual membrane-bound protein components has been well characterized. In particular, the use of Blue-native polyacrylamide gel electrophoresis has been instrumental in recent years in providing evidence that these components are organized into supercomplexes. Single particle electron microscopy studies have enabled a structural characterization of some of the mitochondrial supercomplexes. This has provided the opportunity to define a functional role for these supercomplexes for the first time, in particular for the dimeric ATP synthase complex, which appears to be responsible for the folding of the inner mitochondrial membrane.

Structure and function of the mitochondrial OXPHOS system

The mitochondrial oxidative phosphorylation (OXPHOS) system consists of four multi-subunit oxidoreductases involved in respiratory electron transport (Complexes I to IV) and the ATP synthase complex (Complex V). Except for Complex I, a considerable amount of information is known about the structure of the OXPHOS complexes of fungi and animals based on X-ray crystallography and biochemical investigations.

Complex I

Complex I (NADH-ubiquinone oxidoreductase) is the major entrance point of electrons to the respiratory chain [1]. It has a molecular mass of ~1 MDa and is composed of two elongated domains that together form an L-like structure. One domain is localized within the inner mitochondrial membrane and is involved in proton translocation; the other domain protrudes out of the plain of the membrane into the mitochondrial matrix and is responsible for oxidation of NADH. Approximately 40 different subunits are known to form part of Complex I [2,3].

Corresponding authors: Boekema, E.J. (e.j.boekema@rug.nl), Braun, H-P. (braun@genetik.uni-hannover.de).

* These authors contributed equally to this article.

Available online 17 April 2006

Complex II

Complex II (succinate-ubiquinone oxidoreductase) is a second entrance point of electrons to the respiratory chain [4,5]. It is the smallest complex of the OXPHOS system and consists of two soluble matrix-exposed subunits that are attached to two hydrophobic membrane proteins.

Complex III

Complex III (ubiquinol-cytochrome *c* oxidoreductase) represents the central component of the OXPHOS system [6,7]. It is a functional dimer of ~500 kDa composed of 2×10 or 11 distinct subunits. About a quarter of the complex is embedded within the inner mitochondrial membrane, a small part protrudes out into the mitochondrial intermembrane space and a larger part protrudes into the mitochondrial matrix.

Complex IV

Complex IV (cytochrome *c*-O₂ oxidoreductase) represents the terminal complex of the respiratory chain [8,9]: 12 to 13 subunits together form a monomer of ~220 kDa. It can exist as a monomer or a dimer within the membrane.

Complex V

The ATP synthase complex (Complex V) is a bipartite structure composed of a so-called F₁ headpiece within the mitochondrial matrix, which is anchored to a hydrophobic F₀-part within the inner mitochondrial membrane [10]. The two parts of Complex V are linked by a central stalk that rotates during catalysis and by a peripheral stalk that prevents rotation of the entire headpiece. The rotation of subunits within the two subcomplexes of Complex V is caused by the proton gradient across the inner mitochondrial membrane and forms the basis for phosphorylation of ADP. Complex V comprises ~15 distinct subunits, which partially are present in multiple copies within the holo-enzyme. The total molecular mass of Complex V is between 500 and 600 kDa.

Structure and function of the mitochondrial OXPHOS system in plants

The general structure and function of the plant OXPHOS complexes is considered to be closely related to those of the heterotrophic eukaryotes, although no particular structures have been analysed by X-ray crystallography. All five complexes include similar numbers of subunits, most

of which are homologous to components of the corresponding yeast or bovine protein complexes [11]. However, some plant-specific subunits occur, which in some cases introduce side-activities into OXPHOS complexes. In all organisms, the acyl carrier protein of the mitochondrial fatty acid biosynthesis pathway forms part of Complex I [12,13]. In addition, in plants, L-galactono-1,4-lactone dehydrogenase (which represents the terminal enzyme of the mitochondrial ascorbic acid biosynthesis pathway) and carbonic anhydrases form part of Complex I [14,15]. Complex III includes the two subunits of the mitochondrial processing peptidase in plants, which is responsible for removing mitochondrial pre-sequences from nuclear-encoded mitochondrial proteins after transport has been completed [16]. Also, complexes II and IV include some additional plant-specific subunits that probably integrate extra functions into these OXPHOS complexes [17,18].

The functional context of mitochondrial respiration differs in autotrophic and heterotrophic organisms. In plants, mitochondria and plastids are involved in the redox balance of the cell [19]. Furthermore, mitochondria indirectly participate in photosynthesis through the 'photorespiration' pathway. Probably to accomplish these extra functions, additional oxidoreductases form part of the OXPHOS system in plants, such as the 'alternative oxidase' and three to four different 'rotenone-insensitive NAD(P)H dehydrogenases' [20–23]. All these enzymes participate in electron transport without contributing to the proton gradient across the inner mitochondrial membrane and therefore appear to catalyse wasteful reactions that are nevertheless considered to be of great importance under certain physiological conditions. Structurally, these enzymes do not form part of multi-enzyme complexes but instead exist as monomers or homo-dimers [22]. Unlike the classical OXPHOS enzyme complexes, which include nuclear and mitochondrially encoded subunits, these enzymes are all encoded by the nuclear genome.

Fluid state versus Solid state model of the OXPHOS system

The supramolecular organization of the OXPHOS system in mitochondria is a matter of debate. According to the 'Fluid-state' model, the five OXPHOS complexes independently diffuse within the inner mitochondrial membrane; electron transfer from one complex to another is based on random collisions between the complexes. By contrast, the 'Solid-state' model postulates stable interactions between the OXPHOS complexes under *in vivo* conditions. Experimental results supporting the Fluid-state model are based on the finding that all OXPHOS complexes can be biochemically purified in an enzymatically active form, and on diffusion rate measurements of OXPHOS complexes reconstituted into phospholipid vesicles (reviewed in [24]). The Solid-state model is supported by results obtained by reconstitution experiments [25,26], flux control experiments [27,28], and results concerning mutants with respect to subunits of individual OXPHOS complexes that specifically affect other OXPHOS complexes [29–31]. A useful strategy to investigate the supramolecular association of the OXPHOS proteins

is based on mild solubilization of mitochondrial membranes using non-ionic detergents and separation of the solubilized protein complexes using Blue-native polyacrylamide gel electrophoresis (BN-PAGE) [32,33]. Using this strategy, defined supercomplexes could be described that have a I+III₂, III₂+IV₁₋₂, I+III₂+IV₁₋₄ and V₂ composition (Figure 1 and Table 1). Here we highlight recent studies of the plant OXPHOS mitochondrial system that used BN-PAGE and other biochemical procedures to investigate the supramolecular association of the OXPHOS proteins. Some of the respiratory supercomplexes discovered are extremely stable in plants, enabling their low-resolution structure to be defined by single particle electron microscopy (EM) for the first time [15,34,35].

Methodological strategies for characterizing mitochondrial supercomplexes in plants

BN-PAGE has proved to be a powerful procedure for characterizing mitochondrial supercomplexes. The method is based on solubilizing mitochondrial membranes with non-ionic detergents and incubating the generated protein fractions with Coomassie-blue, which introduces negative charge into proteins without denaturing them [36]. Protein complexes and supercomplexes are subsequently resolved on polyacrylamide gradient gels. Upon combining with SDS-PAGE as the second gel dimension, complexes are dissected into their subunits, which form vertical rows of spots on the resulting 2D gels (Figure 1a,c–h). Alternatively, first dimension BN-PAGE can be combined with a second BN-PAGE (BN/BN-PAGE), which is carried out in the presence of a different detergent. For example, protein solubilization and the first gel dimension are carried out in the presence of digitonin and the second gel dimension in the presence of dodecylmaltoside. All supercomplexes specifically destabilized by the conditions of the second gel dimension are (partially) dissected into protein complexes, which migrate beneath the diagonal line on the resulting 2D gels (Figure 1b). Both 2D gel systems enable the supramolecular association of proteins of the OXPHOS system and of other systems (e.g. the photosystem-supercomplexes of chloroplasts) to be investigated [37].

Supercomplexes of sufficient stability can be structurally analysed by single particle EM. For this approach, isolated mitochondria are treated with non-ionic detergents and supercomplexes are resolved by sucrose gradient ultracentrifugation. Selected fractions can be directly used for EM analyses and image processing [15,34,35].

Complex I and the I+III₂ supercomplex of plants

Until recently, our knowledge of the composition and configuration of plant Complex I was limited. The location of most of the ~40 subunits within the L-shaped complex is still not known. However, some useful conclusions can be drawn from a comparison of the low-resolution structure of a series of Complex I molecules of animals and fungi obtained by EM (<http://www.scripps.edu/biochem/CI/research.html>). A structural scheme of the *Arabidopsis* Complex I is presented in Figure 2. The complex

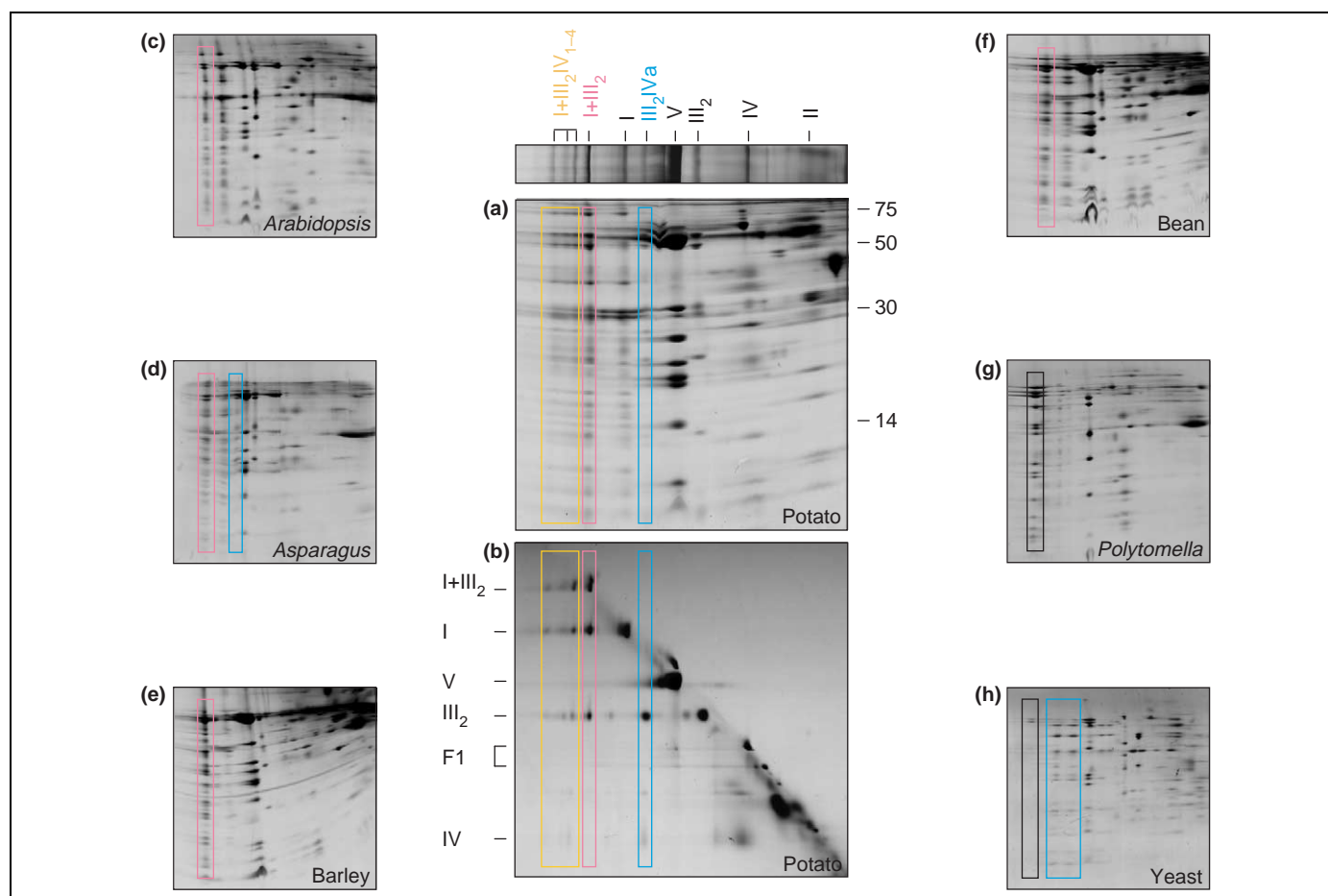


Figure 1. Separation of mitochondrial protein complexes by BN-PAGE. Mitochondrial fractions from potato, *Arabidopsis*, *Asparagus*, barley, bean, *Polytomella* and yeast were treated by digitonin (3 g detergent/g mitochondrial protein) and prepared for gel electrophoresis by addition of Coomassie Blue. Separation of mitochondrial protein complexes and supercomplexes from potato by (a) 2D BN/SDS-PAGE and (b) 2D BN/BN-PAGE (protocols according to [64] and [65]). Identity of protein complexes and supercomplexes of the OXPHOS system are indicated above the BN/SDS gel (a) and to the left of the BN/BN gel (b). Abbreviations: I+III₂+IV₁₋₄, supercomplex composed of Complex I, dimeric Complex III and 1-4 copies of Complex IV (boxed in yellow); I+III₂, supercomplex composed of Complex I and dimeric Complex III (boxed in pink); I, Complex I; V, ATP synthase complex; III₂, dimeric Complex III; III₂+IV, supercomplex composed of dimeric Complex III and Complex IV (boxed in blue); IV, Complex IV; II, Complex II. The molecular masses of standard proteins are given to the right of (a) (in kDa). Separation of mitochondrial protein complexes and supercomplexes from (c) *Arabidopsis*, (d) *Asparagus* (S. Sunderhaus, unpublished), (e) barley, (f) bean, (g) *Polytomella* and (h) yeast by BN/SDS-PAGE. Pink boxes indicate a supercomplex composed of Complex I and dimeric Complex III and blue boxes indicate a supercomplex composed of dimeric Complex III and Complex IV. Black boxes indicate a supercomplex composed of two ATP synthase complexes. (a) and (b) reproduced, with permission, from Ref. [44].

Table 1. OXPHOS supercomplexes in mitochondria identified by Blue-native PAGE^a

| Organism | V ₂ | I+III ₂ | III ₂ +IV ₁₋₂ | I+III ₂ +IV ₁₋₄ | Refs ^b |
|---------------------------------|----------------|--------------------|-------------------------------------|---------------------------------------|-------------------|
| <i>Arabidopsis</i> | X | X | | | [17,49] |
| Barley | | X | | | [17] |
| Bean | | X | | | [17] |
| Potato | | X ^c | X | X | [17,44] |
| Spinach | X | X | X | X | [48] |
| Tobacco | | X | | | [66] |
| Pea | | X | | | [67] |
| Sunflower | | | | (X) ^d | [68] |
| <i>Asparagus</i> | | X | X | | ^g |
| <i>Chlamydomonas</i> | X | | | | [55] |
| <i>Polytomella</i> | X | X | | | [35,56] |
| <i>Saccharomyces cerevisiae</i> | X | - ^e | X | - ^e | [32,33] |
| <i>Podospira anserina</i> | X | X ^f | | X ^f | [69] |
| Bovine | X | X | X | X | [33] |
| <i>Homo sapiens</i> | | X | | X | [70] |

^aEmpty cells in the table indicate that, to date, the corresponding supercomplexes have not been discovered, which could be due to low stability or their absence under *in vivo* conditions.

^bReference including the first report on the occurrence of a specific supercomplex.

^cIn potato two forms of I+III supercomplexes occur, which have I+III₂ and I₂+III₄ composition.

^dIn sunflower, a complex IV containing supercomplex of >1000 kDa was described, which probably has I+III₂+IV₁₋₄ composition.

^eThe respiratory chain of *Saccharomyces cerevisiae* does not include complex I, therefore complex-I-containing supercomplexes are absent.

^fIn *Podospira anserina*, Complex I containing supercomplexes were reported to have I₂ and I₂III₂ composition.

^gS. Sunderhaus, unpublished. See Figure 1d.

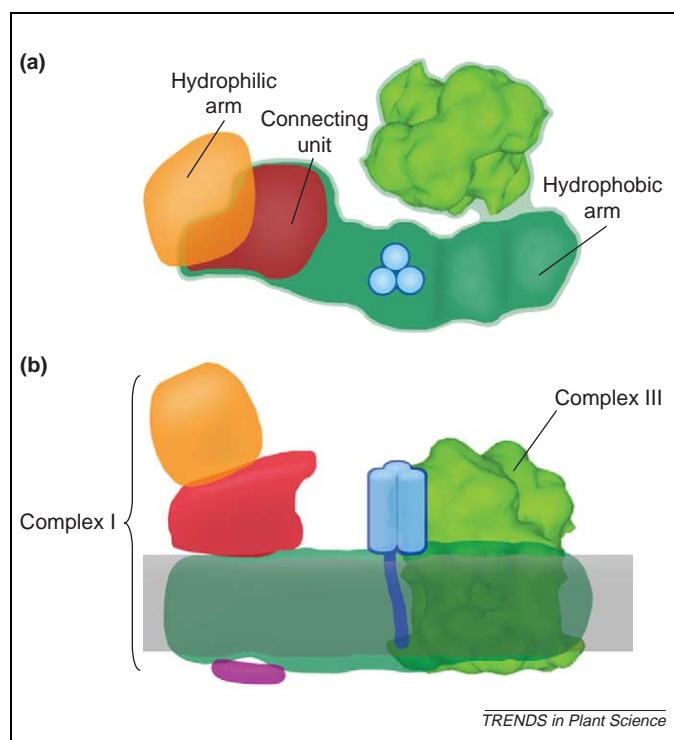


Figure 2. Structural scheme of the plant I + III₂ supercomplex within the membrane plane (a) and from the side (b). The L-shaped Complex I comprises a membrane-bound hydrophobic arm (dark green) and a hydrophilic arm consisting of the NADH oxidizing unit (orange) and the connecting unit (red). These features have also been observed by electron microscopy in yeast and bovine mitochondria [1]. The NADH oxidizing unit is loosely attached in plants and algae but appears to be lacking in cyanobacteria [38]. A second hydrophilic protrusion (blue) is firmly fixed at the centre. It has been assigned to the heterotrimer of carbonic anhydrase and is present in the plant *Arabidopsis* and the alga *Polytomella* [15], but not in cyanobacteria [38]. An unknown third mass (not shown) is present at the tip of the hydrophobic arm in *Polytomella* [15] but not in *Arabidopsis*. A small intermembrane space-exposed protrusion (purple) is specific for *Arabidopsis* and *Polytomella* [15] but absent in Complex I particles from other organisms. Complex III (bright green) is connected to the membrane arm of Complex I mainly via its membrane-inserted portion.

is L-shaped, with a membrane-bound hydrophobic domain (dark green) and a matrix exposed hydrophilic domain (red and orange). The NADH oxidizing unit (orange) is loosely attached in *Arabidopsis* and in the alga *Polytomella* because breakdown products are often observed [15,34]. However, the NADH oxidizing unit appears to be absent in cyanobacteria [38]. A small intermembrane-space-exposed protrusion (purple) is specific for *Arabidopsis* and *Polytomella* [15,34] but absent in the Complex I particles of animals and fungi. Another striking special feature of the Complex I of plants and algae is the presence of a second matrix-exposed domain that is attached to the central part of the membrane arm (blue mass, Figure 2) [15,34]. Complex I from plants includes approximately ten plant-specific subunits [39,40], between three and five of which resemble a γ -type carbonic anhydrase of the archaeobacterium *Methanosarcina thermophila* [41,42]. Analyses of Complex I sub-complexes of *Arabidopsis* using mass spectrometry and protease protection experiments suggest that the carbonic anhydrase subunits represent the second matrix-exposed domain of Complex I [15]. These subunits are probably present as a heterotrimer because the plant proteins have trimer-specific homologies to the archaeobacterial protein.

The carbonic anhydrase domain appears to be firmly attached to the membrane arm of Complex I because no particles without this protrusion were observed; this is probably achieved by membrane-inserted helical anchors close to the C-termini of the proteins. Possibly these carbonic anhydrases of Complex I are involved in an inner-cellular carbon transport system in higher plants that resembles the carbon concentration system of cyanobacteria [43]. Carbonic anhydrases also form part of the cyanobacterial Complex I. However, they do not form a similar second luminal-exposed domain upon EM analysis (A.A. Arteni *et al.*, unpublished). An unknown third additional mass is present at the tip of the hydrophobic arm in *Polytomella* [15] but not in *Arabidopsis*.

On BN gels, Complex I forms part of a 1.5 MDa supercomplex that includes dimeric Complex III (Figure 1). This supercomplex is composed of all visible subunits of Complex I and Complex III and consequently is assumed to comprise at least 50 different types of polypeptides [17]. Using BN/PAGE, the supercomplex becomes partially dissected into monomeric Complex I and dimeric Complex III (Figure 1b). No additional protein components form part of the I + III₂ supercomplex. In contrast to yeast and bovine mitochondria [33], the I + III₂ supercomplex of plant mitochondria is one of the dominant structures on BN gels, indicating high abundance or stability. More than 50% of Complex I is present within the I + III₂ supercomplex in potato and barley and ~50% of Complex I forms part of the supercomplex in *Arabidopsis*, *Asparagus*, bean and *Polytomella* [17,35,44]. Based on flux control experiments and BN-PAGE, supercomplexes and corresponding monomeric OXPHOS complexes are assumed to co-exist in mitochondria under *in vivo* conditions [28,44] and possibly assemble and disassemble in a dynamic manner. In potato, tissue-specific differences concerning supercomplex occurrence were observed [44]. Because of its high stability, the I + III₂ supercomplex of *Arabidopsis* was the first OXPHOS supercomplex to be characterized by single particle EM [34].

Computer modelling using the three-dimensional structure of bovine Complex III (reviewed in [5]) and the single particle EM structure of *Neurospora* and bovine Complex I [45,46] revealed that the interaction between both structures is within the membrane and that the matrix exposed hydrophilic parts of both complexes are not in close contact (Figure 2) [34]. Complex III is laterally attached to the membrane arm of Complex I, which is slightly bent around Complex III. The high stability of the I + III₂ supercomplex in plants might be due to the length of the membrane arm of Complex I, which is extended compared with the corresponding arm in animals and fungi (~230 Å versus ~190 Å). The physiological implications of the interaction between Complexes I and III₂ are not yet fully understood. The bovine I + III₂ supercomplex was shown to have higher NADH:cytochrome *c* oxidoreductase activity than the corresponding separate complexes under *in vitro* conditions [33]. This increase in activity can probably not be explained by direct ubiquinone channeling because the ubiquinone reduction site is believed to be located at the membrane arm close to its

interface with the matrix arm [1]. However, the physiology of the membrane arm of Complex I is largely unknown. It is speculated to include further proton (and other) translocation activities that might interact with the physiological processes of Complex III.

The III₂+IV and I+III₂+IV₁₋₄ supercomplexes of plants

Analyses of bovine mitochondria by BN-PAGE revealed abundant supercomplexes consisting of the OXPHOS complexes I, III₂ and IV [33]. Up to four copies of Complex IV are present within these supercomplexes. Corresponding particles were given the name ‘respirasomes’ because they can autonomously carry out respiration in the presence of the mobile electron carriers ubiquinone and cytochrome *c*. In mitochondria of *Saccharomyces cerevisiae*, which do not contain Complex I, stable III₂+IV₁₋₂ supercomplexes were described by BN-PAGE [33,47]. These particles were also identified in bovine mitochondria but are of lower concentration [33]. In plants, supercomplexes containing Complexes III and IV are of low abundance on BN gels (Figure 1). Respirasomes were described for potato and spinach and a III₂+IV supercomplex for potato, spinach and *Asparagus* [44,48]. Hardly any Complex IV-containing supercomplexes were observed in *Arabidopsis* upon analysis by BN-PAGE and, to date, no single particle EM structures have been published of Complex IV-containing supercomplexes from any organism.

Dimeric ATP synthase supercomplex of plants

A dimeric ATP synthase supercomplex was first discovered for yeast mitochondria by BN/SDS-PAGE [32]. The supercomplex includes dimer-specific subunits termed e, g and k. More recently, a dimeric ATP synthase supercomplex was described for *Arabidopsis* on the basis of BN-PAGE [17,49]. This supercomplex is most stable upon solubilization of mitochondrial membranes using low Triton X-100 concentrations, which was previously reported for yeast [32]. However, compared with the I+III₂ supercomplex, dimeric ATP synthase is a fragile structure in higher plants. Disruption of the nuclear gene encoding the yeast subunit g led to the absence of dimers, indicating an important role for this protein in supercomplex assembly or stability. Ultrastructural studies on this yeast mutant also indicated that cristae were absent, which led to the suggestion that dimeric ATP synthase is essential for folding the inner mitochondrial membrane into cristae [50,51]. A similar prevention of cristae formation was described upon *in vivo* crosslinking of F₁ headpieces in yeast [52]. Previously, oligomeric ATP synthase complexes were identified by rapid-freeze deep-etch EM. These oligomers were proposed to be essential for folding the inner mitochondrial membrane [53,54]. However, until recently, precise information about the role of dimerizing ATP synthase was lacking.

A stable ATP synthase supercomplex was found in the algae *Chlamydomonas* and *Polytomella* [55,56] (Figure 1). This supercomplex could be purified by sucrose gradient ultracentrifugation and studied by single particle EM [35]. In these dimers, the monomers make an angle of ~70° with their long axes (Figure 3b). The kink in the lower part

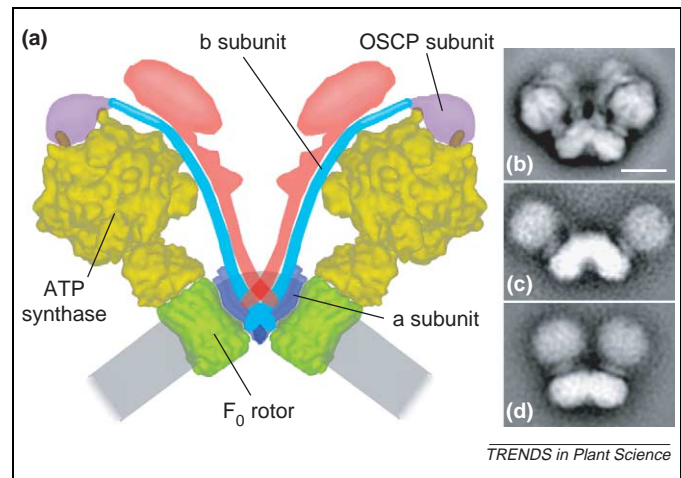


Figure 3. (a) Scheme for dimeric ATP synthase from mitochondria. Each ATP synthase monomer consists of the F₁ headpiece and a central stalk region (yellow) connected to the membrane-embedded F₀ rotor (green). Rotation of the complete headpiece is prevented by the b subunit of the peripheral stalk (blue), which is connected to the top of F₁ by the OSCP subunit (purple) and to the rotor by subunit a (dark blue). Other dimer-specific subunits that do not have direct functional importance for the monomers are depicted in red. (b) Projection map of *Polytomella* ATP synthase dimers [35]. Scale bar = 10 nm. (c) Projection map of *Saccharomyces cerevisiae* ATP synthase true-dimers (N.V. Dudkina *et al.*, unpublished). (d) Projection map of *S. cerevisiae* ATP synthase pseudo-dimers.

of the dimer causes a remarkable separation of the F₁ headpieces by more than 50 Å, preventing any direct contact between them. Hence, interaction of the monomers can only be realized by dimer-specific subunits within the membrane plane (Figure 3a, red). Interaction is probably also facilitated by the two peripheral stalks, which are facing each other. The ATP synthase supercomplex from *Polytomella* includes an additional 60 kDa protein termed ‘Mitochondrial ATP synthase associated protein’ or MASAP, which is supposed to be responsible for the high stability of the dimers. The MASAP subunit is probably part of the large mass in the upper half of the dimer (Figure 3a, red) close to the OSCP subunit (Figure 3a, purple), which links the b subunit of the peripheral stalk (Figure 3a, blue) to the F₁ headpiece. Such a large additional mass is lacking from analysed dimers of the yeast *S. cerevisiae* (Figure 3c). The yeast dimers were purified and analysed in a similar way to those of *Polytomella* (N.V. Dudkina *et al.*, unpublished) but show some distinct differences. Because of the lack of a large additional dimer-specific mass outside the membrane, tentatively assigned to the MASAP subunit, the peripheral stalks are thinner or hardly visible. However, the membrane-embedded F₀ parts are wider and kinked even more strongly, making an angle of ~90°. The wider diameter of the F₀ parts causes the F₁ headpieces to be separated even more strongly. It has been suggested that the yeast subunits 6, 8 (homologous to bovine A6L), b, f, g, i and k are present in this larger interface together with the peripheral stalk [50], but their exact location is not yet established. The precise homologues of some of these subunits in plants and *Polytomella*, if present, also need to be established. But, given the smaller membrane interface in *Polytomella*, it is likely that some of the yeast subunits do not have a counterpart.

In parallel to the ATP synthase dimer from *Polytomella*, the ATP synthase dimer of bovine mitochondria was analysed by EM [57]. This dimer has a configuration in which the headpieces are (almost) in contact, mainly because the angle between the monomers is only $\sim 40^\circ$, which is strikingly different to the maps presented in Figure 3b,c. However, similar particles with an angle of 35° are also present in yeast (Figure 3d) (N.V. Dudkina *et al.*, unpublished). No intermediate angles were observed so it appears that both types of yeast particles could represent specific associates. The most logical explanation would be that these two dimers have a different composition. According to a scheme presented by Patrick Paumard *et al.* [50], the dimers arrange into linear oligomers in the membrane. We hypothesize that detergent solubilization of the oligomers could lead to 'true (native) dimers' as depicted in Figure 3b,c and to 'pseudo-dimers' consisting of two close-neighbour monomers from two different broken native dimers, as shown in Figure 3d. If correct, this interpretation would explain why the width of the F_0 moiety in the pseudo-dimer (Figure 3d) and in the bovine dimer [57] is much smaller than it is in the yeast true dimer (Figure 3c).

There must be a special reason for the occurrence of ATP synthase dimers in mitochondria because the monomer is perfectly designed for catalysing the synthesis of ATP,

including mechanisms to regulate its activity. The shape of the *Polytomella*, bovine and yeast ATP synthase super-complexes gives a clue as to the role of dimerization. The unique orientation of the out-of-plane association of the F_0 membrane domains (Figure 3) will force a strong local curvature of the membrane [35,57]. Most of the ATP synthase complexes are not part of a flat inner mitochondrial membrane but occur within strongly curved invaginations known as cristae lamellae and tubules. For tubular membranes, the diameter is often in the range of 30 nm [58]. If the bent membrane in the region of the dimers is regarded as an arc section of radius 15 nm, this configuration could by extrapolation induce a tubule with a diameter of ~ 30 nm. Such a diameter would fit the observed cristae dimensions. It is likely that the ATP synthase dimers associate into specific oligomers and that the other respiratory chain supercomplexes are arranged between the ATP synthase oligomers. Indeed, oligomeric ATP synthase rows were previously described by rapid-freeze deep-etch EM [53,54]. We propose that ATP synthase dimers are the building blocks of ATP synthase oligomers, which are helically arranged in tubular cristae, as originally proposed by Richard Allen *et al.* [53]. The formation of these helical structures is the driving force for cristae formation and overall mitochondrial morphology as shown in Figure 4.

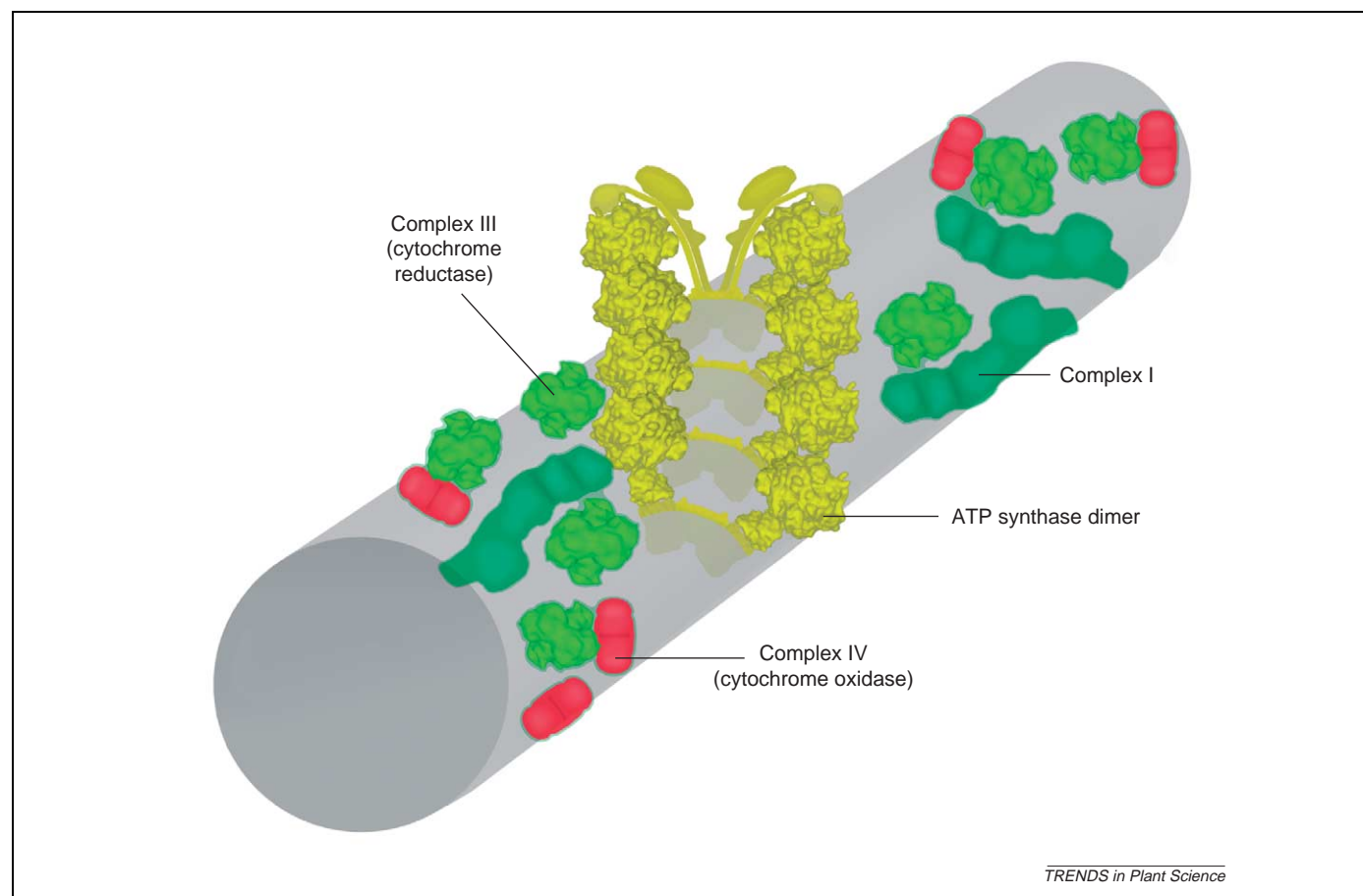


Figure 4. Proposed scheme for mitochondrial supercomplex packing within a tubular cristae membrane. The ATP synthase dimers (yellow) are arranged in row-like oligomers in a helical fashion, of which four are shown. The oligomers are thought to induce membrane curvature to form cristae rods. The three other large respiratory chain complexes are mostly organized as supercomplexes and are arranged in between the rows of ATP synthase. Dimeric Complex III (cytochrome reductase, bright green), monomeric Complex I (dark green) and dimeric Complex IV (cytochrome oxidase, red) are depicted here to form several types of supercomplexes. The exact interaction between Complex III and Complex IV has not yet been established and it could be possible that Complex III associates with two cytochrome oxidase monomers. The much smaller Complex II has no structural association with the other respiratory chain (Complexes III and IV) and has been omitted.

In this model, the other types of supercomplexes, composed of Complexes I, III and IV, are arranged in densely packed arrays between the rows of ATP synthase dimers. Wider or flattened tubules also appear to occur so there might be some variation on this theme and variation between species given that the dimers of *Polytomella* and yeast differ in shape (Figure 4).

A further question is whether the ATP synthase supercomplex arrangement (Figures 3 and 4) is unique to mitochondria. Based on BN-gel electrophoresis studies, the ATP synthase from *Chlamydomonas* chloroplasts is claimed to be dimeric as well [59]. However, an EM study of spinach chloroplasts indicated that the F₁ headpieces do not have any specific interaction within the membrane [60]. Because the chloroplast membranes are flat in the parts where the ATP synthase is located [60], there is no obvious reason why there should be (kinked) dimers in the chloroplast membranes. Hence, it can be concluded that the dimers are probably unique to mitochondria and that their interaction is primarily essential to enlarge the surface of the inner mitochondrial membrane by inducing its heavy folding.

Perspectives

The proposed organization of mitochondrial membranes rules out the possibility that this membrane is organized according to the 'Fluid-state' model. However, mitochondria and their membranes are regarded as flexible structures that can rapidly adapt in response to changing physiological requirements. Consequently, the OXPHOS system cannot be described by the static 'Solid-state' model. Single OXPHOS complexes and their supercomplexes probably dynamically co-exist within the inner mitochondrial membrane (Figure 4): this idea is supported by results obtained by BN-PAGE and by flux control measurements [28]. Furthermore, the stoichiometry of different OXPHOS complexes within the inner mitochondrial membrane differs, excluding the possibility that all complexes form part of a supercomplex at a given time. Cardiolipin is reported to play an important role in supercomplex formation in yeast mitochondria [61,62].

The physiological roles of OXPHOS supercomplexes have not yet been determined. *In vitro* activity measurements indicate that they form the basis for enhanced electron transfer rates between the complexes of the respiratory chain [33]. Furthermore, supercomplex formation has implications for the structural organization of the inner mitochondrial membrane. The morphology of the folds of the inner mitochondrial membrane varies in different organisms and, therefore, abundance and composition of specific respiratory supercomplexes can be expected to differ, which is supported by the results obtained by BN-PAGE (Figure 1). Based on classical thin sectioning it appears that three types of inner membrane folds can be distinguished: lamellar cristae, vesicular cristae and tubular cristae. The formation of ATP synthase dimers and oligomers is likely to be particularly important for tubular cristae, which is in line with results obtained by transmission EM for *Paramecium* and *Polytomella* [53] (N.V. Dudkina *et al.*, unpublished). The inner membrane folds of higher plants are thought to be

more of the lamellar cristae type, which perhaps explains the comparatively weak interaction of ATP synthase monomers in this group of organisms. However, this is speculative and, moreover, classical techniques such as thin sectioning might give a rather distorted view of membrane morphology [58]. Higher-resolution EM tomography investigations [63] need to be performed on intact mitochondria to better understand correlations between the folding types of the inner mitochondrial membrane and the supercomplex composition within in this membrane.

Many other hypotheses concerning supercomplex function have been proposed [33,34]. Supercomplexes possibly allow reciprocal stabilization of OXPHOS complexes, they might offer efficient regulation of the respiratory chain or they could simply be important for increasing the amount of protein that can be inserted into the inner mitochondrial membrane. I + III₂ supercomplex formation was thought to regulate alternative respiration in plants because it possibly limits the access of the alternative oxidase to its substrate ubiquinol. The alternative oxidoreductases of plant mitochondria do not appear to form part of any of the respiratory supercomplexes described [17] and to date the regulation of these enzymes is not well understood. More precise information on the supramolecular organization of the OXPHOS system must await the structural characterization of further supercomplexes, particularly those that include Complex IV, the terminal respiratory chain oxidoreductase.

Acknowledgements

This work was supported by the Deutsche Forschungsgemeinschaft and the Dutch science foundation NWO-CW.

References

- 1 Friedrich, T. and Böttcher, B. (2004) The gross structure of the respiratory Complex I: a Lego system. *Biochim. Biophys. Acta* 1608, 1–9
- 2 Carroll, J. *et al.* (2003) Analysis of the subunit composition of Complex I from bovine heart mitochondria. *Mol. Cell. Proteomics* 2, 117–126
- 3 Abdrakhmanova, A. *et al.* (2004) Subunit composition of mitochondrial Complex I from the yeast *Yarrowia lipolytica*. *Biochim. Biophys. Acta* 1658, 148–156
- 4 Yankovskaya, V. *et al.* (2003) Architecture of succinate dehydrogenase and reactive oxygen species generation. *Science* 299, 700–704
- 5 Horsefield, R. *et al.* (2004) Complex II from a structural perspective. *Curr. Protein Pept. Sci.* 5, 107–118
- 6 Berry, E.A. *et al.* (2000) Structure and function of cytochrome *bc* complexes. *Annu. Rev. Biochem.* 69, 1005–1075
- 7 Hunte, C. *et al.* (2000) Structure at 2.3 Å resolution of the cytochrome *bc*₁ complex. from the yeast *Saccharomyces cerevisiae* co-crystallized with an antibody fragment. *Structure* 8, 669–684
- 8 Tsukihara, T. *et al.* (1996) The whole structure of the 13-subunit oxidized cytochrome *c* oxidase at 2.8 Å. *Science* 272, 1136–1144
- 9 Michel, H. *et al.* (1998) Cytochrome *c* oxidase: structure and spectroscopy. *Annu. Rev. Biophys. Biomol. Struct.* 27, 329–356
- 10 Stock, D. *et al.* (2000) Rotary mechanism of ATP synthase. *Curr. Opin. Struct. Biol.* 10, 672–679
- 11 Vedel, F. *et al.* (1999) The mitochondrial respiratory chain and ATP synthase complexes: composition, structure and mutational studies. *Plant Physiol. Biochem.* 37, 629–643
- 12 Runswick, M.J. *et al.* (1991) Presence of an acyl carrier protein in NADH:ubiquinone oxidoreductase from bovine heart mitochondria. *FEBS Lett.* 286, 121–124

- 13 Sackmann, U. *et al.* (1991) The acyl-carrier protein in *Neurospora crassa* mitochondria is a subunit of NADH: ubiquinone reductase (Complex I). *Eur. J. Biochem.* 200, 463–469
- 14 Millar, A.H. *et al.* (2003) Control of ascorbate synthesis by respiration and its implications for stress responses. *Plant Physiol.* 133, 443–447
- 15 Sunderhaus, S. *et al.* (2006) Carbonic anhydrase subunits form a matrix-exposed domain attached to the membrane arm of mitochondrial Complex I in plants. *J. Biol. Chem.* 281, 6482–6488
- 16 Braun, H.P. *et al.* (1992) The general mitochondrial processing peptidase from potato is an integral part of cytochrome c reductase of the respiratory chain. *EMBO J.* 11, 3219–3227
- 17 Eubel, H. *et al.* (2003) New insights into the respiratory chain of plant mitochondria: supercomplexes and a unique composition of Complex II. *Plant Physiol.* 133, 274–286
- 18 Millar, A.H. *et al.* (2004) Mitochondrial cytochrome c oxidase and succinate dehydrogenase contain plant-specific subunits. *Plant Mol. Biol.* 56, 77–89
- 19 Dutilleul, C. *et al.* (2003) Leaf mitochondria modulate whole cell redox homeostasis, set antioxidant capacity, and determine stress resistance through altered signalling and diurnal regulation. *Plant Cell* 15, 1212–1226
- 20 Siedow, J.N. and Umbach, A.L. (1995) Plant mitochondrial electron transfer and molecular biology. *Plant Cell* 7, 821–831
- 21 Moller, I.M. (2002) A new dawn for plant mitochondrial NAD(P)H dehydrogenases. *Trends Plant Sci.* 7, 235–237
- 22 Juszczuk, I.M. and Rychter, A.M. (2003) Alternative oxidase in higher plants. *Acta Biochim Pol.* 50, 1257–1271
- 23 Rasmusson, A.G. *et al.* (2004) Alternative NAD(P)H dehydrogenases of plant mitochondria. *Annu. Rev. Plant Biol.* 55, 23–39
- 24 Hackenbrock, C.R. *et al.* (1986) The random collision model and a critical assessment of the diffusion and collision in mitochondrial electron transport. *J. Bioenerg. Biomembr.* 18, 331–368
- 25 Fowler, L.R. and Hatefi, Y. (1961) Reconstitution of the electron transport system III. Reconstitution of DPNH oxidase, succinic oxidase, and DPNH succinic oxidase. *Biochem. Biophys. Res. Commun.* 5, 203–208
- 26 Fowler, L.R. and Richardson, H.S. (1963) Studies on the electron transfer system. *J. Biol. Chem.* 238, 456–463
- 27 Boumans, H. *et al.* (1998) The respiratory chain in yeast behaves as a single functional unit. *J. Biol. Chem.* 273, 4872–4877
- 28 Bianchi, C. *et al.* (2004) The mitochondrial respiratory chain is partially organized in a supercomplex assembly: kinetic evidence using flux control analysis. *J. Biol. Chem.* 279, 36562–36569
- 29 Grad, L.I. and Lemire, B.D. (2004) Mitochondrial Complex I mutations in *Caenorhabditis elegans* produce cytochrome c oxidase deficiency, oxidative stress and vitamin-responsive lactic acidosis. *Hum. Mol. Genet.* 13, 303–314
- 30 Acin-Perez, R. *et al.* (2004) Respiratory Complex III is required to maintain Complex I in mammalian mitochondria. *Mol. Cell* 13, 805–815
- 31 Ugalde, C. *et al.* (2004) Differences in assembly or stability of Complex I and other mitochondrial OXPHOS complexes in inherited Complex I deficiency. *Hum. Mol. Genet.* 13, 659–667
- 32 Arnold, I. *et al.* (1998) Yeast mitochondrial F₁F₀-ATP synthase exists as a dimer: identification of three dimer-specific subunits. *EMBO J.* 17, 7170–7178
- 33 Schagger, H. and Pfeiffer, K. (2000) Supercomplexes in the respiratory chains of yeast and mammalian mitochondria. *EMBO J.* 19, 1777–1783
- 34 Dudkina, N.V. *et al.* (2005) Structure of a mitochondrial supercomplex formed by respiratory chain Complexes I and III. *Proc. Natl. Acad. Sci. U. S. A.* 102, 3225–3229
- 35 Dudkina, N.V. *et al.* (2005) Structure of dimeric ATP synthase from mitochondria: an angular association of monomers induces the strong curvature of the inner membrane. *FEBS Lett.* 579, 5769–5772
- 36 Schagger, H. and von Jagow, G. (1991) Blue native electrophoresis for isolation of membrane protein complexes in enzymatically active form. *Anal. Biochem.* 199, 223–231
- 37 Heinemeyer, J. *et al.* (2004) Proteomic approach to characterize the supramolecular organization of photosystems in higher plants. *Phytochemistry* 65, 1683–1692
- 38 Arteni, A.A. *et al.* (2005) Single particle electron microscopy in combination with mass spectrometry to investigate novel complexes of membrane proteins. *J. Struct. Biol.* 149, 325–331
- 39 Heazlewood, J.L. *et al.* (2003) Mitochondrial Complex I from *Arabidopsis* and rice: orthologs of mammalian and yeast components coupled to plant-specific subunits. *Biochim. Biophys. Acta* 1604, 159–169
- 40 Cardol, P. *et al.* (2004) Higher plant-like subunit composition of mitochondrial Complex I from *Chlamydomonas reinhardtii*: 31 conserved components among eukaryotes. *Biochim. Biophys. Acta* 1658, 212–224
- 41 Parisi, G. *et al.* (2004) Gamma carbonic anhydrases in plant mitochondria. *Plant Mol. Biol.* 55, 193–207
- 42 Perales, M. *et al.* (2005) Disruption of a nuclear gene encoding a mitochondrial gamma carbonic anhydrase reduces Complex I and supercomplex I+III2 levels and alters mitochondrial physiology in *Arabidopsis*. *J. Mol. Biol.* 350, 263–277
- 43 Badger, M.R. and Price, G.D. (2003) CO₂ concentrating mechanisms in cyanobacteria: molecular components, their diversity and evolution. *J. Exp. Bot.* 54, 609–622
- 44 Eubel, H. *et al.* (2004) Identification and characterization of respirasomes in potato mitochondria. *Plant Physiol.* 134, 1450–1459
- 45 Guénebaut, V. *et al.* (1997) Three-dimensional structure of NADH-dehydrogenase from *Neurospora crassa* by electron microscopy and conical tilt reconstruction. *J. Mol. Biol.* 265, 409–418
- 46 Grigorieff, N. (1998) Three-dimensional structure of bovine NADH:ubiquinone oxidoreductase (Complex I) at 22 Å in ice. *J. Mol. Biol.* 277, 1033–1046
- 47 Cruciat, C.M. *et al.* (2000) The cytochrome bc₁ and cytochrome c oxidase complexes associate to form a single supracomplex in yeast mitochondria. *J. Biol. Chem.* 275, 18093–18098
- 48 Krause, F. *et al.* (2004) “Respirasome”-like supercomplexes in green leaf mitochondria of spinach. *J. Biol. Chem.* 279, 48369–48375
- 49 Eubel, H. *et al.* (2004) Respiratory chain supercomplexes in plant mitochondria. *Plant Physiol.* 132, 937–942
- 50 Paumard, P. *et al.* (2002) The ATP synthase is involved in generating mitochondrial cristae morphology. *EMBO J.* 21, 221–230
- 51 Giraud, M.F. *et al.* (2002) Is there a relationship between the supramolecular organization of the mitochondrial ATP synthase and the formation of cristae? *Biochim. Biophys. Acta* 1555, 174–180
- 52 Gavin, P.D. *et al.* (2004) Cross-linking ATP synthase complexes *in vivo* eliminates mitochondrial cristae. *J. Cell Sci.* 117, 2333–2343
- 53 Allen, R.D. *et al.* (1989) An investigation of mitochondrial inner membranes by rapid-freeze deep-etch techniques. *J. Cell Biol.* 108, 2233–2240
- 54 Allen, R.D. (1995) Membrane tubulation and proton pumps. *Protoplasma* 189, 1–8
- 55 van Lis, R. *et al.* (2003) Identification of novel mitochondrial protein components of *Chlamydomonas reinhardtii*. A proteomic approach. *Plant Physiol.* 132, 318–330
- 56 Atteia, A. *et al.* (2003) Bifunctional aldehyde/alcohol dehydrogenase (ADHE) in chlorophyte algal mitochondria. *Plant Mol. Biol.* 53, 175–188
- 57 Minauro-Sanmiguel, F. *et al.* (2005) Structure of dimeric mitochondrial ATP synthase: novel F₀ bridging features and the structural basis of mitochondrial cristae biogenesis. *Proc. Natl. Acad. Sci. U. S. A.* 102, 12356–12358
- 58 Frey, T.G. and Mannella, C.A. (2000) The structure of mitochondria. *Trends Biochem. Sci.* 25, 319–324
- 59 Rexroth, S. *et al.* (2004) Dimeric H⁺-ATP synthase in the chloroplast of *Chlamydomonas reinhardtii*. *Biochim. Biophys. Acta* 1658, 202–211
- 60 Dekker, J.P. and Boekema, E.J. (2005) Supermolecular organization of the thylakoid membrane proteins in green plants. *Biochim. Biophys. Acta* 1706, 12–39
- 61 Zhang, M. *et al.* (2002) Gluing the respiratory chain together. Cardiolipin is required for supercomplex formation in the inner mitochondrial membrane. *J. Biol. Chem.* 277, 43553–43556
- 62 Pfeiffer, K. *et al.* (2003) Cardiolipin stabilizes respiratory chain supercomplexes. *J. Biol. Chem.* 278, 52873–52880
- 63 Medalia, O. *et al.* (2002) Macromolecular architecture in eukaryotic cells visualized by cryoelectron tomography. *Science* 298, 1209–1213

- 64 Heinemeyer, J. *et al.* Blue-native gel electrophoresis for the characterization of protein complexes in plants. In *Plant Proteomics (Methods in Molecular Biology Series)* (Thiellement, H., ed.), Humana Press (in press)
- 65 Sunderhaus, S. *et al.* Two dimensional blue native/blue native polyacrylamide gel electrophoresis for the characterization of mitochondrial protein complexes and supercomplexes. In *Mitochondrial Genomics and Proteomics Protocols (Methods in Molecular Biology Series)* (Leister, D and Herrmann, J.H., eds), Humana Press (in press)
- 66 Pineau, B. *et al.* (2005) Targeting the NAD7 subunit to mitochondria restores a functional Complex I and a wild type phenotype in the *Nicotiana sylvestris* CMS II mutant lacking nad7. *J. Biol. Chem.* 280, 25994–26001
- 67 Taylor, N.L. *et al.* (2005) Differential impact of environmental stresses on the pea mitochondrial proteome. *Mol. Cell. Proteomics* 4, 1122–1133
- 68 Sabar, M. *et al.* (2005) Histochemical staining and quantification of plant mitochondrial respiratory chain complexes using blue-native polyacrylamide gel electrophoresis. *Plant J.* 44, 893–901
- 69 Krause, F. *et al.* (2004) Supramolecular organization of cytochrome c oxidase- and alternative oxidase-dependent respiratory chains in the filamentous fungus *Podospora anserina*. *J. Biol. Chem.* 279, 26453–26461
- 70 Schagger, H. *et al.* (2004) Significance of respirasomes for the assembly/stability of human respiratory chain complex I. *J. Biol. Chem.* 279, 36349–36353

Plant Science meetings in July 2006

Plant Growth Regulation Society of America (PGRSA) 33rd Annual Conference 9–12 July 2006

Quebec City Hilton, Quebec City, Canada
<http://www.griffin.peachnet.edu/pgrsa>

17th International Symposium on Plant Lipids 16–21 July 2006

East Lansing, MI, USA
<http://www.ispl2006.msu.edu/index.html>

XV FESPB 2006: Plants, People, Ecosystems and Applications 17–21 July 2006

Lyon, France
<http://www.fespb2006.org/>

5th International Conference on Mycorrhiza 23–27 July 2006

Granada, Spain
<http://www.eez.csic.es/icom5/>

Botany 2006 28 July – 3 August 2006

Chico, CA, USA
<http://www.2006.botanyconference.org/>

American Phytopathological Society 29 July – 2 August 2006

Québec, Canada
<http://meeting.apsnet.org/>

6 Supramolecular structure of the oxidative phosphorylation system in plants

Jesco Heinemeyer, Natalya V. Dudkina, Egbert J. Boekema and Hans-Peter Braun

6.1 Introduction

The oxidative phosphorylation (OXPHOS) system is localized in the inner mitochondrial membrane (IMM) and consists of various oxidoreductases and the ATP synthase complex. By the combined action of the oxidoreductases, electrons are transferred from metabolites (mainly NADH and FADH₂) within the mitochondrial matrix, or the intermembrane space to the terminal electron acceptor O₂. Four multisubunit complexes are of central importance for this so-called respiratory electron transport, the NADH dehydrogenase complex (complex I), the succinate dehydrogenase (complex II), the cytochrome *c* reductase (complex III) and the cytochrome *c* oxidase (complex IV). The lipid ubiquinone mediates transfer of electrons from the dehydrogenases to complex III, and the monomeric protein cytochrome *c* mediates transfer of electrons from complex III to complex IV. Complexes I, III and IV couple electron transfer to proton translocation across the IMM, causing the generation of a chemiosmotic gradient. The adenosine triphosphate (ATP) synthase complex, which is also designated complex V, finally uses this gradient to catalyse the formation of ATP by adenosine diphosphate phosphorylation at the matrix-exposed side of the IMM. Besides the classical oxidoreductase complexes of the respiratory chain, some organisms have further so-called alternative oxidoreductases. As a result, respiratory electron transport is branched. Numerous alternative oxidoreductases occur in plants, including the four distinct alternative NAD(P)H dehydrogenases, and one alternative terminal oxidase (see Chapter 7).

6.2 Structure and function of OXPHOS complexes I–V

Complexes I–V were discovered more than 40 years ago (for review, see Hatefi, 1985). The structure and function of these complexes have since been studied extensively by biochemical procedures in combination with site-directed mutagenesis, electron microscopy and X-ray crystallography. In particular, the detailed structures of the mammalian and yeast OXPHOS complexes have been determined.

6.2.1 Complex I

Complex I has a molecular mass of about 1 MDa, and is composed of 40–45 distinct protein types (for review, see Friedrich and Böttcher, 2004). At least ten cofactors are attached to this complex (one flavin mononucleotide and nine Fe–S clusters). Two large functional domains can be defined: an elongated membrane domain (membrane arm) involved in proton translocation, and a matrix-exposed domain (matrix arm) attached to one end of the membrane arm, which is responsible for NADH oxidation. Overall, the enzyme has an L-like shape. In plants, at least 10 of the approximately 40 subunits do not exhibit sequence similarity to subunits of complex I from heterotrophic eukaryotes (Heazlewood *et al.*, 2003a; Cardol *et al.*, 2004). One of these plant-specific subunits is an L-galactono-1,4-lactone dehydrogenase, which represents the terminal enzyme of the mitochondrial ascorbic acid biosynthesis pathway (Millar *et al.*, 2003); five other subunits exhibit sequence homology to an archaeobacterial γ -type carbonic anhydrase (Parisi *et al.*, 2004; Perales *et al.*, 2004, 2005). The carbonic anhydrase subunits form an extra matrix-exposed domain, which, as revealed by single-particle electron microscopy, is attached to the central part of the membrane arm of complex I in plants (Sunderhaus *et al.*, 2006). Furthermore, an acyl-carrier protein for mitochondrial fatty acid biosynthesis forms part of complex I, as also reported for yeast, and bovine heart mitochondria (Runswick *et al.*, 1991; Sackmann *et al.*, 1991; Heazlewood *et al.*, 2003a). Plant complex I is therefore a multifunctional enzyme complex.

6.2.2 Complex II

Complex II is the smallest OXPHOS complex (for review, see Horsefield *et al.*, 2004). In most organisms it includes four types of subunits, and five cofactors (one flavin adenine dinucleotide, three Fe–S clusters and one heme b). *In vivo*, it most likely has a dimeric or trimeric structure (Yankovskaya *et al.*, 2003). Complex II from plants has at least four additional subunits of unknown function (Eubel *et al.*, 2003; Millar *et al.*, 2004), and these might bring secondary activities to this OXPHOS complex.

6.2.3 Complex III

Complex III is a functional dimer of about 500 kDa. Each monomer is composed of 10–11 proteins and 4 cofactors (three hemes and one Fe–S cluster; reviewed in Braun and Schmitz, 1995a; Berry *et al.*, 2000; Hunte *et al.*, 2000). Its overall structure is very similar in *Arabidopsis*, yeast and bovine heart (Dudkina *et al.*, 2005a). The two largest subunits of complex III are termed core proteins (core I and core II), because they were originally thought to form the center of the complex (Silman *et al.*, 1967). However, it is now known that they protrude into the mitochondrial matrix. The core proteins exhibit sequence similarity to the two subunits of the mitochondrial processing peptidase (MPP), which removes the presequences from nuclear-encoded mitochondrial proteins after import. In most heterotrophic organisms,

the MPP subunits are localized in the mitochondrial matrix. In contrast, in plants the core subunits of complex III represent the MPP subunits (Braun *et al.*, 1992, 1995; Eriksson *et al.*, 1994). Structural prerequisites for MPP activity are a zinc-binding and a substrate-binding domain, which are completely conserved in core subunits of plant complex III, but incomplete in most core proteins from heterotrophic organisms (Braun and Schmitz, 1995b). Isolated complex III from plants was shown to efficiently remove presequences from mitochondrial precursor proteins. Thus, complex III is a bifunctional enzyme in plants.

6.2.4 Complex IV

Complex IV of mammals has a molecular mass of about 210 kDa and includes 13 subunits, some of which are very hydrophobic (Richter and Ludwig, 2003). Four cofactors are attached to the complex (two heme a and two Cu^{2+}). X-ray crystallography revealed that bovine complex IV is a dimer (Tsukihara *et al.*, 1996). However, the supramolecular structure of complex IV is still a matter of debate (Lee *et al.*, 2001). *Arabidopsis* complex IV has a similar number of subunits as the mammalian complex (Millar *et al.*, 2004). Some of the smaller subunits seem to be plant specific. It is possible that plant complex I has subsidiary activities, but this remains to be confirmed.

6.2.5 Complex V

Complex V has a molecular mass of about 600 kDa (for review, see Stock *et al.*, 2000). It is composed of two domains, one within the IMM termed F_0 and the other within the mitochondrial matrix termed F_1 , which are linked by a central and a peripheral stalk. Complex V catalysis involves rotation of the central stalk assembly together with an oligomeric ring of c subunits within F_0 . Five different subunits form F_1 (α , β , γ , δ and ϵ) and about ten subunits of F_0 (a, b, c and several additional small subunits which are designated differentially in different organisms). The structure and composition of complex V of plants is very similar to that of heterotrophic eukaryotes as revealed by single-particle electron microscopy (Dudkina *et al.*, 2005b). The number of mitochondrially encoded subunits is especially high in plants (Heazlewood *et al.*, 2003b).

6.3 Supramolecular organization of the OXPHOS system

6.3.1 Solid-state versus fluid-state model

Historically, there has been some controversy regarding the supramolecular organization of the OXPHOS system. Two extreme models were proposed (for review, see Rich, 1984; Hackenbrock *et al.*, 1986; Lenaz, 2001; Schagger, 2001a, 2002). According to the solid-state model, OXPHOS complexes stably interact and form supramolecular structures called respiratory supercomplexes. In contrast, the

fluid-state model posits that OXPHOS complexes can diffuse freely in a lateral direction within the membrane. Based on this model, electron transfer is believed to take place by random collisions between components (also referred to as the random-collision model; Hackenbrock *et al.*, 1986).

The fluid-state model was based originally on the finding that physiologically active portions of the OXPHOS system could be biochemically purified (for review, see Hatefi, 1985). However, purification protocols applied for the isolation of these portions often resulted in copurification of more than one OXPHOS complex (Fowler and Hatefi, 1961; Hatefi *et al.*, 1961, 1962b; Fowler and Richardson, 1963; Hatefi and Rieske, 1967). Furthermore, isolated OXPHOS complexes were found to assemble in specific stoichiometric ratios (Hatefi *et al.*, 1962a; Fowler and Richardson, 1963; Ragan and Heron, 1978), and the combined activity of the assembled complexes could not be increased upon addition of any of the individual purified OXPHOS complexes (Ragan and Heron, 1978). Together, these data were interpreted in favor of the solid-state model.

In contrast, results of lipid dilution experiments were interpreted in support of the fluid-state model (Schneider *et al.*, 1980a,b). Fusion of IMM with exogenous lipids was found to cause an increase in the average distance between integral membrane proteins, and at the same time a decrease in respiration rates. Also, measurement of rotation of complexes III and IV reconstituted in artificial liposomes indicated the independent presence of these components (Kawato *et al.*, 1981). However, based on recent findings on the essential role of specific lipids for the structure, and activity of membrane-bound protein complexes (Lange *et al.*, 2001; Domonkos *et al.*, 2004; Fyfe and Jones, 2005), these results may have to be reinterpreted. For instance, the mitochondrial-specific lipid cardiolipin was found to be important for the formation of respiratory supercomplexes in yeast (Zhang *et al.*, 2002; Pfeiffer *et al.*, 2003; Zhang *et al.*, 2005). Dilution of mitochondrial membranes with exogenous phospholipids or reconstitution of OXPHOS complexes into artificial vesicles alters the natural lipid composition surrounding the OXPHOS complexes that might cause destabilization of supramolecular structures.

Theoretical considerations, based on the relationship between the measured activity rates for OXPHOS complexes and their diffusion rates within the IMM under *in vitro* and *in vivo* conditions, did not quite resolve the questions concerning the supramolecular organization of the OXPHOS complexes, but were interpreted in favor of a rather dynamic system (Rich, 1984).

Evidence in support of respiratory supercomplexes came from genetic investigations in mouse, humans and nematodes. Mutations affecting subunits of individual OXPHOS complexes were found to have specific effects on the stability of other OXPHOS complexes (Acin-Perez *et al.*, 2004; Grad and Lemire, 2004; Schagger *et al.*, 2004; Ugalde *et al.*, 2004). However, other data are contradictory. Mutations affecting complex I subunits in tobacco, *Arabidopsis* and trypanosomes were recently shown not to affect complex III abundance or stability (Horváth *et al.*, 2005; Perales *et al.*, 2005; Pineau *et al.*, 2005). Crosswise stabilization between different OXPHOS complex types therefore appears to occur only in some organisms. Evidence in favor of defined associations of OXPHOS complexes also comes

from investigations on the homologous electron transfer system in bacteria. Stable respiratory supercomplexes were discovered in several microorganisms (Berry and Trumppower, 1985; Sone *et al.*, 1987; Iwasaki *et al.*, 1995; Niebisch and Bott, 2003; Stroh *et al.*, 2004). A functional fusion of respiratory complexes III and IV, devoid of cytochrome *c* protein, was reported for a thermoacidophilic archaeon (Iwasaki *et al.*, 1995).

Some years ago, a novel experimental strategy to characterize the OXPHOS system was introduced by Hermann Schägger, based on the mild solubilization of mitochondrial membranes with nonionic detergents and subsequent separation of the solubilized protein complexes by blue-native polyacrylamide gel electrophoresis (PAGE) (Arnold *et al.*, 1998; Schägger and Pfeiffer, 2000; Schägger, 2001b). Distinct respiratory supercomplexes could be described by this procedure, such as a dimeric ATP synthase, a I + III₂ supercomplex, and even larger supercomplexes including OXPHOS complexes I, III and IV. It was suggested that the larger structures should be termed respirasomes, because they can perform respiration autonomously in the presence of ubiquinol and cytochrome *c* (Schägger and Pfeiffer, 2000). Detergent-solubilized OXPHOS supercomplexes also proved to be stable during protein separations by sucrose-gradient ultracentrifugation (Dudkina *et al.*, 2005a,b). Of course, detergent treatment of biological membranes could also lead to artificial associations of membrane-protein complexes on the basis of random hydrophobic interaction. However, so far, there is no clear evidence that detergent treatment generates artifacts upon solubilization of mitochondrial membranes. Data based on detergent-treated mitochondrial membrane fractions correspond nicely with biochemical data obtained by other procedures, e.g. cross-linking experiments. In addition, the observed interactions between OXPHOS complexes within supramolecular structures on blue-native gels always make sense with respect to the known physiological context, e.g. complex III associates with complex IV in yeast (see below), or complex I with dimeric complex III in bovine and *Arabidopsis* mitochondria (see below).

Recently, detergent-solubilized supercomplexes purified by sucrose-gradient ultracentrifugation were analyzed by electron microscopy in combination with single-particle analysis (Plate 6.1; Dudkina *et al.*, 2005a,b). The results clearly exclude the possibility that OXPHOS complexes interact on the basis of nonspecific hydrophobic interaction. All supercomplexes investigated revealed highly specific associations of OXPHOS complexes, e.g. within the I + III₂ supercomplex of *Arabidopsis*, or the V₂ supercomplex of the nonphotosynthetic alga *Polytomella*.

Very convincing evidence supporting defined associations of OXPHOS complexes also comes from flux-control experiments in combination with inhibitor titrations. The data obtained reveal that the yeast respiratory chain behaves as a single functional unit (Boumans *et al.*, 1998). Furthermore, inhibitor titrations indicate an interaction between complexes I and III₂ (Bianchi *et al.*, 2003, 2004; Genova *et al.*, 2003). Flux-control analyses are of special value, because they can be carried out *in organello* in the absence of detergent.

In summary, the fluid-state model and the random-collision model cannot explain many of the reported results obtained for the structure of the mitochondrial OXPHOS system. On the other hand, not all OXPHOS complexes can form

Au: Kindly cite Plate 6.2 at an appropriate place in the text.

respiratory supercomplexes at the same time, since their abundances vary within the IMM (Schägger and Pfeiffer, 2001). Most likely, monomeric complexes and supramolecular assemblies coexist under *in vivo* conditions (Lenaz, 2001).

6.3.2 Composition of OXPHOS supercomplexes in plants

Respiratory supercomplexes of plant mitochondria were first described by blue-native/sodium dodecyl sulfate (SDS) PAGE (Eubel *et al.*, 2003). Using membrane solubilization with dodecylmaltoside, Triton X-100, or digitonin, a 1500-kDa supercomplex, composed of the subunits of monomeric complex I and dimeric complex III, was visible on the two-dimensional gels (Figure 6.1). The supercomplex does not include proteins that are not components of complexes I or III₂. It is best stabilized in the presence of digitonin. Under these conditions, 50–90% of complex I is associated with dimeric complex III in *Arabidopsis*, potato, bean and barley (Eubel *et al.*, 2003). A small percentage of complex I forms part of an even larger particle of 3000 kDa, which most likely has I₂III₄ composition. Recently, the 1500-kDa I + III₂ supercomplex was described for spinach, pea, tobacco and asparagus by blue-native PAGE (Krause *et al.*, 2004; Pineau *et al.*, 2005; Taylor *et al.*, 2005; Dudkina

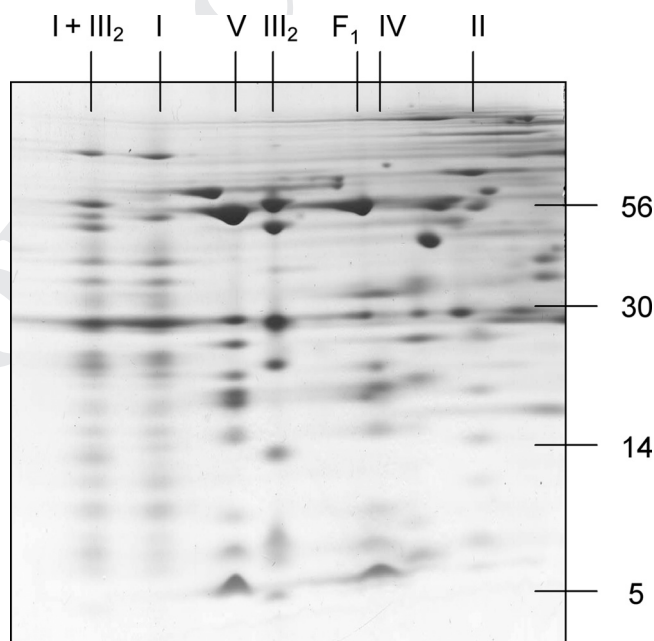


Figure 6.1 Two-dimensional resolution of OXPHOS complexes of *Arabidopsis* by blue-native/SDS PAGE. Mitochondrial membranes were solubilized by digitonin (5 g/g protein). The molecular masses of standard proteins are given to the right and the identities of the protein complexes above the gel. I + III₂: supercomplex formed of complexes I and dimeric complex III, I: complex I, V: ATP synthase; III₂: dimeric complex III, F₁: F₁ part of ATP synthase, IV: complex IV, II: complex II.

et al., 2006). Some larger supercomplexes of 1700–3000 kDa, which additionally include one or multiple copies of complex IV, were described for potato, spinach and sunflower (Eubel *et al.*, 2004a; Krause *et al.*, 2004; Sabar *et al.*, 2005). However, compared to mammalian mitochondria, these respirasomelike structures are of comparatively low abundance or stability in plants. Only a very small percentage of complex IV forms part of respiratory supercomplexes under all conditions tested. In contrast, the I + III₂ supercomplex proved to be of extraordinary stability in plants, and therefore was subject to single-particle electron microscopy in order to obtain structural information on supercomplex architecture (see below).

Very low detergent concentration during mitochondrial membrane solubilization enables the visualization of a dimeric ATP synthase supercomplex (Arnold *et al.*, 1998; Schägger and Pfeiffer, 2000). This supercomplex was first described for yeast and mammals using blue-native PAGE (Arnold *et al.*, 1998). In yeast, the supercomplex includes three dimer-specific proteins termed subunit e, g and k. If the gene for subunit g is deleted in yeast, the supercomplex is not formed. Furthermore, the characteristic foldings of the inner membrane do not develop in the mutant yeast line, leading to speculation that dimerization of ATP synthase is important for cristae formation (Giraud *et al.*, 2002; Paumard *et al.*, 2002). A similar ultrastructural phenotype was obtained upon *in vivo* cross-linking of the matrix-exposed F₁ parts of ATP synthase, indicating an important role of the F₀ membrane domain of ATP synthase during dimer formation (Gavin *et al.*, 2004).

A dimeric ATP synthase supercomplex could also be described for plant mitochondria upon solubilization of mitochondrial membranes by low concentrations of nonionic detergent in combination with blue-native PAGE (Eubel *et al.*, 2003, 2004b). The supercomplex is best stabilized by very low Triton X-100 concentrations (>0.5 g/g protein). However, overall this supercomplex seems to be less stable/abundant in higher plants. In contrast, the algae *Chlamydomonas* and *Polytomella* were shown to have an exceptionally stable ATP synthase supercomplex (Atteia *et al.*, 2003; van Lis *et al.*, 2003, 2005). In these algae, ATP synthase is exclusively dimeric on blue-native gels, independent of the type and concentration of nonionic detergent used for membrane solubilization (J. Heinemeyer, unpublished results). Compared with other organisms, the algal ATP synthase supercomplex includes an additional 60-kDa subunit termed *mitochondrial ATP synthase associated protein* (MASAP). This protein is speculated to be responsible for dimer stability (van Lis *et al.*, 2003).

6.3.3 Structure of OXPHOS supercomplexes in plants

The I + III₂ supercomplex of higher plants and the dimeric ATP synthase supercomplex from green algae proved to be extraordinary stable particles. Therefore, they were selected for structural investigations using electron microscopy in combination with single-particle analyses. In order to omit binding of Coomassie blue during protein purification, which confers negative charge to protein surfaces and, therefore, possibly interferes with native protein structures, protein complexes and supercomplexes were separated by sucrose-gradient ultracentrifugation. Fractions

of these gradients were directly analyzed by electron microscopy. Single-particle analyses revealed a highly defined interaction of monomeric complex I and dimeric complex III within the I + III₂ supercomplex of *Arabidopsis* (Plate 6.1). The complex III dimer is laterally attached to the membrane arm of complex I. At the region of interaction, the membrane arm is slightly bent around the complex III dimer. The overall length of the membrane arm of plant complex I, which exceeds that in mammals, is most likely responsible for the enhanced stability of the I + III₂ supercomplex.

Analysis of the dimeric ATP synthase supercomplex of *Polytomella* also revealed a highly defined interaction between ATP synthase monomers within the V₂ supercomplex (Dudkina *et al.*, 2005b). Interaction takes place exclusively between the membrane-bound F₀ parts of the monomeric complex. The long axis of the two ATP synthase monomers forms an angle of about 70°, causing a local bending of the IMM in the region of the dimeric supercomplex. These data nicely support the hypothesized role for ATP synthase dimerization in the formation of cristae (see above). A parallel investigation of bovine ATP synthase supercomplexes by single-particle electron microscopy revealed an angle of 30° between the monomers (Minauro-Sanmiguel *et al.*, 2005). Furthermore, monomers within yeast ATP synthase dimers were recently found to have angles of either 40° or 90° (Dudkina *et al.*, 2006). Therefore, angles between ATP synthase monomers of ATP synthase supercomplexes seem to vary in different organisms. On the other hand, angles fall into two classes, a narrow-angle (30–40°) and a wide-angle (70–90°) class. It is possible that these classes represent two alternative binding arrangements for ATP synthase monomers in oligomeric ATP synthase structures, as described previously based on the results of rapid-freeze deep-etch electron microscopy (Allen *et al.*, 1989; Allen, 1995) or blue-native PAGE (Paumard *et al.*, 2002; Arselin *et al.*, 2003; Krause *et al.*, 2005; Wittig and Schägger, 2005). Recently, it was suggested that the wide-angle ATP synthase dimers are true dimers that represent the building blocks of ATP synthase oligomerization, whereas the narrow-angle dimers are artificial dimers which consist of two monomeric ATP synthase complexes of two neighboring ATP synthase dimers within the oligomers (Dudkina *et al.*, 2006). It has been suggested that the latter dimers are artificially generated as a result of the breakdown of ATP synthase oligomers during the solubilization step. However, it should be pointed out that, according to this hypothesis, both dimer types represent specific interactions of functional relevance. The presence of two different classes of ATP dimers in yeast is also supported by biochemical analyses. Using fluorescence resonance energy transfer, b subunits of different ATP synthase monomers were shown to interact physically (Gavin *et al.*, 2005). Therefore, yeast ATP synthase dimers might be formed by the interaction of either g subunits or b subunits.

6.3.4 Function of OXPHOS supercomplexes in plants

The function of the OXPHOS supercomplexes is only partially understood. ATP synthase supercomplexes probably have an important role in the formation of IMM

ultrastructure in mitochondria. This might also be the case for other OXPHOS supercomplexes, such as the I + III₂ supercomplex. However, membrane bending due to the binding of monomeric complex I and dimeric complex III is less evident. Dimerization of ATP synthase complexes has been suggested to have a positive effect on the fixation of the nonrotating parts of the ATP synthase monomers because they are attached to each other back-to-back in the region of the peripheral stalks, thereby causing torsional forces of opposite orientation (Rexroth *et al.*, 2004).

Respiratory supercomplexes might allow an overall increase in electron transfer rates as a result of substrate channeling between different OXPHOS components. This has been demonstrated for the NADH-cytochrome *c* oxidoreductase activity of the bovine I + III₂ supercomplex under *in vitro* conditions (Schägger and Pfeiffer, 2001). However, the I + III₂ supercomplex structure, as revealed by single-particle electron microscopy, does not support ubiquinone/ubiquinol channeling between complex I and complex III₂, because the location of the ubiquinone pocket of complex I is not in the region of the complex I–complex III₂ interface (Sazanov and Hinchliffe, 2006). The role of the membrane arm of complex I in proton translocation is still not known. It is possible that there are secondary electron transport chains present within this part of complex I, which could interact with electron transport in dimeric complex III.

Supercomplexes are likely also important for the regulation of respiration. The I + III₂ supercomplex was suggested to be involved in the regulation of the alternative oxidase in plants, because it might reduce access of this enzyme to its substrate, ubiquinol (Eubel *et al.*, 2003). However, as stated above, ubiquinone/ubiquinol channeling between complexes I and III₂ has not been proven. The alternative oxidoreductases of plant mitochondria were not found to form part of the respiratory supercomplexes (Eubel *et al.*, 2003), which might be an important prerequisite for the independent regulation of alternative electron transport pathways.

6.4 Concluding remarks

The OXPHOS supercomplexes have many functions in addition to electron transport and ATP generation, such as providing structural stabilization of the individual membrane–protein complexes or increasing the protein-insertion capacity of the IMM. At present, the physiological roles of the respiratory supercomplexes are poorly understood, and there is much more to learn about supercomplex structure. Unfortunately, this quaternary level of protein structure is fragile, making investigations technically challenging; it is likely that X-ray crystallography will not be applicable for the resolution of supercomplex structure, at least in the near future. However, alternative, noninvasive procedures to investigate the three-dimensional interaction network of proteins and protein complexes should generate much useful data. What is certain is that investigation of protein supercomplexes and protein interaction networks will be crucial for the understanding of the molecular basis of life.

Acknowledgments

Research in our laboratories is supported by the Deutsche Forschungsgemeinschaft (DFG) and the Dutch science foundation, NOW.

References

- Acin-Perez R, Bayona-Bafaluy MP, Fernandez-Silva P, *et al.* (2004) Respiratory complex III is required to maintain complex I in mammalian mitochondria. *Mol Cell* **13**, 805–815.
- Allen RD (1995) Membrane tubulation and proton pumps. *Protoplasma* **189**, 1–8.
- Allen RD, Schroeder CC and Fok AK (1989) An Investigation of mitochondrial inner membranes by rapid-freeze deep-etch techniques. *J Cell Biol* **108**, 2233–2240.
- Arnold I, Pfeiffer K, Neupert W, Stuart RA and Schagger H (1998) Yeast mitochondrial F1FO-ATP synthase exists as a dimer: identification of three dimer-specific subunits. *EMBO J* **17**, 7170–7178.
- Arselin G, Giraud MF, Dautant A, *et al.* (2003) The GxxxG motif of the transmembrane domain of subunit e is involved in the dimerization/oligomerization of the yeast ATP synthase complex in the mitochondrial membrane. *Eur J Biochem* **170**, 1875–1884.
- Atteia A, van Lis R, Mendoza-Hernandez G, *et al.* (2003) Bifunctional aldehyde/alcohol dehydrogenase (ADHE) in chlorophyte algal mitochondria. *Plant Mol Biol* **53**, 175–188.
- Berry EA, Guergova-Kuras M, Huang LS and Crofts AR (2000) Structure and function of cytochrome bc complexes. *Annu Rev Biochem* **69**, 1005–1075.
- Berry EA and Trumpower BL (1985) Isolation of ubiquinol oxidase from *Paracoccus denitrificans* and resolution into cytochrome bc₁ and cytochrome c-aa₃ complexes. *J Biol Chem* **260**, 2458–2467.
- Bianchi C, Fato R, Genova ML, Castelli GP and Lenaz G (2003) Structural and functional organization of complex I in the mitochondrial respiratory chain. *Biofactors* **18**, 3–9.
- Bianchi C, Genova ML, Castelli GP and Lenaz G (2004) The mitochondrial respiratory chain is partially organized in a supercomplex assembly: kinetic evidence using flux control analysis. *J Biol Chem* **279**, 36562–36569.
- Boumans H, Grivell LA and Berden JA (1998) The respiratory chain in yeast behaves as a single functional unit. *J Biol Chem* **273**, 4872–4877.
- Braun HP, Emmermann M, Kruff V, Bodicker M and Schmitz UK (1995) The general mitochondrial processing peptidase from wheat is integrated into the cytochrome bc₁ complex of the respiratory chain. *Planta* **195**, 396–402.
- Braun HP, Emmermann M, Kruff V and Schmitz UK (1992) The general mitochondrial processing peptidase from potato is an integral part of cytochrome c reductase of the respiratory chain. *EMBO J* **11**, 3219–3227.
- Braun HP and Schmitz UK (1995a) The bifunctional cytochrome c reductase/processing peptidase complex from plant mitochondria. *J Bioenerg Biomembr* **27**, 423–436.
- Braun HP and Schmitz UK (1995b) Are the ‘core’ proteins of the mitochondrial bc₁ complex evolutionary relics of a processing peptidase? *Trends Biochem Sci* **20**, 171–175.
- Cardol P, Vanrobaeys F, Devreese B, van Beeuman J, Matagne RF and Remacle C (2004) Higher plant-like subunit composition of mitochondrial complex I from *Chlamydomonas reinhardtii*: 31 conserved components among eukaryotes. *Biochim Biophys Acta* **1658**, 212–224.
- Domonkos I, Malec P, Sallai A, *et al.* (2004) Phosphatidylglycerol is essential for oligomerization of photosystem I reaction center. *Plant Physiol* **134**, 1471–1478.
- Dudkina NV, Eubel H, Keegstra W, Boekema EJ and Braun HP (2005a) Structure of a mitochondrial supercomplex formed by respiratory chain complexes I and III. *Proc Natl Acad Sci USA* **102**, 3225–3229.
- Dudkina NV, Heinemeyer J, Keegstra W, Boekema EJ and Braun HP (2005b) Structure of dimeric ATP synthase from mitochondria: an angular association of monomers induces the strong curvature of the inner membrane. *FEBS Lett* **579**, 5769–5772.

- Dudkina NV, Sunderhaus S, Braun HP and Boekema EJ (2006) Characterization of dimeric ATP synthase and cristae membrane ultrastructure from *Saccharomyces* and *Polytomella* mitochondria. *FEBS Lett* **580**, 3427–3432.
- Eriksson AC, Sjöling S and Glaser E (1994) The ubiquinol cytochrome *c* oxidoreductase complex of spinach leaf mitochondria is involved in both respiration and protein processing. *Biochim Biophys Acta* **1186**, 221–231.
- Eubel H, Heinemeyer J and Braun HP (2004a) Identification and characterization of respirasomes in potato mitochondria. *Plant Physiol* **134**, 1450–1459.
- Eubel H, Heinemeyer J, Sunderhaus S and Braun HP (2004b) Respiratory chain supercomplexes in plant mitochondria. *Plant Physiol Biochem* **42**, 937–942.
- Eubel H, Jansch L and Braun HP (2003) New insights into the respiratory chain of plant mitochondria: supercomplexes and a unique composition of complex II. *Plant Physiol* **133**, 274–286.
- Fowler LR and Hatefi Y (1961) Reconstitution of the electron transport system III. Reconstitution of DPNH oxidase, succinic oxidase, and DPNH succinic oxidase. *Biochem Biophys Res Commun* **5**, 203–208.
- Fowler LR and Richardson HS (1963) Studies on the electron transfer system. *J Biol Chem* **238**, 456–463.
- Friedrich T and Böttcher B (2004) The gross structure of the respiratory complex I: a Lego system. *Biochim Biophys Acta* **1608**, 1–9.
- Fyfe PK and Jones MR (2005) Lipids in and around photosynthetic reaction centres. *Biochem Soc Trans* **33**, 924–930.
- Gavin PD, Prescott M and Devenish RJ (2005) Yeast F_1F_0 -ATP synthase complex interactions *in vivo* can occur in the absence of the dimer specific subunit *e*. *J Bioenerg Biomembr* **37**, 55–66.
- Gavin PD, Prescott M, Luff SE and Devenish RJ (2004) Cross-linking ATP synthase complexes *in vivo* eliminates mitochondrial cristae. *J Cell Sci* **117**, 2233–2243.
- Genova ML, Bianchi C and Lenaz G (2003) Structural organization of the mitochondrial respiratory chain. *Ital J Biochem* **52**, 58–61.
- Giraud MF, Paumard P, Soubannier V, *et al.* (2002) Is there a relationship between the supramolecular organization of the mitochondrial ATP synthase and the formation of cristae? *Biochim Biophys Acta* **1555**, 174–180.
- Grad LI and Lemire BD (2004) Mitochondrial complex I mutations in *Caenorhabditis elegans* produce cytochrome *c* oxidase deficiency, oxidative stress and vitamin-responsive lactic acidosis. *Hum Mol Genet* **13**, 303–314.
- Hackenbrock CR, Chazotte B and Gupta SS (1986) The random collision model and a critical assessment of the diffusion and collision in mitochondrial electron transport. *J Bioenerg Biomembr* **18**, 331–368.
- Hatefi Y (1985) The mitochondrial electron transport and oxidative phosphorylation system. *Ann Rev Biochem* **54**, 1015–1069.
- Hatefi Y, Haavik AG, Fowler LR and Griffiths DE (1962a) Studies on the electron transfer system. Reconstitution of the electron transfer system. *J Biol Chem* **237**, 2661–2669.
- Hatefi Y, Haavik AG and Griffiths E (1962b) Studies on the electron transfer system XL: preparation and properties of mitochondrial DPNH-Coenzyme Q reductase. *J Biol Chem* **237**, 1676–1680.
- Hatefi Y, Haavik AG and Jurtschuk P (1961) Studies on the electron transport system XXX. DPNH-cytochrome *c* reductase I. *Biochim Biophys Acta* **52**, 106–118.
- Hatefi Y and Rieske JS (1967) The preparation and properties of DPNH-cytochrome *c* reductase (complex I–III of the respiratory chain). *Meth Enzymol* **10**, 225–231.
- Heazlewood JL, Howell KA and Millar AH (2003a) Mitochondrial complex I from *Arabidopsis* and rice: orthologs of mammalian and yeast components coupled to plant-specific subunits. *Biochim Biophys Acta* **1604**, 159–169.
- Heazlewood JL, Whelan J and Millar AH (2003b) The products of the mitochondrial ORF25 and ORFB genes are F_0 components of the plant F_1F_0 ATP synthase. *FEBS Lett* **540**, 201–205.
- Horsefield R, Iwata S and Byrne B (2004) Complex II from a structural perspective. *Curr Protein Pept Sci* **5**, 107–118.

- Horváth A, Horáková E, Dunajcikova P, *et al.* (2005) Downregulation of the nuclear-encoded subunits of the complexes III and IV disrupts their respective complexes but not complex I in procyclic *Trypanosoma brucei*. *Mol Microbiol* **58**, 116–130.
- Hunte C, Koepke J, Lange C, Rossmann T and Michel H (2000) Structure at 2.3 Å resolution of the cytochrome bc₁ complex from the yeast *Saccharomyces cerevisiae* co-crystallized with an antibody fragment. *Structure* **8**, 669–684.
- Iwasaki T, Matsuura K and Oshima T (1995) Resolution of the aerobic respiratory system of the thermoacidophilic archaeon, *Sulfolobus* sp. strain 7. I: The archaeal terminal oxidase supercomplex is a functional fusion of respiratory complexes III and IV with no c-type cytochromes. *J Biol Chem* **270**, 30881–30892.
- Kawato S, Sigel E, Carafoli E and Cherry RJ (1981) Rotation of cytochrome oxidase in phospholipid vesicles. *J Biol Chem* **256**, 7518–7527.
- Krause F, Reifschneider NF, Goto S and Dencher NA (2005) Active oligomeric ATP synthases in mammalian mitochondria. *Biochem Biophys Res Commun* **329**, 583–590.
- Krause F, Reifschneider NH, Vocke D, Seelert H, Rexroth S and Dencher NA (2004) ‘Respirasome’-like supercomplexes in green leaf mitochondria of spinach. *J Biol Chem* **279**, 48369–48375.
- Lange C, Nett JH, Trumpower BL and Hunte C (2001) Specific roles of protein-phospholipid interactions in the yeast cytochrome bc₁ complex. *EMBO J* **20**, 6591–6600.
- Lee SJ, Yamashita E, Abe T, *et al.* (2001) Intermonomer interactions in dimer of bovine heart cytochrome c oxidase. *Acta Crystallogr D Biol Crystallogr* **57**, 941–947.
- Lenaz G (2001) A critical appraisal of the mitochondrial coenzyme Q pool. *FEBS Lett* **509**, 151–155.
- Millar AH, Eubel H, Jansch L, Kruft V, Heazlewood JL and Braun HP (2004) Mitochondrial cytochrome c oxidase and succinate dehydrogenase contain plant-specific subunits. *Plant Mol Biol* **56**, 77–89.
- Millar AH, Mittova V, Kiddle G, *et al.* (2003) Control of ascorbate synthesis by respiration and its implications for stress responses. *Plant Physiol* **133**, 443–447.
- Minauro-Sanmiguel F, Wilkens S and Garcia JJ (2005) Structure of dimeric mitochondrial ATP synthase: novel F₀ bridging features and the structural basis of mitochondrial cristae biogenesis. *Proc Natl Acad Sci USA* **102**, 12356–12358.
- Niebisch A and Bott M (2003) Purification of a cytochrome bc₁-aa₃ supercomplex with quinol oxidase activity from *Corynebacterium glutamicum*. Identification of a fourth subunit of cytochrome aa₃ oxidase and mutational analysis of dihemeric cytochrome c₁. *J Biol Chem* **278**, 4339–4346.
- Parisi G, Perales M, Fornasari MS, *et al.* (2004) Gamma carbonic anhydrases in plant mitochondria. *Plant Mol Biol* **55**, 193–207.
- Paumard P, Vaillier J, Coulary B, *et al.* (2002) The ATP synthase is involved in generating mitochondrial cristae morphology. *EMBO J* **21**, 221–230.
- Pfeiffer K, Gohil V, Stuart RA, *et al.* (2003) Cardiolipin stabilizes respiratory chain supercomplexes. *J Biol Chem* **278**, 52873–52880.
- Perales M, Eubel H, Heinemeyer J, Colaneri A, Zabaleta E and Braun HP (2005) Disruption of a nuclear gene encoding a mitochondrial gamma carbonic anhydrase reduces complex I and supercomplex I + III₂ levels and alters mitochondrial physiology in *Arabidopsis*. *J Mol Biol* **350**, 263–277.
- Perales M, Parisi G, Fornasari MS, *et al.* (2004) Gamma carbonic anhydrase subunits physically interact within complex I of plant mitochondria. *Plant Mol Biol* **56**, 947–957.
- Pineau B, Mathieu C, Gerard-Hime C, De Paepe R and Chetrit P (2005) Targeting the NAD7 subunit to mitochondria restores a functional complex I and a wild type phenotype in the *Nicotiana glauca* CMS II mutant lacking nad7. *J Biol Chem* **280**, 25994–26001.
- Ragan CI and Heron C (1978) The interaction between mitochondrial NADH-ubiquinone oxidoreductase and ubiquinol-cytochrome c oxidoreductase. *Biochem J* **174**, 783–790.
- Rexroth S, Meyer zu Tittingdorf JM, Schwassmann HJ, Krause F, Seelert H and Dencher NA (2004) Dimeric H⁺-ATP synthase in the chloroplast of *Chlamydomonas reinhardtii*. *Biochim Biophys Acta* **1658**, 202–211.
- Rich PR (1984) Electron and proton transfer through quinones and cytochrome bc complexes. *Biochim Biophys Acta* **768**, 53–79.

- Richter OMH and Ludwig B (2003) Cytochrome *c* oxidase – structure, function, and physiology of a redox-driven molecular machine. *Rev Physiol Biochem Pharmacol* **147**, 47–74.
- Runswick MJ, Fearnley IM, Skehel JM and Walker JE (1991) Presence of an acyl carrier protein in NADH: ubiquinone oxidoreductase from bovine heart mitochondria. *FEBS Lett* **286**, 121–124.
- Sabar M, Balk J and Leaver CJ (2005) Histochemical staining and quantification of plant mitochondrial respiratory chain complexes using blue-native polyacrylamide gel electrophoresis. *Plant J* **44**, 893–901.
- Sackmann U, Zensen R, Röhlen D, Jahnke U and Weiss H (1991) The acyl-carrier protein in *Neurospora crassa* mitochondria is a subunit of NADH: ubiquinone reductase (complex I). *Eur J Biochem* **200**, 463–469.
- Sazanov LA and Hinchliffe P (2006) Structure of the hydrophilic domain of respiratory complex I from *Thermus thermophilus*. *Science* **311**, 1430–1436.
- Schägger H (2001a) Respiratory chain super complexes. *IUBMB Life* **52**, 119–128.
- Schägger H (2001b) Blue-native gels to isolate protein complexes from mitochondria. *Methods Cell Biol* **65**, 231–244.
- Schägger H (2002) Respiratory supercomplexes of mitochondria and bacteria. *Biochim Biophys Acta* **1555**, 154–159.
- Schägger H, De Coo R, Bauer MF, Hofmann S, Godinot C and Brandt U (2004). Significance of respirasomes for the assembly/stability of human respiratory chain complex I. *J Biol Chem* **279**, 36349–36353.
- Schneider H, Lemasters JL, Höchli M and Hackenbrock CR (1980a) Fusion of liposomes with mitochondrial inner membranes. *Proc Natl Acad Sci USA* **77**, 442–446.
- Schneider H, Lemasters JL, Höchli M and Hackenbrock CR (1980b) Liposome-mitochondrial inner membrane fusions. *J Biol Chem* **255**, 3748–3756.
- Schägger H and Pfeiffer K (2000) Supercomplexes in the respiratory chains of yeast and mammalian mitochondria. *EMBO J* **19**, 1777–1783.
- Schägger H and Pfeiffer K (2001) The ratio of oxidative phosphorylation complexes I–V in bovine heart mitochondria and the composition of respiratory chain supercomplexes. *J Biol Chem* **276**, 37861–37867.
- Silman HI, Rieske JS, Lipton SH and Baum H (1967) A new protein component of complex III of the mitochondrial electron transfer chain. *J Biol Chem* **242**, 4867–4875.
- Sone N, Sekimachi M and Kutoh E (1987) Identification and properties of a quinol oxidase supercomplex composed of a bc₁ complex and cytochrome oxidase in the thermophilic bacterium PS3. *J Biol Chem* **262**, 15386–15391.
- Stock D, Gibbons C, Arechaga I, Leslie AGW and Walker JE (2000) Rotary mechanism of ATP synthase. *Curr Opin Struct Biol* **10**, 672–679.
- Stroh A, Anderka O, Pfeiffer K, *et al.* (2004) Assembly of respiratory complexes I, III and IV into NADH oxidase supercomplexes stabilizes complex I in *Paracoccus denitrificans*. *J Biol Chem* **279**, 5000–5007.
- Sunderhaus S, Dudkina NV, Jansch L, *et al.* (2006) Carbonic anhydrase subunits form a matrix-exposed domain attached to the membrane arm of mitochondrial complex I in plants. *J Biol Chem* **281**, 6482–6488.
- Taylor NL, Heazlewood JL, Day DA and Millar AH (2005) Differential impact of environmental stresses on the pea mitochondrial proteome. *Mol Cell Proteomics* **4**, 1122–1133.
- Tsukihara T, Aoyama H, Yamashita E, *et al.* (1996) The whole structure of the 13-subunit oxidized cytochrome *c* oxidase at 2.8 Å. *Science* **272**, 1136–1144.
- Ugalde C, Janssen RJRJ, Van Den Heuvel LP, Smeitink JAM and Nijtmans LGJ (2004) Differences in assembly or stability of complex I and other mitochondrial OXPHOS complexes in inherited complex I deficiency. *Hum Mol Genet* **13**, 659–667.
- Van Lis R, Atteia A, Mendoza-Hernandez G and Gonzalez-Halphen D (2003) Identification of novel mitochondrial protein components of *Chlamydomonas reinhardtii*. A proteomic approach. *Plant Physiol* **132**, 318–330.

- Van Lis R, Mendoza-Hernandez G and Gonzalez-Halphen D (2005) Divergence of the mitochondrial electron transport chains from the green alga *Chlamydomonas reinhardtii* and its colorless close relative *Polytomella* sp. *Biochim Biophys Acta* **1708**, 23–34.
- Wittig I and Schägger H (2005) Advantages and limitations of clear native polyacrylamide gel electrophoresis. *Proteomics* **5**, 4338–4346.
- Yankovskaya V, Horsefield R, Tornroth S, *et al.* (2003) Architecture of succinate dehydrogenase and reactive oxygen species generation. *Science* **299**, 700–704.
- Zhang M, Mileykovskaya E and Dowhan W (2002) Gluing the respiratory chain together. Cardiolipin is required for supercomplex formation in the IMM. *J Biol Chem* **277**, 43553–43556.
- Zhang M, Mileykovskaya E and Dowhan W (2005) Cardiolipin is essential for the organization of complexes III and IV into a supercomplex in intact yeast mitochondria. *J Biol Chem* **280**, 29403–29408.

UNCORRECTED PROOF

Supplementary Discussion and Outlook

8.1 Discussion

This PhD thesis presents experimental evidence that the occurrence of protein supercomplexes is a wide spread phenomenon in membrane systems involved in the generation of ATP. In chapter 2, the occurrence of respirasomes in potato mitochondria is demonstrated by the use of Blue-native PAGE. Using the same experimental approach the existence of chloroplast supercomplexes composed of PS I + LHC I and dimeric PS II + LHC II is demonstrated in the thylakoid membrane of Arabidopsis (chapter 3). Chapter 4 provides structural information of a supercomplex that consists of two ATP synthase complexes from the colorless green alga *Polytomella*. Furthermore, the pseudoatomic model of a supercomplex consisting of complex III and IV from yeast is presented. Beside the chapters of this PhD thesis a considerable number of recent publications also report the existence of supercomplexes. Nevertheless, the pure depiction of such structures should not be considered to represent sufficient evidences for their *in vivo* appearance. As a consequence, the debate on the occurrence of supercomplexes continues (see chapters 6 and 7 of this PhD thesis). Indeed, all techniques used to investigate the supramolecular organization of membrane-bound protein complexes somehow disturb the system to be analyzed and might generate artifacts. The following discussion focuses on supercomplex function. If the described supercomplexes are meaningful structures they must have a function.

8.1.1 Function of OXPHOS supercomplexes

Proposed functions for OXPHOS supercomplexes are:

1. Structural stabilization of the individual protein complexes
2. Regulation of the electron transfer
3. Acceleration of electron transfer between the individual protein complexes
4. Structural organization of the associated membranes systems
5. Enhancement of the protein-insertion capacity of the associated membrane systems

Concerning the functions listed by points one to three data are contradictory. The chapter 6 and 7 of this PhD thesis include an extensive discussion. However, recent data on the structure of

the III+IV supercomplex in yeast newly support a role of respiratory supercomplexes in accelerating electron transfer. In the past, the discovery of supercomplexes consisting of two or more individual complexes which constitute an electron transfer sequence gave rise to the idea these supramolecular structures could enhance electron transfer. This hypothesis is based on the assumption that the active sites of respiratory complexes are in close proximity within supercomplexes. However, the structural model of the I+III₂ supercomplex from *Arabidopsis* does not support this hypothesis. Within this supercomplex, binding sites for ubiquinone and ubiquinol are postulated to be rather distant from each other (Dudkina et al. 2005). The EM data for mammalian respirasomes point into the same direction (Schäfer et al. 2006). On the other hand the data presented in chapter 5 of this work clearly show that in the case of the yeast III+IV supercomplex enhanced electron transfer is deducible. Based on the pseudoatomic model for these supercomplexes the cytochrome c binding sites of the complexes III and IV are in very close proximity, allowing cytochrome c to move between them by a rapid ping-pong like mechanism. The data obtained from the work in chapter 3 of this PhD thesis add another aspect to this controversy. In the photophosphorylation apparatus supercomplexes consisting of different oxidoreductases could not be detected. These findings do not support a role of supercomplexes of the photophosphorylation system in accelerated electron transfer (Lavergne et al. 1992, Kirchhoff et al. 2002).

In contrast to the contradicting hints for supercomplex functions outlined by points one to three the proposed functions by points 4 and 5 seem to be less strongly challenged by experimental results. Indeed, several arguments support the idea that OXPHOS supercomplexes play a role in membrane architecture:

Folding of the inner mitochondrial membrane is mediated by proteins

In general, folding of the inner mitochondrial membrane (IMM) is assumed to be facilitated by its two main components, the lipids and the proteins. In case of lipids an asymmetrically distribution of different lipid species in the two leaflets of the membrane bilayer could curve the membrane. Such an asymmetrical distribution could be achieved and maintained by the activities of flippases or lipid modifying enzymes (for review see Pomorski et al. 2006). Since lipid asymmetry is considered to be unable to create large and stable membrane structures and since little is known about a continuously and asymmetrically lipid distribution in the IMM the protein mediated folding is more likely (Voeltz et al. 2007). Indeed several proteins of the IMM were found to be important for the folding. For example, the reduced level of a

protein called mitofilin was shown to lead to a concentric onion like configuration of inner mitochondrial membranes; Tubular foldings of the inner mitochondrial membranes were absent (John et al. 2005). Furthermore, a protein called OPA1 in man and Mgm1 in yeast also has an influence on the membrane morphology. Impaired expression of this protein results in cristae disorganization accompanied by matrix dilatation and mitochondrial constriction (Olichon et al. 2003, Griparic et al. 2004). Finally, decreased amounts of ATP6 result in rounded compartments contiguous with lamellar regions of the same membrane (Celotto et al. 2006). Beside the mentioned proteins also TIM23, a subunit of the protein translocation machinery of the mitochondrial membranes, which includes domains in both mitochondrial membranes, is thought to affect the IMM shape (Donzeau et al. 2000).

Membrane folding proteins have a preferential localization

The role of proteins in membrane folding processes requires a defined localization of them. This was for instance shown for the TIM23 subunit, which mainly is localized within the IBM (Wurm et al (2006) and Vogel et al. (2006). The same localization was found for the Opa/Mgm1 protein (Vogel et al. (2006). In contrast, the localization of mitofilin is so far unclear. However, recent experimental results point towards a localization close to cristae junctions (John et al. 2005).

Membrane folding is proposed to occur through the constitution of large protein assemblies

The membrane forming function of mitofilin is proposed to rely on its ability to constitute large protein assemblies of approximately 1200 kDa (John et al. 2005). The proteins of the mitochondrial protein import machinery associate to constitute the TIM and TOM complexes. Mokranjac et al. (2005) and Albrecht et al. (2006) have demonstrated that the newly discovered Tim21 subunit of the TIM complex interacts with the TOM40 and TOM22 subunits of the TOM complex within a TOM/TIM supercomplex. Furthermore, as stated above, the TIM23 subunit was found to span both the OMM and IMM (Donzeau et al. 2000). It can be assumed that formation of the TOM/TIM supercomplex is due to these features and mediates membrane tethering of the IBM to the outer mitochondrial membrane. It was suggested that the two membrane spanning domain of TIM23 alone is responsible for permanent membrane tethering of outer and inner mitochondrial membranes (Donzeau et al. 2000). This is supported by the fact that TOM/TIM supercomplexes are only stable during preprotein translocation and therefore seem to be transient structures (Berthold et al. 1995, Horst et al. 1995; Dekker et al. 1997, Endres et al. 1999). Also the membrane shaping function of OPA1 is be-

lieved to be based on the formation of large membrane assemblies. Putative binding partners of OPA1 within these assemblies are the Fzo1 and Ugo1 proteins, which together with OPA1 form part of the mitochondrial fusion and fission machinery (for review see Escobar-Henriques et al 2006).

Also OXPHOS supercomplexes represent large protein assemblies which have a preferential localization within the inner mitochondrial membrane (Wurm et al. 2006, Vogel et al. 2006). Additionally, the proteins of the OXPHOS system are the most abundant proteins within the cristae membrane. It therefore is quite likely that they have a strong influence on membrane shape, as reported by several recent investigations. The angular association of ATP synthase monomers within ATP synthase dimers (chapter 4) demonstrates how inner mitochondrial membranes can be shaped by the formation of a supercomplex. This conclusion is further supported by the observation that yeast mutants deficient in ATP synthase dimerization lack foldings of the inner mitochondrial membranes and instead show an onion-like structure of the IMM (Paumard et al. 2002). Similar results were reported on the basis of artificial cross-linking of ATP synthase monomers between their F_1 parts (Gavin et al. 2004).

As in the case of dimeric ATP synthase the structure of the III+IV supercomplex from yeast presented in chapter 5 also is the starting point of speculations on its possible role in shaping the IMM. The structure of the supercomplex reveals that complex IV monomers are attached to a complex III dimer on opposite sides. The interaction takes place in a way that does not occupy the proposed complex IV side responsible for complex IV dimerization. In theory, this way of supercomplex formation allows the formation of long strings of III+IV supercomplexes. String like structures of respiratory supercomplexes were already proposed by Wittig et al. (2006) for mammalian mitochondria. In the case of dimeric ATP synthase formation of oligomers were proposed to create a scaffold that determines the shape of tubular cristae (Allen et al. 1989, chapter 4, and 6 of this work, Dudkina et al. 2006, Voeltz et al. 2007). However, for the III+IV supercomplex of yeast results pointing into this direction until now are lacking.

A rather indirect hint towards the role of not only dimeric ATP synthase but also respiratory supercomplexes in cristae generation comes from observations on human fibroblasts devoid of mitochondrial DNA (mtDNA). MtDNA depletion was shown to alter the cristae structure (Gilkerson et al. 2000) by the loss of subunits of ATP synthase and the respiratory chain com-

plexes. Since the function of the respiratory chain is disrupted it can be assumed that supercomplexes are absent. A role of dimeric ATP synthase in cristae formation can be excluded because it is assumed that this supercomplex is responsible mainly for tubular cristae and those are already absent in WT cells. Hence, it occurs that the lack of supercomplexes could be responsible for the altered cristae structure.

8.1.2 Function of PHOTPHOS supercomplexes

The intension of the work presented in chapter 2 was to investigate whether or not until now unknown supercomplexes can be detected in the thylakoid membranes of plants. In this respect an association of Cyt b_6f with PS I could be imaginable. This putative supercomplex was proposed to enhance cyclic electron transport (Joliot et al 2002, Joliot et al. 2004). However, in accordance with previous studies, the investigation reported in chapter 2 did not reveal occurrence of such a supercomplex. An alternative supercomplex could be composed of PS II and Cyt b_6f . Presence of this supercomplex was proposed to exist as a consequence of putative microdomains of PS II and Cyt b_6f (Joliot et al. 1992, Kirchhoff et al. 2000). The function of this assembly was suggested to be an enhancement of electron transfer since plastoquinone diffusion in grana membranes was estimated to be very slow (Lavergne et al. 1992, Kirchhoff et al. 2002). However, conclusive evidence for the occurrence of this supercomplex is so far lacking. The absence of an PS II-Cyt b_6f supercomplex in part can be explained by the complementary microlocation of the protein complexes of the thylakoid membranes (reviewed by Dekker et al. 2005). PS II was shown to be located in the grana stacks whereas PS I has a preferential localization within the stroma membranes. This microdistribution possibly also is due to the membrane protruding parts of PS I which are too large to fit into the narrow stacks of the grana. Also the membrane protruding parts of Cyt b_6f are assumed to be a hindrance to enter the grana stacks. Hence the occurrence of PS II-Cyt b_6f supercomplexes is unlikely. However, results on the microlocalization of Cyt b_6f so far are not quite clear (e.g. Berthold 1981, Anderson 1982).

Supercomplexes composed of PS II and LHC II and PS I and LHC I, which previously were described by single particle electron microscopy, could be confirmed by the investigation of this dissertation (chapter 3). One of the functions of these structures is to facilitate the transfer of light energy onto the photoreaction centers of PS I and PS II. Additionally, it is generally accepted that LHC II can be detached from PS II to become attached to PS I. The reversible binding of LHC II complexes to PS II or PS I is important to balance light energy absorbed by

the two photoreaction centers. It is regulated by phosphorylation. (for review see Allen et al. 2001).

In contrast to the membrane shaping function of ATP synthase dimers in mitochondria an analogous role of chloroplast ATP synthase supercomplexes is uncertain. However, using Blue-native PAGE, such supercomplexes were recently reported (Schwassmann et al. 2007). The two photosystems and the Cyt b_6f complex are not known to directly influence the membrane shape of the thylakoids. Rather, interactions of PS II and LHC II complexes in opposing membranes are considered to cause the membrane stackings within the grana. In contrast, the PS II + LHC II and PS I + LHC I supercomplexes are not known to induce membrane bending and the margins of the grana membrane stacks are supposed to be free of proteins (Murphy et al. 1986, Dekker et al. 2005). On the other hand, Kovacs et al. (2006) demonstrate that absence of the CP24 subunit leads to an altered structure of the grana membrane due to PS II + LHC II supercomplex disassembly, but if this in turn alters grana stacking was not shown. In conclusion, the precise influence of supramolecular protein structures on the shape of the thylakoid membrane so far is largely unknown.

8.2 Outlook

8.2.1 Further investigations of the supramolecular organization of membrane bound protein supercomplexes

Although experimental results strongly support a role of dimeric ATP synthase in the formation of tubular cristae, further investigations should be carried out to get deeper insights into mechanisms that determine the shape of the inner mitochondrial membrane. A project to systematically search for the correlation between the oligomeric state of ATP synthase and the shape of the inner mitochondrial membrane could reveal exciting information. In this respect, initial investigations that aim to characterize dimeric ATP synthase of *Paramecium* by Blue-native PAGE are underway in our laboratory. The results possibly allow a confirmation of interpretations published earlier by Allen et al. (1989). Using “rapid-freeze deep-etch” electron microscopy, Allen et al. visualized double rows of particles which form helical structures on the surface of tubular cristae. These structures were interpreted to represent ATP synthase oligomers. However, biochemical analyses of the mitochondrial membranes of *Paramecium* are so far lacking.

Beyond an investigation on the influence of the oligomeric state of ATP synthase on the structure of the inner mitochondrial membrane a quantitative determination of ATP synthase dimers in relation to the abundance of tubular cristae would be telling. It has been shown by the work of Hanaki et al. (1985) that the amount of tubular cristae in rat adrenal cortex mitochondria varies in dependence to their specific localization of cells within this tissue. While the cristae of the zona glomerula and the external zone of the zona fasciculata have an almost tubular shape, those of the internal zone of the zona fasciculata are mainly vesicular but also lamellar. Furthermore, the cristae of the zona reticularis are mainly tubules and vesicles. The varying amounts of tubular cristae in mitochondria of different zones of the adrenal cortex represent an ideal starting point to investigate the role of the oligomeric state of ATP synthase on the shaping of the inner mitochondrial membrane. So far, only the investigation by Dudkina et al. (2006) on *Polytomella* mitochondria includes a biochemical characterization of ATP synthase dimers and at the same time demonstrates the presence of cristae rich in tubular foldings.

As in the case of dimeric ATP synthase also the data obtained for the structure of the yeast III+IV supercomplex need further validation. In particular, an investigation of the string hypothesis that conciliates the presented pseudoatomic model of the III+IV supercomplex with the crystal structure of dimeric complex IV would be exciting. Clarifying evidence could come from a check whether yeast complex IV *in vivo* exists as a dimer or not. This could be done by crosslink experiments. Further hints to answer the question if strings are a possible organization form of complexes III and IV could come from an investigation of the cristae structure of mutants with a deficiency to form III+IV supercomplexes. Since chapter 4 assumes that the III+IV supercomplex can bend the membrane solely by four degree, only long strings of III+IV supercomplexes would be able to organize the IMM. In this respect, III+IV supercomplex deficiency accompanied by an atypical cristae structure would be telling. An available subject for the mentioned investigation could be the yeast strain Δ Taz1 which was shown to comprise reduced amounts of the III+IV supercomplex due to defects in cardiolipin biosynthesis (Brandner et al. 2005). In this respect it has to be taken into account that a putative altered cristae structure could also be a direct effect of the cardiolipin defect. Nevertheless, the investigation of the cristae structure of the yeast Δ Taz1 mutant appears to be attractive because in man a Taz1 mutation causing the Bath syndrome was correlated to impaired supercomplex assembly. Indeed, in human Bath syndrome an altered cristae morphology was demonstrated (Acehan et al. 2007). However, the discussion of these findings does not take

into account that impaired supercomplex formation might be the cause. Instead, along with the possibility that lack of Taz1 itself is the cause of the observed abnormalities, an unspecific aggregation of protein complexes due to the lack of cardiolipin is assumed. It is worth mentioning that unspecific aggregations of respiratory protein complexes due to the lack of cardiolipin to my knowledge were never shown.

8.2.2. Further investigations of the supramolecular organization of membrane bound protein supercomplexes on the basis of DIGE

If strings of III+IV supercomplexes in yeast are absent *in vivo*, dimerization of complex IV is in conflict with the findings of chapter 4. Besides the proposed cross-linking experiments to search for evidence in favor of the presence of yeast complex IV dimers, another possibility would be the development of a new approach capable to identify whether the proposed dimer interaction side of the complex IV monomer is *in vivo* occupied or not. If occupied, one can assume that amino acid (AS) residues of subunits at the dimer interaction side are inaccessible for the binding of reactive chemicals. In case of a dimeric configuration of complex IV, impaired binding of chemicals could be visualized by the combination of Blue-native PAGE and the use of fluorescent dyes. In general, this approach would be based on the assumption that residues of internal protein subunits within a protein complex have a lower accessibility while peripheral proteins have a higher accessibility for binding fluorescent dyes. This in turn would result in weakly respectively strongly labeled protein subunits depending on their position within the (super-) complex. The differentially labeled proteins subsequently could be separated and identified by the use of 2D Blue-native/SDS-PAGE. If dimerization of complex IV is true, subunits which are predicted to be at the dimerization interface should belong to the group of weakly labeled proteins. Appropriate fluorescence dyes are the CyDyes™ of GE Healthcare. These dyes are part of the differential gel electrophoresis (DIGE) system offered by this company. Originally, this system was intended to quantify differences within related protein mixtures. By the use of three available CyDyes™, up to three related samples can be differentially labeled and subsequently subjected to isoelectric focusing/sodium dodecyl sulfate gel electrophoresis (IEF/SDS-PAGE) within one single gel. Detection of the resolved samples is achieved by scanning the obtained gel at different wavelengths corresponding to the dyes used. This results in a distinct image for each sample and allows to compare the fluorescence intensities quantitatively to a resolved protein species in the different samples. Additionally, an overlay image can be generated to illustrate the differences. Since the single im-

ages in this mode have different colors, unaltered protein species are displayed in a combination color. The idea to divert the DIGE system from its originally intended use comes from the observation that the protein pattern of a fluorescence scanned 2D Blue-native/SDS gel differs from the pattern obtained when the same gel is Coomassie colloidal stained. It is assumed that the differences are due to the inaccessibility of proteins for the fluorescence dye if the labeling is carried out in the presence of native conditions. This in turn could reflect topological information of proteins within protein complexes.

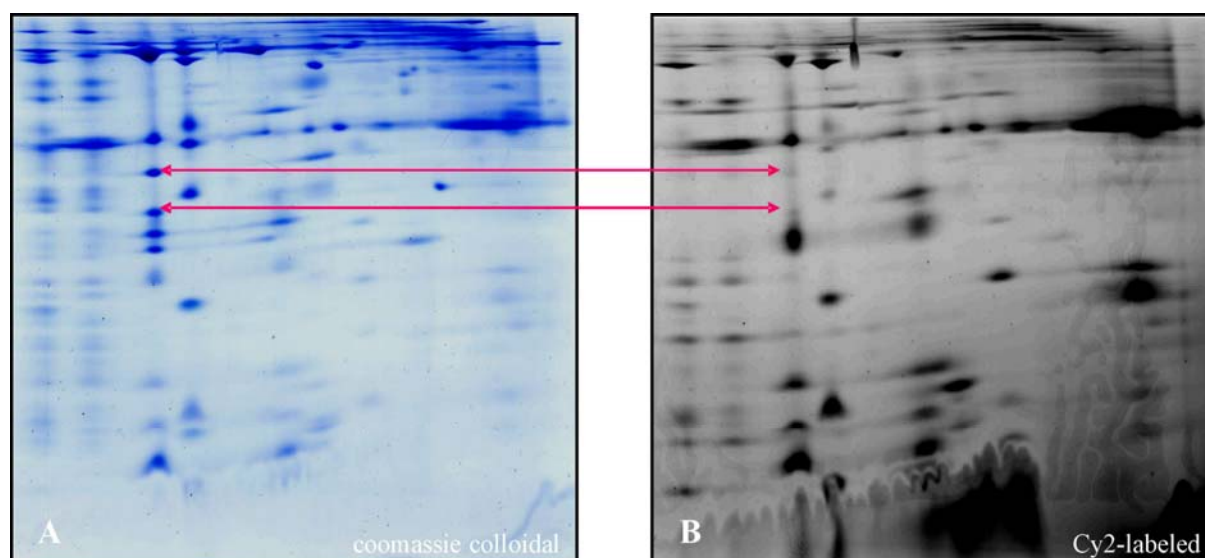


Figure 2: Comparison of two images of the same 2D BN/SDS gel obtained after different detection procedures. **A:** Coomassie colloidal staining. **B:** Fluorescence detection. The gross pattern of proteins is unaltered while detection of distinct proteins is remarkably different (red arrows indicate subunits of complex V hardly detectable by fluorescence detection).

For developing a reliable procedure, an optimized DIGE system based on the observations and ideas presented above has to be established. Apart from the efforts to use an optimized DIGE system for topological investigations other fields of applications exist. In the course of this thesis it could be demonstrated that a combination of Blue-native PAGE and DIGE is suitable to map the protein subunits belonging to a protein complex within IEF/SDS gels without the use of mass spectrometry. Furthermore it was shown that this combination also is a suitable tool to facilitate precise size comparisons between protein complexes and super-complexes of different species or organelles.

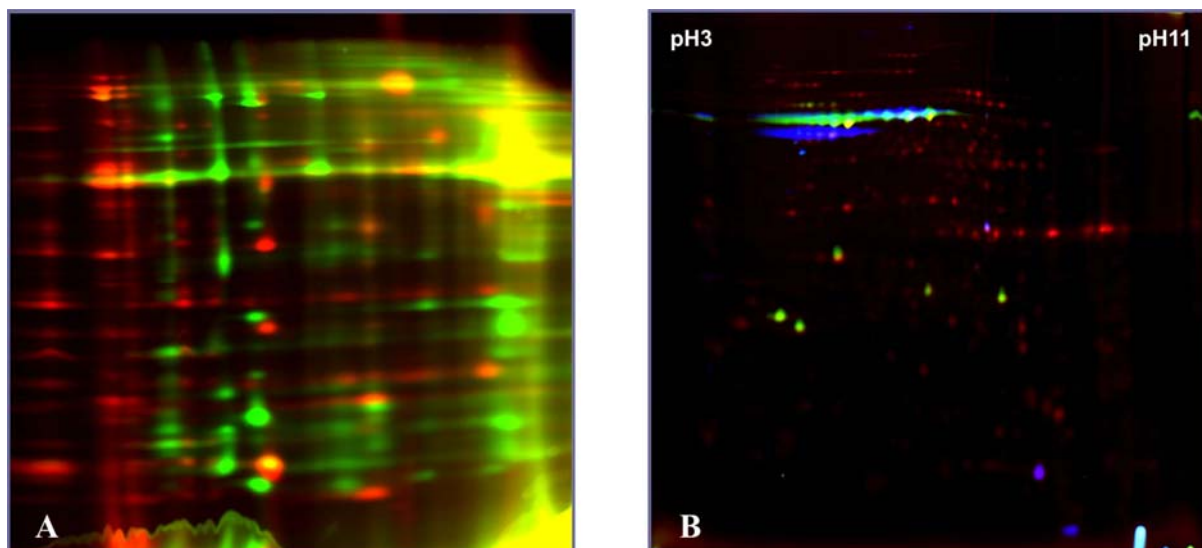


Figure 3: 2D gel separations using new DIGE approaches A: BN/SDS gel of a co-separation of mitochondrial protein complexes and protein supercomplexes from Polytomella (in red) and Arabidopsis (in green). B: IEF/SDS gel of a three dimensional separation of mitochondrial proteins. Members of protein complex V (in green) and of protein complex III (in blue) are mapped within the Arabidopsis proteome (in red).

The demonstrated transfer of established techniques to new fields of research as well as the extension of techniques with respect to their intended use can help to promote scientific progress. In this respect it might be possible that even larger structures than those of the OXPHOS and PHOTPHOS system will be discovered once. Oligomeric ATP synthase can be regarded as a first example of such very large protein structures but so far its presence under *in vivo* conditions is highly speculative and has to await further investigations. Nevertheless, it is interesting to realize that the concept of a supramolecular organization of many biochemical pathways is looming, especially in the functional context of the OXPHOS and the PHOTPHOS system. The Calvin cycle as well as the citric acid cycle are assumed to be organized in supercomplexes (Süss et al. 1993, Velot 1997, Velot et al. 2000). Since both, by means of their demand on NADPH or their offer of NADH are functionally linked to the OXPHOS or the PHOTPHOS system, one can question whether even larger structures do exist. Data supporting this idea come from an investigation that reports capability of complex I to bind citric acid cycle enzymes (Sumegi et al. 1984). This would be in conflict with the view that complex II is the best candidate to tether the citric acid cycle to the inner mitochondrial membrane. Since this protein complex itself is part of the enzyme sequence of the citric acid cycle, this also appears imaginable and maybe both is true. Weak evidence comes from the work of Hatefi et al. (1961) who described the reconstruction of a protein supercomplex of complexes I, II and III, but until today this complex could not be confirmed by other experimental strategies.

8.3 Literature cited

Acehan D., Xu Y., Stokes DL., Schlame M. (2007)

Comparison of lymphoblast mitochondria from normal subjects and patients with Barth syndrome using electron microscopic tomography.

Lab Invest. 87(1): 40-48

Albrecht R., Rehling P., Chacinska A., Brix J., Cadamuro SA., Volkmer R., Guiard B., Pfanner N., Zeth K. (2006)

The Tim21 binding domain connects the preprotein translocases of both mitochondrial membranes.

EMBO Rep. 7(12): 1233-1238

Allen RD., Schroeder CC., Fok AK. (1989)

An investigation of mitochondrial inner membranes by rapid-freeze deep-etch techniques.

J Cell Biol. 108(6): 2233-2240

Allen JF., Forsberg J. (2001)

Molecular recognition in thylakoid structure and function.

Trends Plant Sci. 6: 317-326

Anderson JM. (1982)

Distribution of the cytochromes of spinach chloroplasts between the appressed membranes of grana stacks and stroma-exposed thylakoid regions.

FEBS Lett. 138: 62-66

Berthold DA., Babcock GT., Yocum CF. (1981)

A highly-resolved oxygen-evolving photosystem II preparation from spinach thylakoid membranes.

FEBS Lett. 134: 231-234

Berthold J., Bauer MF., Schneider HC., Klaus C., Dietmeier K., Neupert W., Brunner M. (2005)

The MIM complex mediates preprotein translocation across the mitochondrial inner membrane and couples it to the mt-Hsp70/ATP driving system.

Cell. 81(7): 1085-1093

Brandner K., Mick DU., Frazier AE., Taylor RD., Meisinger C., Rehling P. (2005)

Taz1, an outer mitochondrial membrane protein, affects stability and assembly of inner membrane protein complexes: implications for Barth Syndrome.

Mol Biol Cell. 16(11): 5202-5214

Celotto AM., Frank AC., McGrath SW., Fergestad T., van Voorhies WA., Buttle KF., Mannella CA., Palladino MJ. (2006)

Mitochondrial encephalomyopathy in *Drosophila*.

J Neurosci. 26(3): 810-820

Dekker PJ., Martin F., Maarse AC., Bomer U., Muller H., Guiard B., Meijer M., Rassow J., Pfanner N. (1997)

The Tim core complex defines the number of mitochondrial translocation contact sites and can hold arrested preproteins in the absence of matrix Hsp70-Tim44.

EMBO J. 16(17): 5408-5419

Dekker JP., Boekema EJ. (2005)

Supramolecular organization of thylakoid membrane proteins in green plants.

Biochim. Biophys. Acta. 1706(1-2): 12-39. Review

Donzeau M., Kaldi K., Adam A., Paschen S., Wanner G., Guiard B., Bauer MF., Neupert W., Brunner M. (2000)

Tim23 links the inner and outer mitochondrial membranes.

Cell. 101(4): 401-412

Dudkina NV., Eubel H., Keegstra W., Boekema EJ., Braun HP. (2005)

Structure of a mitochondrial supercomplex formed by respiratory-chain complexes I and III.

Proc Natl Acad Sci U S A. 102(9): 3225-3229

Dudkina NV., Sunderhaus S., Braun HP., Boekema EJ. (2006)

Characterization of dimeric ATP synthase and cristae membrane ultrastructure from *Saccharomyces* and *Polytomella* mitochondria.

FEBS Lett. 580(14): 3427-3432

Endres M., Neupert W., Brunner M. (1999)

Transport of the ADP/ATP carrier of mitochondria from the TOM complex to the TIM22.54 complex.

EMBO J. 18(12): 3214-3221

Escobar-Henriques M., Langer T. (2006)

Mitochondrial shaping cuts.

Biochim. Biophys. Acta. 1763(5-6): 422-429. Review

Gavin PD., Prescott M., Luff SE., Devenish RJ. (2004)

Cross-linking ATP synthase complexes in vivo eliminates mitochondrial cristae.

J Cell Sci. 117(Pt 11): 2333-2343

Gilkerson RW., Margineantu DH., Capaldi RA., Selker JM. (2000)

Mitochondrial DNA depletion causes morphological changes in the mitochondrial reticulum of cultured human cells.

FEBS Lett. 474(1): 1-4

Griparic L., van der Wel NN., Orozco JJ., Peters PJ., van der Blik AM. (2004)

Loss of the intermembrane space protein Mgm1/OPA1 induces swelling and localized constrictions along the lengths of mitochondria.

J Biol Chem. 279(18): 18792-18798

Hanaki M., Tanaka K., Kashima Y. (1985)

Scanning electron microscopy study on mitochondrial cristae in the rat adrenal cortex.

J. Electron Microsc. 4: 373-380

Hatefi Y., Haavik AG., Griffiths DE. (1961)

Reconstitution of the electron transport system II. Reconstitution of DPNH-cytochrome c reductase. succinic-cytochrome c reductase and DPNH, succinic-cytochrome c reductase.

Biochem. Biophys. Res. Comm. 4: 447-453

Horst M., Hilfiker-Rothenfluh S., Oppliger W., Schatz G. (1995)

Dynamic interaction of the protein translocation systems in the inner and outer membranes of yeast mitochondria.

EMBO J. 14(10): 2293-2297

John GB., Shang Y., Li L., Renken C., Mannella CA., Selker JM., Rangell L., Bennett MJ., Zha J. (2005)

The mitochondrial inner membrane protein mitofilin controls cristae morphology.

Mol Biol Cell. 16(3):1543-1554

Joliot P., Lavergne J., Beal D. (1992)

Plastoquinone compartmentation in chloroplasts: 1. Evidence for domains with different rates of photoreduction.

Biochim. Biophys. Acta. 1101: 1-12

Joliot P., Joliot A. (2002)

Cyclic electron transfer in plant leaf.

Proc Natl Acad Sci U S A. 99(15): 10209-10214

Joliot P., Beal D., Joliot A. (2004)

Cyclic electron flow under saturating excitation of dark-adapted Arabidopsis leaves.

Biochim. Biophys. Acta. 1656: 166-176

Kirchhoff H., Horstmann S., Weiss E. (2000)

Control of the photosynthetic electron transport by PQ diffusion microdomains in thylakoids of higher plants.

Biochim. Biophys. Acta. 1459: 148-168

Kirchhoff H., Mukherjee U., Galla HJ. (2002)

Molecular architecture of the thylakoid membrane: lipid diffusion space for plastoquinone.

Biochemistry 41: 4872– 4882

Kovacs L., Damkjaer J., Kereiche S., Iliaia C., Ruban AV., Boekema EJ., Jansson S., Horton P. (2006)

Lack of the light-harvesting complex CP24 affects the structure and function of the grana membranes of higher plant chloroplasts.

Plant Cell. 18(11): 3106-3120

Lavergne J., Bouchaud JP., Joliot P. (1992)

Plastoquinone compartmentation in chloroplasts. 2. Theoretical aspects.

Biochim. Biophys. Acta. 1101: 13-22

Mokranjac D., Popov-Celeketic D., Hell K., Neupert W. (2005)

Role of Tim21 in mitochondrial translocation contact sites.

J Biol Chem. 280(25): 23437-23440

Murphy DJ. (1986)

The molecular organization of the photosynthetic membranes of higher plants.

Biochim. Biophys. Acta. 864: 33-94

Olichon A., Baricault L., Gas N., Guillou E., Valette A., Belenguer P., Lenaers G. (2003)

Loss of OPA1 perturbs the mitochondrial inner membrane structure and integrity, leading to cytochrome c release and apoptosis.

J Biol Chem. 278(10): 7743-7746

Paumard P., Vaillier J., Couлары B., Schaeffer J., Soubannier V., Mueller DM., Brethes D., di Rago JP., Velours J. (2002)

The ATP synthase is involved in generating mitochondrial cristae morphology.

EMBO J. 21(3): 221-230

Pomorski T., Menon AK. (2006)

Lipid flippases and their biological functions.

Cell Mol Life Sci. 63(24): 2908-2921. Review

Schäfer E., Seelert H., Reifschneider NH., Krause F., Dencher NA., Vonck J. (2006)

Architecture of active mammalian respiratory chain supercomplexes.

J Biol Chem. 281(22): 15370-15375

Schwassmann HJ., Rexroth S., Seelert H., Dencher NA. (2007)

Metabolism controls dimerization of the chloroplast FoF1 ATP synthase in *Chlamydomonas reinhardtii*.

FEBS Lett. 581(7): 1391-1396

Sumegi B., Srere PA. (1984)

Complex I binds several mitochondrial NAD-coupled dehydrogenases.

J Biol Chem. 259(24): 15040-15045

Suss KH., Arkona C., Manteuffel R., Adler K. (1993)

Calvin cycle multienzyme complexes are bound to chloroplast thylakoid membranes of higher plants in situ.

Proc Natl Acad Sci U S A. 90(12): 5514-5518

Velot C., Mixon MB., Teige M., Srere PA. (1997)

Model of a quinary structure between Krebs TCA cycle enzymes: a model for the metabolon.

Biochemistry. 36(47): 14271-1476

Velot C., Srere PA. (2000)

Reversible transdominant inhibition of a metabolic pathway. In vivo evidence of interaction between two sequential tricarboxylic acid cycle enzymes in yeast.

J Biol Chem. 275(17): 12926-12933

Voeltz GK., Prinz WA. (2007)

Sheets, ribbons and tubules - how organelles get their shape.

Nat Rev Mol Cell Biol. 8(3): 258-264

Vogel F., Bornhovd C., Neupert W., Reichert AS. (2006)

Dynamic subcompartmentalization of the mitochondrial inner membrane.

J Cell Biol. 175(2): 237-247

Wittig I., Carozzo R., Santorelli FM., Schagger H. (2006)

Supercomplexes and subcomplexes of mitochondrial oxidative phosphorylation.

Biochim. Biophys. Acta. 1757(9-10): 1066-1072

Wurm CA., Jakobs S. (2006)

Differential protein distributions define two sub-compartments of the mitochondrial inner membrane in yeast.

FEBS Lett. 580(24): 5628-5634

Abbreviations

| | |
|----------------------|---|
| 1D | one dimensional |
| 2D | two dimensional |
| ADP | adenosine diphosphate |
| AS | amino acid |
| ATP | adenosine triphosphate |
| BN | Blue-native |
| C-atom | carbon atom |
| CO ₂ | carbon dioxide |
| Complex I | NADH dehydrogenase |
| Complex II | succinate dehydrogenase |
| Complex III | cytochrome c reductase |
| Complex IV | cytochrome c oxidase |
| Complex V | ATP synthase |
| Cyt b ₆ f | cytochrome b ₆ f complex |
| DDM | n-dodecylmaltoside |
| DIGE | differential gel electrophoresis |
| DNA | desoxy ribonucleic acid |
| EM | electron microscopy |
| F ₀ | F ₀ part of f-type ATP synthase |
| F ₁ | F ₁ part of f-type ATP synthase |
| FAD ⁺ | Flavin adenine dinucleotide (oxidized form) |
| FADH ₂ | Flavin adenine dinucleotide (reduced form) |
| GDP | Guanosine diphosphate |
| GTP | Guanosine triphosphate |
| IEF | isoelectric focusing |
| IMB | inner boundary membrane |
| IMM | inner mitochondrial membrane |
| KDa | kilo Dalton |
| LHC I | light harvesting complex I |
| LHC II | light harvesting complex II |
| MtDNA | mitochondrial DNA |
| NAD ⁺ | Nicotinamide adenine dinucleotide (oxidized form) |
| NADH | Nicotinamide adenine dinucleotide (reduced form) |
| NADP ⁺ | Nicotinamide adenine dinucleotide phosphate (oxidized form) |
| NADPH | Nicotinamide adenine dinucleotide phosphate (reduced form) |
| O ₂ | molecular oxygen |
| OMM | outer mitochondrial membrane |
| OXPPOS | oxidative phosphorylation |
| P _i | inorganic orthophosphate |
| PAGE | polyacrylamide gel electrophoresis |
| PHOTPHOS | photophosphorylation |
| PS I | photosystem I |
| PS II | photosystem II |
| SDS | sodium dodecyl sulfate |
| TIM | translocase of the inner mitochondrial membrane |
| TOM | translocase of the outer mitochondrial membrane |
| WT | wild type |
| µm | micrometer |

Publications 2004-2007

Heinemeyer J., Braun HP., Boekema EJ., Kouril R. (2007)

A structural model of the cytochrome c reductase / oxidase supercomplex from yeast mitochondria.

J. Biol. Chem. 282: 12240-12248

Heinemeyer J., Dudkina NV., Boekema EJ., Braun HP. (2006)

Supramolecular structure of the OXPHOS system in plants.

In: "Plant Mitochondria", Logan, DC. (ed.), Annual Plant Reviews series, Blackwell Publishing, Oxford, UK, in press

Dudkina NV.*, Heinemeyer J.*, Sunderhaus S., Boekema EJ., Braun HP. (2006)

Respiratory chain supercomplexes in the plant mitochondrial membrane.

Trend in Plant Science 11: 232-240

*Equally contributing first authors

Sunderhaus S., Dudkina NV., Jansch L., Klodmann J., Heinemeyer J., Perales M., Zabaleta E., Boekema EJ., Braun HP. (2006)

Carbonic anhydrase subunits form a matrix-exposed domain attached to the membrane arm of mitochondrial complex I in plants.

J. Biol. Chem. 281: 6482-6488

Heinemeyer J., Lewejohann D., Braun HP. (2006)

Blue-native gel electrophoresis for the characterization of protein complexes in plants.

Meth. Mol. Biol. 335: 343-352

Dudkina NV., Heinemeyer J., Keegstra W., Boekema EJ., Braun HP. (2005)

Structure of dimeric ATP synthase from mitochondria: An angular association of monomers induces the strong curvature of the inner membrane.

FEBS Lett. 579: 5769-5772

Perales M., Eubel H., Heinemeyer J., Colaneri A., Zabaleta E., Braun HP. (2005)

Disruption of a nuclear gene encoding a mitochondrial gamma carbonic anhydrase reduces complex I and supercomplex I+III₂ levels and alters mitochondrial physiology in Arabidopsis.

J. Mol. Biol. 350: 263-277

Eubel H., Heinemeyer J., Sunderhaus S., Braun HP. (2004)

Respiratory chain supercomplexes in plant mitochondria.

Plant Physiol. and Biochem. 42: 937-942

Heinemeyer J., Eubel H., Wehmhöhn D., Jansch L., Braun HP. (2004)

Proteomic approach to characterize the supramolecular organization of photosystems in higher plants.

Phytochemistry 65: 1683-1692

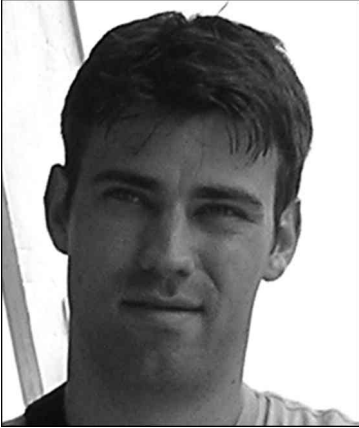
Eubel H., Heinemeyer J., Braun HP. (2004)

Identification and characterization of respirasomes in potato mitochondria

Plant Physiol. 134: 1450-1459

Evaluated by "Faculty of 1000"

Curriculum Vitae

| | | |
|-----------------|--|---|
| Name: | Jesco Heinemeyer |  |
| Date of Birth: | June 12, 1976 | |
| Place of Birth: | Hildesheim, Germany | |
| Citizenship: | Citizen of Germany | |
| Marital Status: | unmarried | |
| Parents: | Dr. rer. nat. Otto Heinemeyer Marion Heinemeyer, nee Eggers | |
| Siblings: | Dr. med. Oliver Heinemeyer | |

School Education

| | |
|--------------|--|
| 1982 – 1986 | Primary school „Hohnsen Schule“ in Hildesheim |
| 1986 – 1995 | Comprehensive school „Robert-Bosch-Gesamtschule“ in Hildesheim |
| May 22, 1995 | „Allgemeine Hochschulreife (Abitur)“ |

Civil Service, Traineeships

| | |
|------------------------|--|
| Aug. 1995 - Aug. 1996 | Civil service at the youth hostel of Hildesheim und at the St. Bernward Hospital in Hildesheim |
| Aug. 1996 - Oct. 1996 | Traineeship at the engineering works „Maschinenfabrik Hogendorf GmbH“(further Traineeships: At the County Court of Hildesheim while class 9 and at the Harz Mountains Waterworks while class 12) |
| April 1997 - Dec. 1997 | Temp. assistant at the St. Bernward Hospital in Hildesheim |

Academic Education

| | |
|-----------------------|--|
| Oct. 1997 - Nov. 2003 | Student at the „Gottfried Wilhelm Leibniz Universität Hannover“; major: biology |
| Jan. 2003 | Diploma examination in Microbiology, Genetics and Hydrobiology |
| Feb. 2003 - Oct. 2003 | Diploma thesis at the „Institut für Planzengenetik“, Division „Pflanzenmolekularbiologie“ as a member of the group “Pflanzenproteomik” of Prof. Dr. Hans-Peter Braun |
| 7. Nov. 2003 | Diplom-degree in Biology (grade: very good) |
| Since April 2004 | PhD student at the „Institut für Planzengenetik“, Division „Pflanzenmolekularbiologie“ as a member of the group of Prof. Dr. Hans-Peter Braun |
| Hannover, May 2007 | |

Danksagung

Die vorliegende Arbeit wurde unter der Anleitung von Prof. Dr. Hans-Peter Braun am Institut für Pflanzengenetik, der Naturwissenschaftlichen Fakultät, der Gottfried Wilhelm Leibniz Universität Hannover angefertigt.

Prof. Dr. Hans-Peter Braun danke ich daher an dieser Stelle ganz besonders. Durch seine versierte und zugleich stets freundliche Art hat er ein Arbeitsumfeld geschaffen, in dem ich mit großer Freude vieles gelernt habe. Durch sein außergewöhnliches Engagement hat er seiner Arbeitsgruppe die Teilnahme an so manchem wissenschaftlichen Kongress ermöglicht. Dies hat meine Zeit in seiner Arbeitsgruppe in ganz besonderer Weise bereichert. Des Weiteren danke ich Ihm für seine große Bereitschaft mit mir über diverse wissenschaftliche aber auch nichtwissenschaftliche Dinge zu diskutieren.

Prof. Dr. Udo Schmitz möchte ich dafür danken, dass diese Arbeit innerhalb der Abt. Pflanzenmolekularbiologie entstehen konnte.

Dr. Holger Eubel danke ich für die tolle gemeinsame Zeit in Büro und Labor. Zu Beginn meiner Arbeit waren sein Rat und seine Hilfe so manches Mal die Rettung in der Not.

Stephanie Sunderhaus danke ich ebenfalls für die schöne gemeinsame Zeit und die gegenseitige Hilfe. Ohne ihr Engagement sähe unser Büro wohl immer noch recht ungastlich aus.

Dagmar Lewejohann gebührt Dank für ihre helfende Hand im Labor. Zudem hätte, ohne ihren ordnenden Einfluss, die Labor-Entropie möglicherweise ein ernst zu nehmender Gegner im stetigen „Kampf“ um wissenschaftliche Ergebnisse werden können.

Prof. Dr. Egbert J. Boekema, Dr. Lothar Jänsch, Natalia Dudkina und Roman Kouril danke ich für eine tolle Zusammenarbeit.

Jenny Klodmann, Kathrin Peters, Frank Colditz und Mariano Perales waren prima Kollegen.

Meiner Familie und Inge verdanke ich viel mehr.

Jesco Heinemeyer
In der Schratwanne 45
31141 Hildesheim

Hildesheim, den 02.05.2007

Eidesstattliche Erklärung

Hiermit erkläre ich, dass ich die vorliegende Arbeit selbstständig verfasst und keine anderen als die angegebenen Quellen und Hilfsmittel verwendet habe.

(Jesco Heinemeyer)